Experimental Evaluation of the Strut-and-Tie Model Applied to Deep Beam with Near-Load Openings

Aqeel Talib Fadhil
Assistant Lecturer
College of Engineering-University of Baghdad
aqeel.fadhil@uobaghdad.edu.iq

ABSTRACT

It is commonly known that Euler-Bernoulli's thin beam theorem is not applicable whenever a nonlinear distribution of strain/stress occurs, such as in deep beams, or the stress distribution is discontinuous. In order to design the members experiencing such distorted stress regions, the Strut-and-Tie Model (STM) could be utilized. In this paper, experimental investigation of STM technique for three identical small-scale deep beams was conducted. The beams were simply supported and loaded statically with a concentrated load at the mid span of the beams. These deep beams had two symmetrical openings near the application point of loading. Both the deep beam, where the stress distribution cannot be assumed linear, and the existence of the openings, which causes stress discontinuity, make the use of Euler-Bernoulli's thin beam theorem not applicable. An idealized STM for the beam was first established and then experimental test was carried out to study the capability of STM to deal with the distortion of stress caused by the presence of near-load openings in addition to the nonlinear distribution of stress occurring in deep beam. The test results showed that the beam designed using STM was able to withstand a load higher than the designed ultimate load. The service load, in the other hand, was within the range of the estimated one. The outcome of this study can then be added to the relatively few available experimental studies related to STM technique to enhance the validation of STM to efficiently treat different structural configurations where the linear stress assumption cannot be applied.

Keywords: deep beam; strut-and-tie model; openings; nonlinear stress distribution; distorted stress regions.

دراسة عملية لنظرية الدعامة والشداد لاعتاب عميقة ذات فتحات قريبة من نقاط التحميل

عقيل طالب فاضل
مدرس مساعد
كلية الهندسة- جامعة بغداد

الخلاصة

نظرية اويلر-برنولي للاعتاب لا يمكن تطبيقها عندما يكون توزيع الاجهادات غير خطي اوغير مستمر على عمق المقطع الانشائي. لتصميم هذه العناصر، يمكن استخدام نظرية الدعامة والشداد. يقدم هذا البحث دراسة عملية لتطبيق نظرية الدعامة والشداد على ثلاثة نماذج متماثلة لاعتاب مصغرة. الاعتاب التي تم دراستها مسندة اسناد بسيط و تم تحميلها استاتيكيا بحمل مركز في منتصف العتبة. الاعتاب تحتوي على فتحتين متناظرتين قرب نقطة تحميل القوى. نظرية برنولي لايمكن استخدامها في هذه العتبات نتيجة كون العتبات عميقة والتي لايمكن فيها فرض توزيع الاجهادات خطي ونتيجة وجود الفتحات والتي تؤدي الى انقطاعات في توزيع الاجهادات. في هذا البحث، يتم اجراء دراسة عملية على نظرية الدعامة والشداد لمعرفة قدرتها على التعامل مع تشوه الاجهادات الناتج من وجود الفتحات قرب نقاط التحميل. نتائج البحث اظهرت ان الاعتاب المصممة بطريقة الدعامة والشداد كانت قادرة على مقاومة احمال قصوى اكثر من الاحمال المصممة لها. اما فيما يخص الاحمال الخدمية فكانت ضمن الحدود المتوقعة. النتائج المستخلصة من هذا البحث يمكن ان تكون اضافة للدراسات العملية القليله التي اجريت مسبقا لتأكيد قابلية نظرية الدعامة والشداد على التعامل مع حالات انشائية مختلفة تكون فيها نظرية برنولي غير قابلة للتطبيق.

الكلمات الرئيسية: عتب عميق، نظرية الدعامة والشداد، فتحات، توزيع الاجهادات اللاخطي، تشوه الاجهادات.

1. INTRODUCTION

Structural members come in a variety of configurations to comply with different structural demands. It is, therefore, hard to presume a unified assumption that can be applied precisely to all structural members. Euler-Bernoulli's thin beam theorem is one of those theories that cannot be applied to all structural components.

In general, structural elements can be grouped in two categories, **Wight** and **MacGregor 2012**,:

- B-regions (Beam regions) where the assumptions of Euler-Bernoulli's thin beam theorem can be applied including linear stress distribution assumption.
- D-regions (Disturbed or Discontinuous regions) where Euler-Bernoulli's thin beam theory cannot be used.

Strut-and–tie modeling approach is considered a valuable technique to design D-regions or nonlinear stress regions including deep beams. The strut-and–tie model was first introduced in the **ACI 318-02 code**, **2002**, in 2002 as an appendix. After that, it has been included within the code context as a main chapter including the latest **ACI code 318-14**, **2014**. The strut-and-tie model is a simple method that is basically derived from the truss analogy. The idea is to draw the flow of forces inside the structural member as struts and ties. The force in struts is resisted by concrete while reinforcement is designed and placed to resist the tension in ties. Several patterns of load paths may be constructed for the same loading conditions provided that the truss pattern and components satisfy the recommendations specified by the ACI code, as it is the reference code for this study, or the provisions specified by other codes of practice.

ACI 318-14 code, **2014**, defines the beam as a deep beam if a concentrated load acts within a distance less than twice the depth of the beam, or if the clear span between the beam's supports is less than fourth times the depth of the beam. Once the beam is identified as a deep beam, **ACI 318-14 code**, **2014**, recommends two methods to design the beam; either by taking into consideration the nonlinear distribution of the strains, without mentioning further details, or by using the strut-and-tie model.

One of the earliest and pioneering studies to address the design of deep beams with web openings was carried out by **Kong** and **Sharp**, **1977**. The study continued earlier pilot tests that had also been conducted by **Kong** and **Sharp**, **1973**, which focused on "Shear strength of lightweight reinforced concrete deep beams with web openings." The total beams tested in both studies were 56 deep beams with various beam and opening dimensions and different openings locations. At that time, no regulations within the codes of practice covered the design of deep beam with web opening. The researchers implicitly used the basics of the strut-and-tie model for the design. The final outcome made by **Kong** and **Sharp**, **1977**, was a modified shear strength formula and hints for the design of similar cases.

Following **Kong** and **sharp** several researches addressed the design of deep beams with web openings aiming to introduce a design method for such cases. Many of these researches used in some parts the load path method to bypass the existence of openings in the beam. The results of these assumptions proved that it was a good structural treatment for the presence of openings. After that, the load path treatment was developed to the strut-and-tie model approach as a simple yet a powerful design method. Among these researchers are **Kong et al., 1978**, **Kubik**, **1980**, **Mansur** and **Alwis**, **1984**, **Haque et al.**, **1986**, and **Schlaich et al.**, **1987**.

Several theoretical studies have been introduced later in order to address the use of strut-and-ties models in different structural members. However, a relatively few experimental verification tests

have been made related to the implementation of the strut-and-ties models in various scenarios including tests carried out by **Maxwell** and **Breen**, **2000**, **Chen et al.**, **2002**, **Ley et al.**, **2007**, **Zhang** and **Tan**, **2007**, **Campione** and **Minafò, 2011**, **Arabzadeh et al.**, **2011**, **Nagrodzka-Godycka** and **Piotrkowski, 2012**, **He et al.**, **2012**, and **Tuchscherer et al.**, **2014**. Good amount of experimental verifications will support and encourage engineers to better utilize this simple method in many structural cases where the linear stress beam theory cannot be utilized. It was noted by reviewing the previous experimental tests that the web opening in most of these studies were placed relatively away from the loading source and closer to the supports or to the middle region of the beam. Therefore, it was intended herein to place two openings closer to loading area of beams tested to show that a good strut-and-tie model design can overcome the high stress distortions that occur between the loading point and the openings. The intent from this study is to introduce, test, and verify different untraditional structural problem to help increasing the number of experimental studies that ensure the capabilities of the strut-and–tie model to treat variety of structural scenarios.

2. SPECIMEN DETAILS

The test involved three identical small-scale deep beam specimens. The geometry of the beam is shown in **Fig. 1**. The specimen had a full length of 800mm and a depth of 250mm. The width of the beam was 100mm. The beam had two symmetrical 50mm by 50mm openings near the application of the load.

Regarding the size of the openings, there are no available limitations in the current codes of practice. Many researchers label the openings in their work as "small" or "large" openings without a clear definition of the size limits between both labels. **Mansur M. A., 1998,** related "small" and "large" openings definitions based on the beam response where the large openings result in Vierendeel action. Beams with large openings require special treatment.

The beam was simply supported with a span length of 600mm center-to-center of the support which makes the ratio of clear span to overall beam depth equals to 2.0. **ACI 318 code**, **2014**, classifies the beam as a deep beam if the aforementioned ratio is less than 4. Deep beams can either be designed by taking into consideration the nonlinearity of strain along the depth or by using the strut-and-tie model.

Steel bearing plates of 100mm by 100mm were provided at each support to provide the required bearing width and to simulate the bearing width provided by the columns or supporting girders. The beam was loaded at the mid span through a steel bearing plate of 100mm by 100mm.

When designed, the beam was intended to carry an ultimate concentrated load of 50kN at the middle of the beam. This load was supposed to be a combination of factored dead and live load according to the **ACI 318 code**, **2014**, with load factors equal to 1.2 for the dead load and 1.6 for the live load. The related service load could then be approximated by dividing the ultimate load by an average load factor of 1.4 for both dead and live load combined, **Maxwell and Breen**, **2000**, to obtain an equivalent service condition with load factor of 1.0 resulting in a related service load of 35.71 kN.

3. MATERIAL PROPERTIES

To accommodate the small-scale beam specimen, small reinforcing bar diameters and proper maximum size of coarse aggregate were adopted. Steel reinforcement and concrete used for this

study were tested based on the test methods and procedures recommended by the **ASTM international** standards.

Two different reinforcing steel bars were used in this research;

- 4mm diameter deformed reinforcing bars with cross sectional area of 15.69 mm^2, and
- 6mm diameter deformed reinforcing bars with cross sectional area of 32.15 mm^2.

The reinforcing steel used in the study complies with **ASTM A615** specifications titled "*Standard Specification for Deformed and Plain Carbon Steel Bars for Concrete Reinforcement*." The results showed that Ø4mm deformed bars had an average yield strength of (457 MPa) and an ultimate strength of (606 MPa) while the average yield strength of Ø6mm deformed bars was (544 MPa) and the ultimate strength was (688 MPa).

Fine and coarse aggregate used in the study complies with **ASTM C33** titled *"Standard Specification for Concrete Aggregates*" including grading limits for both fine and coarse aggregate which was conducted in accordance with **ASTM C136** "*Standard Test Method for Sieve Analysis of Fine and Coarse Aggregates."*

Mix design was carried out based on the procedure provided by **ACI 211.1** titled *"Standard Practice for Selecting Proportions for Normal, Heavyweight, and Mass Concrete"* after gathering the required information from sieve analysis as well as mass densities of fine and coarse aggregates conducted in accordance with **ASTM C127** *"Standard Test Method for Density, Relative Density (Specific Gravity), and Absorption of Coarse Aggregate"* and **ASTM C128** *"Standard Test Method for Density, Relative Density (Specific Gravity), and Absorption of Fine Aggregate"* The cylinders that were taken at the day of casting the beams were tested according to **ASTM C39** *"Standard Test Method for Compressive Strength of Cylindrical Concrete Specimens"* and showed that the concrete had an average specified compressive strength (f_c') of (29.6 MPa) at the age of 28 days resulting in modulus of elasticity equal to (25500 MPa) and modulus of rupture equal to (3.3 MPa).

4. STRUT-AND-TIE MODEL DESIGN

4.1 Concept

The design using the strut-and-tie model basically depends on visualizing the stress fields inside the structural member caused by the applied loads. These stress fields are then illustrated based on the truss analogy as a combination of struts, for compression stress fields, and ties, for tension stress fields. Struts and ties are assumed to be connected at nodes to form the complete geometry of the truss.

Different truss configurations can be drawn for the same loading conditions. The process of the design using the strut-and-tie model may involve some iterations to select the optimum truss for the given load. The optimum truss should be able to resist the designed factored load with a minimal use of reinforcement tie weight which ensures that the selected truss satisfies the strength requirement as well as the economic considerations. The final truss selected for design should not only satisfy the strength and economic requirements but also the safety needs regarding the failure type. In order to prevent brittle failure, a safe design can be accomplished by attempting to provide a design that allows the beam to deflect to a minimum deflection of (L/100) at failure, **Ley et al.**, **2007**. This ratio is usually considered among the structural engineers because it is generally thought to be close to the limit of deflection that is noticeable to the human eye.

4.2 Finite Element Implementatıon

As advised by **Schlaich et al.**, **1987**, finite elements model can be utilized to get a better understanding of the stress fields inside the unreinforced structural member. It has not been an obligation for the researchers to implement the use of finite element when designing using the strut-and-tie model as it is supposed to be an optional tool for a better design.

For this study, a two-dimensional finite element modeling was performed for the unreinforced specimen in order to get a better picture about the compression and tension field stresses in the beam which, in turns, could help configuring the outline of the truss. The two-dimensional finite element modeling was carried out using Abaqus FEA software.

Since it is a 2D FE Analysis, the element CPS4R was chosen to model the beam. CPS4R element is a 4-node bilinear plane stress quadrilateral, reduced integration, hourglass control**, Abaqus/CAE, 2011**. The beam was sketched with dimensions equal to 800mm in length and 250mm in depth. Two openings were drawn with dimensions of 50mm by 50mm and placed in its designated position in the tested beam shown in **Fig. 1**. As it is recommended by **Schlaich et al.**, **1987**, to model the unreinforced beam in the FE model to view the stress path in the concrete without the help of reinforcement, the only material that was fed to the program is concrete properties with a mass density of (2400 kg/m^3), Young's Modulus of (25500 MPa) and Poisson's Ratio of (0.15). A concentrated load was applied at the middle of the beam to simulate the loading case at the testing. The output of the major ranges of compression stress field and tension stress field are shown in **Figs. 2** and **3**.

4.3 Idealızed Truss Model

After an extensive study and several iterations of different truss configurations, the idealized truss shown in **Fig. 4** was adopted. The selected truss complies with recommendations of the **ACI 318 code**, **2014**, found in Chapter 23 which is titled "The Strut-and-Tie Models."

The limitation of the **ACI 318 code**, **2014**, of providing a minimum angle of (25˚) between any strut and tie connecting at a single node was considered when designing the idealized truss layout. Also, the strengths of the ties, struts, and nodal zones of the idealized truss were checked to satisfy the following ACI criteria, **ACI 318 code**, **2014**.

$$\phi F_{ns} \geq F_{us} \quad (For\ Struts) \tag{1}$$

$$\phi F_{nt} \geq F_{ut} \quad (For\ Ties) \tag{2}$$

$$\phi F_{nn} \geq F_{us} \quad (For\ Nodal\ zones) \tag{3}$$

where F_{ns}, F_{nt}, and F_{nn} represent the nominal strength of struts, ties, and at nodal zones respectively while F_{us} and F_{ut} represent the factored compressive force in struts and tensile force in ties respectively. The strength reduction factor (ϕ) equals to 0.75 as specified in the **ACI 318 code**, **2014**.

The factored forces in each strut and tie were calculated after performing the analysis on the idealized truss as shown in **Fig. 4**. The nominal strengths of each strut, tie and node were calculated based on the criteria detailed in the **ACI 318 code**, **2014**. For each member of the truss, the inequalities of Eqs. (1) - (3) were checked and; hence, the designed truss should be able to transfer the concentrated load thought the truss to the supports.

4.4 Reınforcement Desıgn and Arrangement

Reinforcement layout and placing in the strut-and-tie model follow the idealized truss model. The reinforcement area is calculated according to the factored tie forces and placed according to the orientations and locations of the ties in the designed truss model.

The reinforcement was placed in three layers; a top layer that is located above the openings, a middle layer placed below the openings, and a bottom layer. According to the analysis performed on the idealized truss and based on the yield strength of the reinforcing steel used in this study, the following reinforcement was provided;

- For the top layer, four reinforcing bars of Ø4mm were provided.
- For the middle layer, three reinforcing bars of Ø4mm were provided.
- For the bottom layer, two reinforcing bars of Ø6mm were provided.

The reinforcement layout for the beam is shown in **Figs. 5(a)-(b)**. The anchorage lengths for the reinforcement were provided to ensure that the failure during the test would not occur due to the lack of anchorage of reinforcement.

It is important to mention that the design of deep beams using the strut-and-tie model does not require providing a minimum reinforcement ratio as per the recommendations of **ACI 318 code**, **2014**, for ordinary flexural members.

5. TEST ASSEMBLY

The test assembly was prepared as shown in **Fig. 6**. The test was carried out at the laboratories of College of Engineering / University of Baghdad. The test assembly consisted of:

- The examined deep beam specimen.
- Two supports; each connected to a bearing plate of 100x100mm to provide the required bearing width, that was checked throughout the design of the idealized truss model, and to simulate the bearing width provided by the columns or supporting girders.
- Hydraulic loading system equipped with a hydraulic shaft to deliver the desired load to the tested beam through a bearing plate with dimensions of 100x100mm.
- Load cell with a loading capacity of 20kN connected to a digital load indicator.
- Digital dial gauge to record the vertical deflections at the mid span of the beam specimens.
- Strain gauges and a digital strain indicator that is connected to a computer supplied with computer software that is designed to read and record strain readings from both concrete and steel reinforcement.

6. TEST RESULTS AND CRACK PATTERNS

The test performed on the three identical deep beams showed comparable results since they were identical in almost every detail. The slight difference between the results of the specimens is normal and due to the inherent randomness in material properties and testing environment for all three specimens.

The results of the test conducted on the beams showed that the beams designed using the strut-and –tie model were able to withstand concentrated loads higher than the designed ultimate load which was in the range of 50kN.

The vertical load-deflection curves of the three beam specimens show almost a linear relation between the applied vertical load and the vertical deflection at the mid span of the beam

(see **Fig. 7**). The test carried out on the first sample showed that the beam resisted an ultimate load of 58.60kN before failure with an increase of 17% in the designed ultimate load. The second specimen was able to carry an ultimate load of 62.40kN before it failed resulting in an increase in the designed ultimate load of approximately 25%. The test on the third beam showed that this sample resisted before failure an ultimate load of 60.70kN with an increase of approximately 21% in the designed ultimate load. **Fig. 8** summarizes the percent of increase in the designed ultimate load for each specimen during the test. The average ultimate load obtained from the test of the three beam specimens was 60.57kN with an average increase of 21% in the designed ultimate load obtained from the strut-and-tie modeling technique.

For all specimens, the initial crack appeared at the lower center of the beam which indicates a flexural action at the service stage of loading. The initial crack at the three specimens occurred at a load approximately equal to 35kN which is close to the specified service load mentioned earlier.

As the load was being increased towards the ultimate load, diagonal cracks started to develop in the vicinity of the supports propagating from the left and right supports approaching the openings, which reflects shear action dominance at this level of loading. When the load was increased so that it became in the neighborhood of the ultimate load, the diagonal cracks kept propagating towards the openings causing the beam specimens to fail at loadings equal to 58.60kN, 62.40kN, and 60.70kN for beam specimens one, two, and three respectively. Initial crack location and general schematic crack pattern for the beam specimens are presented in **Figs. 9-10**.

The deflection recorded at the ultimate load for the first beam specimen was 5.78mm. For the second beam, the deflection measured at failure was 6.33mm. A deflection of 5.45mm was recorded for the third beam specimen. The average deflection of the three specimens was 5.85mm which is close to the deflection obtained from the ratio L/100 where the deflection is considered noticeable.

7. CONCLUSIONS AND RECOMMENDATIONS

The results of this study affirm that the strut-and-tie model is a plasticity method that is based on the lower bound theorem. Some previous experimental researches reported an increase in the ultimate strength of beams designed using the strut-and-tie method by ratios ranging between (0.09% -0.28%), **Chen et al.**, **2002**, while other researchers reported an increase in the ultimate strength up to 95% more than the designed ultimate load, **Maxwell** and **Breen**, **2000**. The average increase of the ultimate strength of the beams studied herein was 21% more than the designed ultimate load.

The strut-and-tie model has proven throughout this study and previous studies that it is a useful, safe, and simple tool to handle untraditional and complicated problems provided that all the limitations recommended by the **ACI-318, 2014**, code or the selected practice code are to be taken into consideration throughout the design process. Successful implementation of the strut-and-tie model also requires providing a good design for the idealized truss which may involve several iterations to achieve the best truss layout. It is worthwhile to mention, however, that the bending and placement of the reinforcement for members designed using the strut-and-tie method is usually more time-consuming than the traditional reinforcement constructions.

The good choice for the idealized truss model in this study successfully helped the beam overcome the diagonal shear forces until the beam reached satisfactory ultimate loads compared to the designed load. The existence of the inclined reinforcement above and below the openings restrained the propagations of the diagonal cracks and prevented the premature failure. The

model was also able to deal with the distorted region existed due to the presence of two openings near the loading source which, in turns, prevented any concrete spalling in this region.

For the future studies, it may be useful to investigate the following cases:

- Perform and suggest different strut-and-ties models for the same loading and beam geometry. Then, conduct an experimental verification to ensure the ability of the strut-and-tie model to offer different adequate designs for the same scenario.
- Conduct a larger-scale experimental test for the same model in this research to investigate whether or not scaling the model will affect the percent of increase in the ultimate load-carrying capacity of the beams designed using the strut-and-tie model.

REFERENCES

- Abaqus/CAE User's Manual Version 6.11, 2011, *Dassault Systèmes Simulia Corp*., Providence, RI, USA.
- ACI 318, 2002, *Building code requirements for structural concrete and commentary*, American Concrete Institute; Farmington Hills, MI, USA.
- ACI 318, 2014, *Building code requirements for structural concrete and commentary*, American Concrete Institute; Farmington Hills, MI, USA.
- ACI 211.1, 1991, *Standard Practice for Selecting Proportions for Normal, Heavyweight, and Mass Concrete*, American Concrete Institute; Farmington Hills, MI, USA.
- ASTM A615/A615M–04, 2004, *Standard Specification for Deformed and Plain Carbon Steel Bars for Concrete Reinforcement*, ASTM International, West Conshohocken, PA, USA.
- ASTM C33–03, 2003, *Standard Specification for Concrete Aggregates*, ASTM International, West Conshohocken, PA, USA.
- ASTM C39–03, 2003, *Standard Test Method for Compressive Strength of Cylindrical Concrete Specimens*, ASTM International, West Conshohocken, PA, USA.
- ASTM C127–01, 2001, *Standard Test Method for Density, Relative Density (Specific Gravity), and Absorption of Coarse Aggregate*, ASTM International, West Conshohocken, PA, USA.
- ASTM C128–01, 2001, *Standard Test Method for Density, Relative Density (Specific Gravity), and Absorption of Fine Aggregate*, ASTM International, West Conshohocken, PA, USA.
- ASTM C136–01, 2001, *Standard Test Method for Sieve Analysis of Fine and Coarse Aggregates*, ASTM International, West Conshohocken, PA, USA.

- Arabzadeh, A., Aghayari, R., and Rahai, A. R., 2011, *Investigation of experimental and analytical shear strength of reinforced concrete deep beams,* International Journal of Civil Engineering, Vol. 9, No. 3, PP. 207-214.

- Campione, G., and Minafò, G., 2011, *Experimental investigation on compressive behavior of bottle-shaped struts,* ACI Structural Journal, Vol. 108, No. 3, PP. 294-303.

- Chen, B. S., Hagenberger, M. J., and Breen, J. E., 2002, *Evaluation of strut-and-tie modeling applied to dapped beam with opening*, ACI Structural Journal, Vol. 99, No. 4, PP. 445-450.

- Haque, M., Rasheeduzzafar, and Al-Tayyib, A. H. J., 1986, *Stress distribution in deep beams with web openings*, Journal of Structural Engineering, Vol. 112, No. 5, PP. 1147-1165.

- He, Z., Liu, Z., and Ma, Z. J., 2012, *Investigation of load-transfer mechanisms in deep beams and corbels,* ACI Structural Journal, Vol. 109, No. 4, PP. 467.

- Kong, F. K., and Sharp, G. R., 1973, *Shear strength of lightweight reinforced concrete deep beams with web openings*, The Structural Engineer, Vol. 51, No. 8, PP. 267-275.

- Kong, F. K., and Sharp, G. R., 1977, *Structural idealization for deep beams with web openings*, Magazine of Concrete Research, Vol. 29, No. 99, PP. 81-91.

- Kong, F. K., Sharp, G. R., Appleton, S. C., Beaumont, C. J., and Kubik, L. A., 1978, *Structural idealization for deep beams with web openings: further evidence*, Magazine of Concrete Research, Vol. 30, No. 103, PP. 89-95.

- Kubik, L. A., 1980, *Predicting the strength of reinforced concrete deep beams with web openings,* Institution of Civil Engineers, Proceedings, Vol. 69, Pt. 2, PP. 939-958.

- Ley, M. T., Riding, K. A., Widianto, Bae, S., and Breen, J. E., 2007, *Experimental verification of strut-and-tie model design method,* ACI Structural Journal, Vol. 104, No. 6, PP. 749-755.

- Mansur, M.A. and Alwis, W.A.M., 1984, *Reinforced fibre concrete deep beams with web openings*, International Journal of Cement Composites and Lightweight Concrete, Vol. 6, No. 4, PP. 263-271.

- Mansur, M.A., 1998, *Effect of openings on the behaviour and strength of R/C beams in shear,* Cement and concrete composites, Vol. 20, No.6, PP. 477-486.

- Maxwell, B. S., and Breen, J. E., 2000, *Experimental evaluation of strut-and-tie model applied to deep beam with opening,* ACI Structural Journal, Vol. 97, No. 1, PP. 142-148.

- Nagrodzka-Godycka, K., and Piotrkowski, P., 2012, *Experimental study of dapped-end beams subjected to inclined load,* ACI Structural Journal,Vol. 109, No. 1, PP. 11-20.

- Schlaich, J., Schäfer, K., and Jennewein, M., 1987, *Toward a consistent design of structural concrete*, PCI Journal, Vol. 32, No. 3, PP. 74-150.

- Tuchscherer, R. G., Birrcher, D. B., Williams, C. S, Deschenes, D. J., and Bayrak, O., 2014, *Evaluation of existing strut-and-tie methods and recommended improvements*, ACI Structural Journal, Vol. 111, No. 6, PP. 1451.

- Wight, J.K. and MacGregor, J.G., 2012, *Reinforced Concrete Mechanics and Design*, 6th Edition, Pearson Education. Inc., Upper Saddle River. NJ, USA.

- Zhang, N., and Tan, K., 2007, *Size effect in RC deep beams: Experimental investigation and STM verification*, Engineering Structures, Vol. 29, No. 12, PP. 3241-3254.

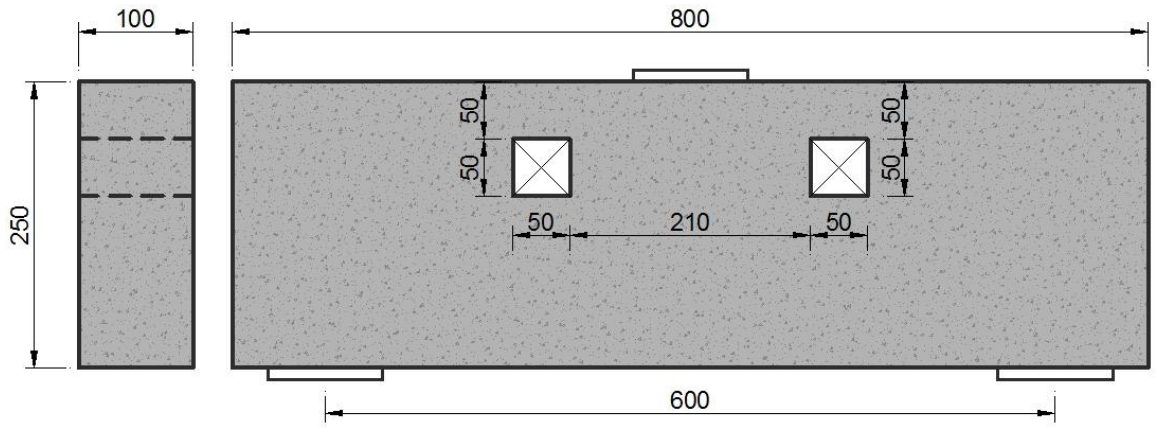

Figure 1. Beam geometry (dimensions are in mm).

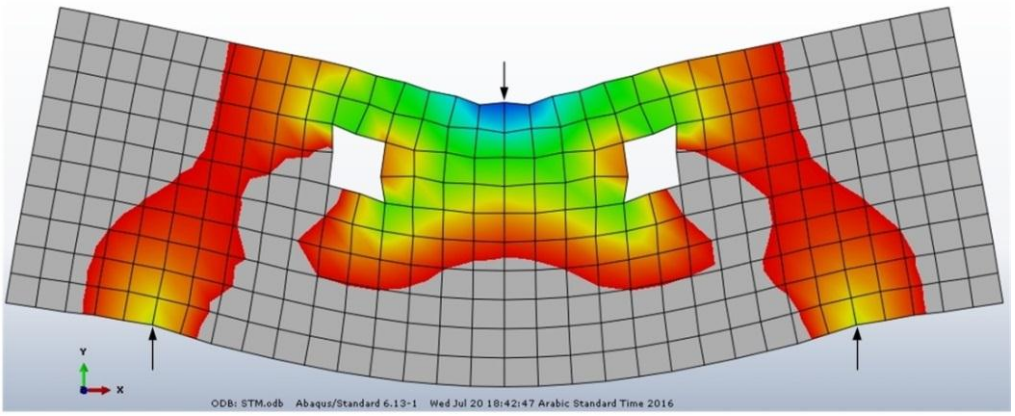

Figure 2. Compression stress field in FE model of the unreinforced beam specimen.

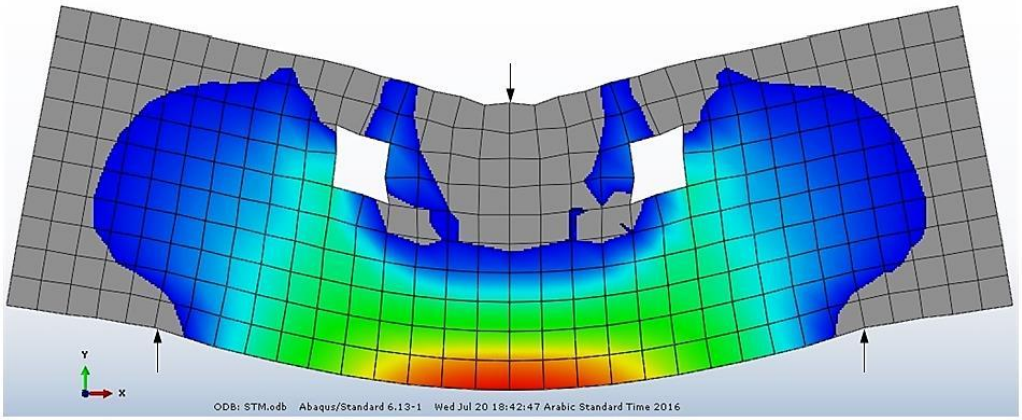

Figure 3. Tension stress field in FE model of the unreinforced beam specimen.

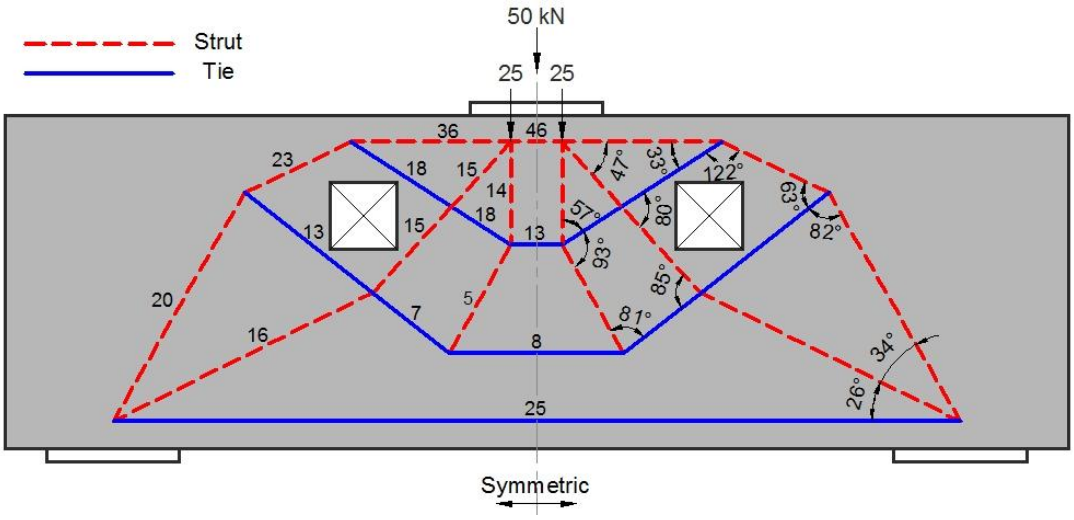

Figure 4. Idealized truss model and factored forces (forces are in kN).

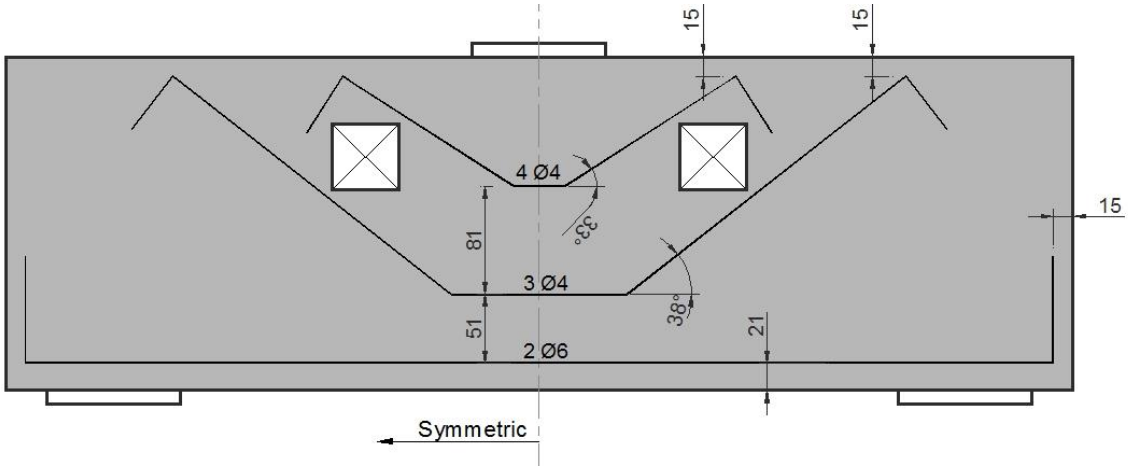

(a) Reinforcement design

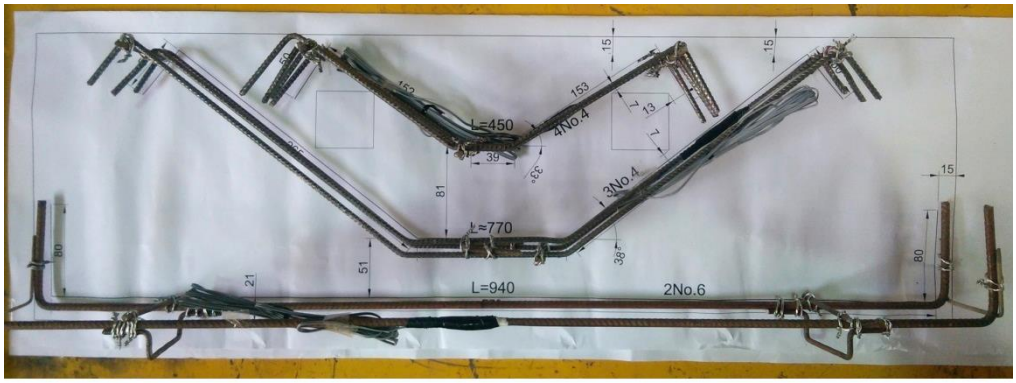

(b) Reinforcement construction

Figure 5. Reinforcement layout and construction (dimensions are in mm).

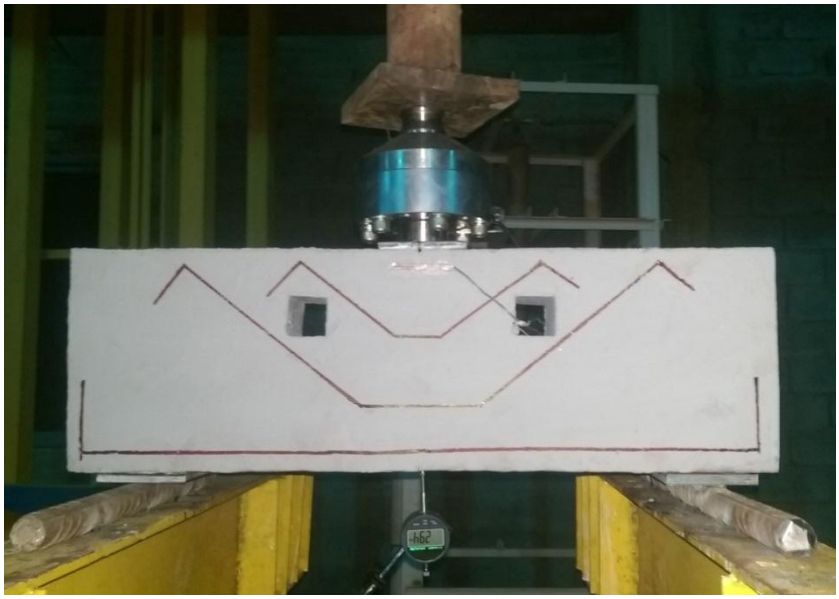

Figure 6. Test assembly.

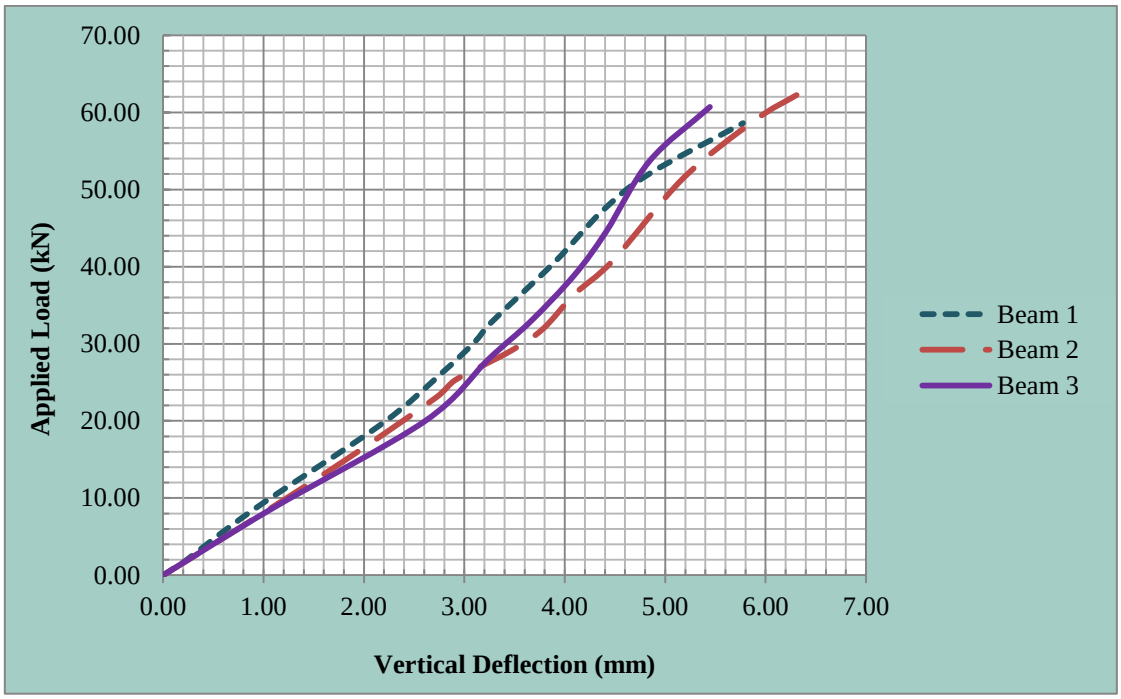

Figure 7. Vertical load-deflection for the tested beams.

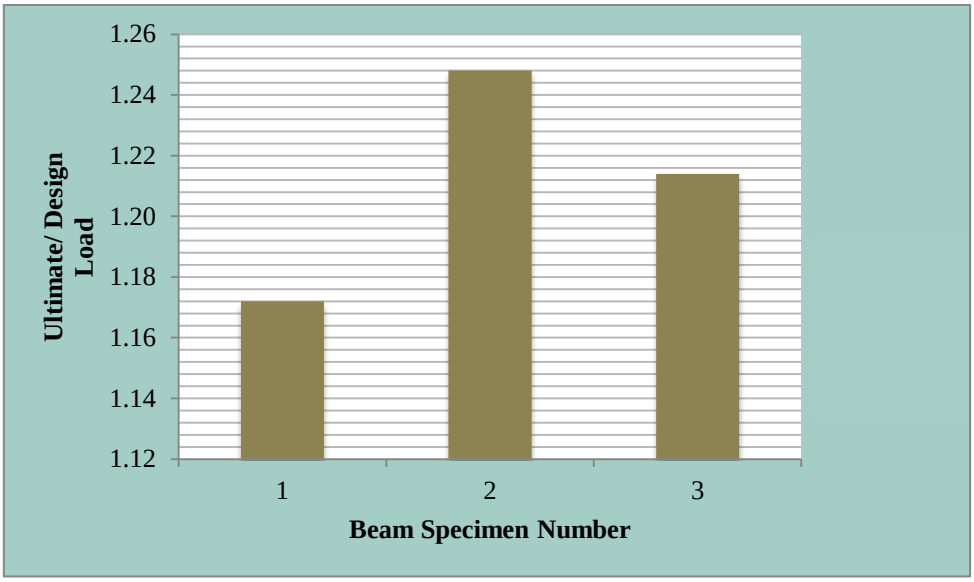

Figure 8. Percent of increase in the ultimate strength with respect to the design load.

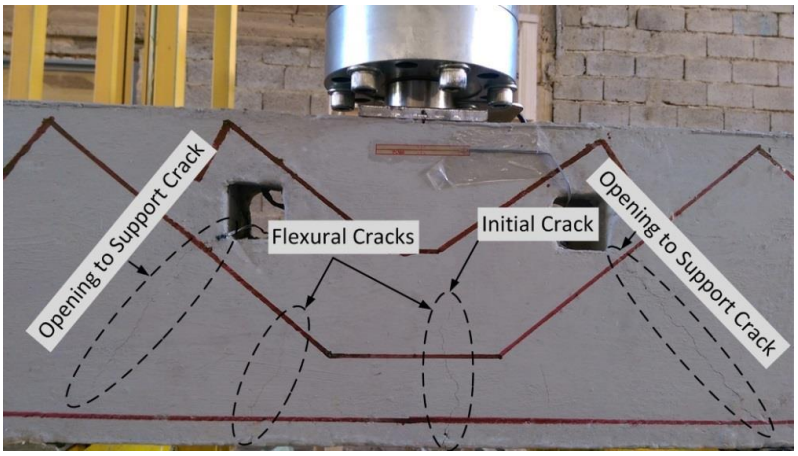

Figure 9. Initial and diagonal cracks captured during the test.

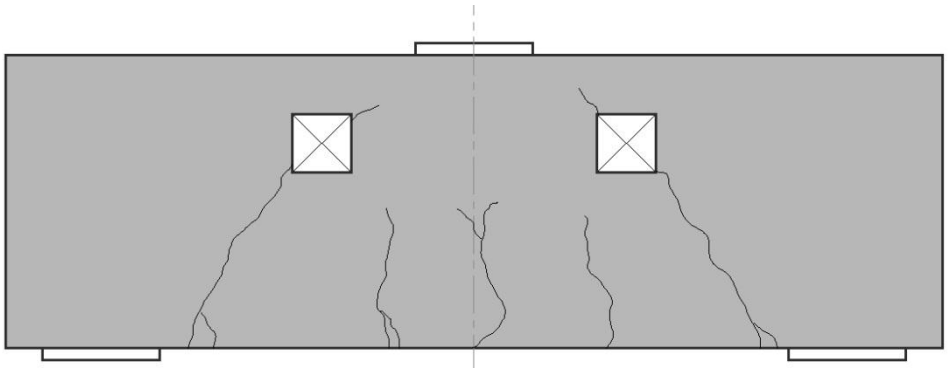

Figure 10. General crack pattern for the tested beams.

Mismanagement Reasons of the Projects Execution Phase

Dr. Hatem Khaleefah Al-Agele
Assistant Professor
Engineering College-Baghdad University
dr.hatem2999@yahoo.com

Abdulmajeed Jafar Ali
Researcher
Engineering College-Baghdad University
Abdulmajeed1110@gmail.com

ABSTRACT

The execution phase of the project is most dangerous and the most drain on the resources during project life cycle, therefore, its need to monitor and control by specialists to exceeded obstructions and achieve the project goals. The study aims to detect the actual reasons behind mismanagement of the execution phase. The study begins with theoretical part, where it deals with the concepts of project, project selection, project management, and project processes. Field part consists of three techniques: 1- brainstorming, 2- open interviews with experts and 3- designed questionnaire (with 49 reason. These reasons result from brainstorming and interviewing with experts.), in order to find the real reasons behind mismanagement of the execution phase. The most important reasons which are negatively impact on management of the execution phase that proven by the study were (Inability of company to meet project requirements because it's specialized and / or large project, Multiple sources of decision and overlap in powers, Inadequate planning, Inaccurate estimation of cost, Delayed cash flows by owners, Poor performance of project manager, inefficient decision making process, and the Negative impact of people in the project area). Finally, submitting a set of recommendations which will contribute to overcome the obstructions of successful management of the execution phase.

Key words: execution phase, project mismanagement**,** brainstorming.

أسباب سوء الادارة في مرحلة تنفيذ المشاريع

د. حاتم خليفة العجيلي
إستاذ مساعد
كلية الهندسة- جامعة بغداد

عبدالمجيد جعفر علي
باحث ماجستير
كلية الهندسة- جامعة بغداد

الخلاصة

تعتبر مرحلة تنفيذ المشروع هي المرحلة الاخطر والاكثر استنزافا للموارد خلال دورة حياة المشروع، لذلك فهي تحتاج الى مراقبة وسيطرة دقيقة يقوم بها اصحاب الاختصاص من اجل تجاوز العقبات وتحقيق اهداف المشروع. إن الهدف من الدراسة هو لبحث وايجاد الاسباب الحقيقية وراء سوء ادارة المشروع في مرحلة التنفيذ. بدأ البحث بالدراسة النظرية وإستطلاع ادبيات الموضوع. بعد ذلك بدأت الدراسة الميدانية والتي استندت على استخدام ثلاثة تقنيات معتمدة وهي: 1- العصف الذهني، 2- المقابلات المفتوحة مع الخبراء، و 3- تصميم استبيان (يحتوي على 49 سببا تم استنباطها من العصف الذهني والمقابلات مع الخبراء)من اجل إيجاد الاسباب الحقيقية المؤدية إلى سوء إدارة المشروع في مرحلة التنفيذ. اثبتت الدراسة ان الاسباب التالية هي الاكثر تأثيرا على ادارة مرحلة التنفيذ: (عدم قدرة الشركة على تلبية متطلبات المشروع لكونه من المشاريع التخصصية و/ او الكبيرة، تعدد مصادر القرار والتداخل في الصلاحيات، ضعف التخطيط للمشروع، عدم دقة تخمين الكلفة، تأخر صرف مستحقات المقاول من قبل صاحب العمل، ضعف اداء مدير المشروع ،ضعف عملية اتخاذ القرار، والتأثير السلبي لسكان منطقة المشروع). واخيرا تقديم مجموعة من التوصيات ستسهم في تجاوز معرقلات الادارة الناجحة لمرحلة التنفيذ.

1. INTRODUCTION

After 2003, Iraq has got a high income and this have encouraged the successive governments to adopt a quick and ambitious programs for reconstruction, either by establish new projects for public infrastructure or by developing the old facilities which are necessary to grow needs of all sectors. Unfortunately, there are many problems in reconstruction programs because improvisatory and unplanned. Therefore, they do not achieve their goals. The selection of an appropriate project for implementation and provide the necessary financial allocations in addition to proper management, all of which are required to achieve a success project.

2. CONSTRUCTION PROJECT

Construction projects are complex, time-consuming undertakings. The development of a project typically consists of several stages requiring a diverse range of specialized services. To some extent each project is unique-no two jobs are ever exactly the same, **Sears, et al., 2008.**

The construction project goal is to build something. What differentiates the industry of construction from other industries is that its project is large, built on –site, and generally unique, **Gould, 1997.**

The major characteristics of a project are as follows:

1- An established objective.
2- A defined life span with a beginning and an end.
3- Usually, the involvement of several departments and professionals.
4- Typically, doing something that has never been done before.
5- Specific time, cost, and performance requirements, **Larson,** and **Gray, 2011**.

2.1 Project Context (Environment)

Construction project is influenced by multiple factors which can be internal or external to the organization responsible for its execution and management. The external factors which making this environment includes the client or customer, contractors, various external consultants, suppliers, national and local government agencies, competitors, politicians, pressure group, public utilities, and the end user. Internal influences include the organization's management, the project team, internal departments, (technical and financial) and possibly the shareholders.

The important thing for the project manager is to recognize what these factors are and how they impact on the project during the various phases from inception to final handover, or even disposal, **Fig.1** illustrates the project surrounded by its external environment**, Lester, 2006.**

2.2 Project Selection

The process of projects selection for implementation is subject to several considerations such as; the needs of organization, realistic expectations for deliverables sophistication, strategic plans, project success attributes, and the restrictions for the project's success. To make logical and consistent decisions in prioritizing and projects selection, a company shall establish a specific process of evaluating projects. Projects ranking is commonly conducted according to certain criteria and in terms of importance with the use of an index, sometimes called a metric, or a group of indices called a model. Indices used for project selection tend to fall into two major categories. The first category includes quantitative indices that are generally based on financial characteristics such as: total cost, cash flow demand, cost-benefit ratio, Payback period, average internal rate of return, net present value. The second category includes qualitative indices that are intended to measure subjective issues, such as operational necessity, competitive necessity, product line extension, market constraints, Profitability, Feasibility, desirability, recognition, and

success. **Fig. 2** shows a simple weighted summation for the results of the of graphical depiction indices to a selection model that is composed of four indices, **Rad, 2002.**

2.3 Project Success Criteria

One of the topics in the project management plan is the project success criteria. These are the most important attributes and objectives which must be met to enable the project to be termed a success. For example if one of the project success criteria is that the project finishes by or before a certain date, then there can be no compromise of the date, but the cost may increase or quality may be sacrificed, **Lester, 2006.**

A project is generally considered to be successfully implemented if it:

a) Comes in on-schedule (time criterion).
b) Comes in on-budget (monetary criterion).
c) Achieves basically all the goals originally set for it (effectiveness criterion).
d) Is accepted and used by the clients for whom the project is intended (client satisfaction criterion), **Pinto**, and **Slevin, 1987.**

2.4 Project Management

Is the planning, monitoring and control of all aspects of a project and the motivation of all those involved in it, in order to achieve the project objectives within agreed criteria of time, cost and performance. **Lester 2006.**

2.4.1 Need for project management

It can be summarized the great importance of project management in the following aspects:

a) Project management allows managers to plan and manage strategic initiatives.
b) Project management tools decrease time to market, manage expenses, ensure quality products, and enhance profitability.
c) Project management helps sell products and services by positively differentiating them from their competitors.
d) Project management is one of the most important management techniques for ensuring the success of an organization, **Richman**, **2011.**

2.4.2 Poor project management

The lack of project management by owners or contractors on projects leads to construction delays and extra costs for both parties. In addition to the problems that occur during construction, poor project management can also result in a completed facility that fails to meet the specified quality and suitability of materials, fails to produce the intended products, or cannot be operated for its intended life. Reasons for project failure that are often cited during disputes: **King**, **2015.**

1- The failure of the project management team to adequately plan the work, or, when a plan developed, to properly execute that plan.
2- The failure to provide adequate human resources, staff or direct labor, to the project.
3- The failure to develop adequate project schedules, or to maintain those schedules throughout project execution.
4- The failure to control costs and changes throughout the execution of the project.

3. UNDERSTANDING PROJECT PROCESSES

All projects progress through five project management process groups:

3.1 Initiating Process

The Initiating process determines which projects should be undertaken (project selection). It examines whether the project is worth doing and if it is beneficial to the company when all is said and done, **PMBOK**, **2013.**

3.2 Planning Process

The planning process requires establish the scope of the project, refine the objectives, and define the course of action required to attain the objectives that the project was undertaken to achieve, **PMBOK**, **2013.**

3.3 Executing Process

It is involves the actual "work" of the project. Materials and resources are procured, the project is produced, and performance capabilities are verified. There are two aspects to the process of project execution. One is to execute the work that must be done to create the product of the project. This is properly called technical work. Executing also refers to implementing the project plan, since without a plan there is no control**, Heagney**, **2012.**

Executing means carrying out the activities described in the work plan, and where visions and plans become reality, **Dillon**, **2008.**

3.4 Monitoring and Controlling Process

Monitoring and controlling can actually be thought of as two separate processes, but because they go hand in hand, they are considered one activity, **Heagney**, **2012.**

Monitoring: Collecting, recording, and reporting information concerning project performance that project manager and others wish to know.

Controlling: Uses data from monitor activity to bring actual performance to planned performance, **Meredith**, and **Mantel**, **2000**.

3.5 Closing Process

Finishing your assigned tasks is only part of bringing your project to a close, **Portny**, **2010**. If you did a good job of planning and execution, the close-out phase should be fairly simple and fun. Some project leaders avoid close out because there are unresolved problems with the project: There are unhappy customers or team members, overrun budgets, and late schedule dates, **Martin**, and **Tate**, **2001**.

4. THE TECHNIQUES

The researcher provides detail explanation about the techniques which are used in this part of the study.

4.1 Brainstorming Technique

It is a creating technique and popular tool of generating ideas to solve a problem. The main outcome of a brainstorm session may be a full solution to the problem, a set of ideas for an approach to a subsequent solution, or a set of ideas resulting in a plan to find a solution.

Brainstorming can be used in:

a) To diagnose problems.
b) Problem solving.
c) Project management.
d) Team building, **Ozmen**, **2006**.

The number of participants with range (6-12), it is good for brainstorming, **Balackova**, **2003**.
The researcher conducted brainstorming session with (8) participants from different sectors and specialties, as shown in **Table 1**.
Brainstorming session consists of two phases, individual and group brainstorming which mixed together in order to diagnose the problem, as follows:

Phase I: The researcher stated the problem in detail and clarity to two groups, each group consisting of (4) persons. They have actual experience not less than (15) years. The participants are from several specialties as shown in **Table 1**. The researcher asked them to record every reason that they believe it may be obstructive to the management of the project execution phase.

Phase II: In the presence of the two groups (8 participants); the study begins with the second phase and it is recalled the problem. Then listened to the reasons offered by the participant No. (1). The reasons are recorded on a large blackboard with a large handwriting and they are clearly seen by everyone. After that, the rest of the participants provide the reasons that they believe it negatively impact on the management of a project. The total reasons that are collected from the first phase are (40). We started the second phase of brainstorming with (40) reason, the process of producing and developing reasons is continued. When the second phase have been finished the study gets (75) reasons. The participants then conduct a review to assess the results that it is obtained. Moreover, the numbers of reasons have been reduced from 75 to 55.

4.2 Interview with Experts

In order to discuss, assess and evaluate the results obtained from the brainstorming session, the researcher conducted interviews with (10) experts who have actual experience not less than (30) years from both public and private sectors, the experts were from various areas of construction projects management, planning, execution, statutory and financial. The experts have been reducing the reasons of mismanagement from 55 to 46, and then added 3 reasons. They believe these (49) reasons have a significant negative impact on the management of the execution phase.

4.3 Questionnaire Design

the questionnaire construction is relied on the reasons that are collected from the techniques of brainstorming and interviews with experts. For the importance and complexity of the research topic and to give a realistic, comprehensive, and strength to the results of the study, the researcher decided to design the questionnaire according to the following steps:

a) Initial questionnaire: after the techniques of brainstorming and interviews with experts have been finished, the researcher classify the reasons that have been collected for, develop hypotheses of the study, and then build the questionnaire in its initial form. The initial questionnaire have been distributes to a small sample of 10 persons, in order to discover weaknesses and ambiguities.
b) Final Questionnaire: After the ten questionnaires are collected and viewing the comments and opinions of the participants, there are some changes to remove the ambiguity and misunderstanding in the formulation of phrases. So, now the questionnaire has been completed in its final form, as details in the paragraph 5.

5. STUDY HYPOTHESES (STUDY PIVOTAL)

The study aims to identify the causes of mismanagement in the execution phase; therefore, to achieve this purpose, the researcher develops three hypotheses as a result of the brainstorming and interviews with experts. Each hypothesis composed of a group of reasons (problems), as follow:

5.1 First Hypothesis (first pivotal): The lack of infrastructure for application of project management leads to mismanagement of the project execution phase. This hypothesis measured with the reasons (1 to 19).

5.2 Second Hypothesis (second pivotal): Lack of awareness of construction companies to the importance of the planning for project management leads to mismanagement of the execution phase. This hypothesis measured with the reasons (20 to 34).

5.3 Third Hypothesis (third pivotal): Lack of awareness of construction companies and employer to the importance of commitment with project management plans, lead to mismanagement of the execution phase. This hypothesis measured with the reasons (35 to 49).

6. QUESTIONNAIRE DISTRIBUTION

The questionnaire forms have been distributed to the target sample which consisting of 90 respondents. The distribution process was in two ways. The first way, the questionnaire distributed directly to the targeted people, where it is offered simple clarifying about the study and its objectives. The method of direct meeting is considered as the ideal way in follow-up the questionnaire and get results conform to reality. This method included 77 respondents, equivalent 88% of the sample size. The second way is indirect meeting with the target people through internet, where we have distributed 13 electronic questionnaire forms, it is also offered simple clarified about the study and its objectives. The number of full forms that we have collected in this way was 10 forms, and only 3 of them do not return. Thus, the study gets 87 complete and correct forms from the total number which is 90; **Table. 2** shows the individual characteristics of the respondents.

7. STATISTICAL ANALYSIS OF THE QUESTIONNAIRE DATA:

Reliability and validity considered as the most important methodology conditions in the design of research tools therefore must be proving the reliability and validity of the questionnaire before conduct the statistical analyses of data**, Jerjaoi**, **2010.**

7.1 Reliability

It is to ensure get almost the same results if re-application the questionnaire more than once on the same group of individuals under similar circumstances**, Jerjaoi**, **2010.**

Reliability coefficient takes values ranging between (0.00) and the (1.00), if there is no reliability in the data it will be equal to (0.00), and on the contrary if data with complete reliability, it will be equal to the (1.00)**, Abdel Fattah**, **2008.**

The appropriate reliability coefficient is (0.7) and more, and high reliability coefficient when it reached (0.8) and more, and is average if ranged between (0.6. and 0.7), and low if it is less than that**, Hassan**, **2006.**

By using SPSS program (version 19), the researcher calculated reliability coefficients of the study were (1^{st} pivotal=0.813, 2^{nd} pivotal =0.796, 3^{rd} pivotal =0.784, and the Reliability coefficient for the study overall =0.919). (Where; 1^{st} pivotal = 1^{st} hypothesis, 2^{nd} pivotal = 2^{nd} hypothesis, and 3^{rd} pivotal = 3^{rd} hypothesis)

7.2 Validity

It is the degree to which a questionnaire reflects reality. The researcher calculates the validity coefficient from calculating the root of reliability coefficient**, Abdel Fattah, 2008.**

Validity coefficients of the study were (1^{st} pivotal =0.902, 2^{nd} pivotal =0.892, 3^{rd} pivotal =0.885, and the Validity coefficient of the study overall =0.959).

Aarbitrators validity is one of the most common and easy methods of validity and the best known among researchers**, Jerjaoi, 2010.**

As it is mentioned earlier, the questionnaire is designed in consulting with ten experts; therefore, we also won the validity of arbitrators

7.3 Test of Normality

Applied researchers should always look at the shape of their data before conducting statistical tests. Looking at data can give you some idea about whether your data are normality distributed, **Larson-Hall, 2010.**

The researcher adopted two tests, Shapiro-wilks and Kolmogorov to test the distribution type of answers is it normal (equinoctial) or not. These tests are necessary to check the study hypotheses, because most of parametric tests require normal distribution for data, **Abu Dakka**, and **Safi**, **2013.**

By using (assume) a significance level ($\alpha = 0.05$), we will test the type of answers distribution of all reasons. In the beginning we assume two hypotheses, the first is the null hypothesis (H0), and the second is the alternative hypothesis (H1). Null hypothesis means that the distribution of the sample answers behaves as normal, accepts this hypothesis if the value of significance (sig. which computed by SPSS program) is greater than (α), and reject if the value of sig. is smaller than (α).

The alternative hypothesis H1 means that the distribution of the answers is random. This hypothesis is accepted if the value of computed sig. is smaller than (α) and it is rejected if the value of computed sig. is greater than value of (α). As it is shown in **Table. 3**, the sig. values are computed for the first four reasons were less than of (α=0.05), therefore, the null hypothesis is rejected and accepts the alternative hypothesis which means that the distribution is random, **Larson-Hall**, **2010.**

The results of normality test for all answers show that the distribution are random.

7.4 Likert Scale

A psychometric response scale mainly used in questionnaires to get participant's preferences or degree of agreement with a statement or group of statements. Ask Respondents to indicate their agreement level with a given statement by using an ordinal scale, **Johns, 2010.**

The design of the questionnaire is based on that the answer of each question is one of five options. So, the likert scale quintet is used. It is usually enter values (weights) as in the **Table. 4. Abdel Fattah, 2008.**

7.5 The Mean

It is the algebraic sum of a set of items divided by their number. It uses with quantitative variables in the case of similar distributions (almost), especially if we take into account all the values, **Larson-Hall**, **2010**.

By using SPSS program (Version 19), the mean of all reasons are calculate, and then compare with the weighted mean to know the trend of answers on each reason, whether it is acceptable or not, or neutral.

7.6 Chi-Square

Chi-square: As it is proved in the paragraph "test of normality", the distributions of respondents' answers were random. Here, non-parametric tests are used, including chi-square. The chi-square test is used to examine the presence of statistically significant differences between answers (approval, neutrality, and disapproval). This test is based on comparison the calculated chi-square against scheduled chi-square at a significance level ($\alpha = 0.05$). It is supposed that:

1) The null hypothesis or (H0) stated: (distribution of the respondents answers are regular, and the differences in those answers can be attributed to chance), this hypothesis is accepted if calculated chi-square is less than scheduled chi-square and it is rejected if calculated chi-square is greater than scheduled one.

2) Alternative hypothesis (H1) stated: (distribution of the respondents answers are irregular), this hypothesis is accepted if the value of calculated chi-square is greater than the value of scheduled chi-square and it is rejects if calculated chi-square is less than a scheduled one**, Bousnina, 2011.**

8. RESULTS

After the statistical operations on the data have finished, it is reached the following results:

8.1 First:

After the statistical analysis on the questionnaire data have been finished, the researcher identified the reasons which have a significant negative impact on the management of project execution phase, which are (26) reasons; below it is mention some of them:

1- Inability of company to meet project requirements because it's specialized and / or large project, with agreement ratio reached (4.68).
2- Inefficient and non- professional supervision committees, with agreement ratio 4.66.
3- Inadequate planning, with agreement ratio 4.62.
4- Relying on manager only to control the project, with agreement ratio 4.53.
5- Unrealistic project plan, with agreement ratio 4.51.
6- Inaccurate estimation of cost, with an agreement ratio 4.48.
7- Poor performance of Project Manager, with agreement ratio 4.39.
8- Delayed cash flows by owners, with agreement ratio 4.37.
9- Poor performance of contractor, with agreement ratio 4.14.
10- Inefficient decision making process, with agreement ratio 3.9.
11- Multiple sources of decision and the overlap in powers, with agreement ratio 3.89.
12- Negative impact of people in the project area, with agreement ratio 3.71.

The agreement ratio on each reason is represent the mean value according to Likert scale quintet. The total (26) reasons which are lead to mismanagement of the execution phase are descendingly arranged according to value of the mean as it is shown in **Table. 5**. All reasons that have been approved by the study have statistically significant differences, since the value of calculated chi is greater than the scheduled chi.

8.2 Second

Prove the hypotheses of the study overall, as follows:

1) Prove the first hypothesis of the study which states that, the lack of infrastructure for application of project management leads to mismanagement of the execution phase, where the ratio of those who agree with this hypothesis reached 54.63%, and the chi calculated (513) greater than chi scheduled (9.488) which indicates the presence of statistically significant difference between answers.

2) Prove the second hypothesis of the study which states that, lack of awareness of construction companies to the importance of planning for project management leads to mismanagement of the execution phase, where the ratio of those who agree with this hypothesis reached 71.34%, and the chi calculated (615) greater than chi scheduled (9.488) which indicates the presence of statistically significant difference between answers.

3) Prove the third hypothesis of the study which states that, lack of awareness of construction companies and employer to the importance of commitment with project management plans leads to mismanagement of the execution phase, where the ratio of those who agree with this hypothesis reached 68.28%, and the chi calculated (553) greater than chi scheduled (9.488) which indicates the presence of statistically significant difference between answers.

9. CONCLUSIONS

The most important conclusions are:

1. The agreement of respondents on hypotheses of the study will imparts realism to the study and its results, (Ranking: 1- 2nd hypothesis, 2- 3rd hypothesis, and 3- 1st hypothesis).

2. The choice of construction project for implementation is subject to improvisational and chaos with a lack of clear criteria in the selection process.

3. The full absence of vocational rehabilitation centers which increases in loss of skilled workers in the construction industry.

4. Most contractors have not any managerial skill.

5. Reliance on personal experience only in full control of the project with full absence of standard tools of performance evaluation.

6. Weakness in the supervision and follow up by employer

7. Inability of company to meet project requirements, because it's specialized and / or large project, is considered as most important factor that leads to mismanagement of the execution phase.

8. The failure of execution management can be considered as the problems that are not borne by one party alone, but due to all parties of the project.

9. Inaccurate estimation of costs is one of mismanagement causes

10. RECOMMENDATIONS

The study presents a group of recommendations which may help to eliminate or reduce the negative impact of the reasons of mismanagement of the project execution phase:

1. Restricted to clauses (2, 11, 14, 15, 42, 44, 47, and 62) of the general conditions for contracts of civil engineering works. because they can help to overcome the reasons of mismanagement.

2. Activating the role of council of reconstruction in provinces and give it wide powers within the terms of reference. It must play a major role to follow the basic design of province and protect it, and to take a consultative role in feasibility studies of the projects and also in prepare their documents.

3. Communicate with competent international bodies is necessary to train the managerial and technical leadership according to international standards.

4. Encourage the site meetings because their necessity for all parties to the project.

5. The construction companies must rely on trained professional staff in the fields of planning and execution, even if the wages are high.

6. The importance of communication between the designers and executants for project's success.

7. Importance of statistical databases of previous projects to the planning process for future projects.

8. Encourage the staff of project, either in the planning or execution and give them reward and incentives to induce them to do work efficiently.

9. Punish those who aggress on public property, (especially in project area).

10. Do not let the contractor who does not fit his financial and technical ability with project to offer the bid for implementation of the work by (list qualified contractors or company selection criteria).

11. Prepare cost estimation depending on WBS, final drawings and direct market surveys.

REFERENCES

- Abdel Fattah, A., 2008, *Introduction to Descriptive and Inferential Statistics by using SPSS.*
- Abu Dakka, S. A., and Safi, S. K., 2013, *Practical Applications by using the (Statistical Packages for Social Sciences) in Educational and Psychological Research.*
- Balackova, H., 2003, *Brainstorming: a creative problem-solving method,* Masaryk Institute of Advanced Studies, Czech Technical University, Prague, Czech Republic.
- Johns, R., 2010, *Likert Items and Scales,* (University of Strathclyde) SQB Methods Fact Sheet 1 (March 2010)
- Bousnina, M. A., 2011, *Study the Delays in Construction Projects Because of the Owner.*

- Dillon, L. B., 2008, *Project Implementation, published on* (http://www.sswm.info/).
- Gould, F. E., 1997, *Managing the Construction Process. Estimating, Scheduling, and Project Control.*
- Hassan, M. A., 2006, *The Psychometric Characteristics of Measurement Tools in Psychological and Educational Research by using SPSS.*
- Heagney, J., 2012, *Fundamentals of Project Management,* Fourth Edition, American Management Association.
- Jerjaoi, Z. A., 2010, *The Educational Methodology Rules for the Construction of the Questionnaire.*
- King, T. D., 2015, *Assessment of Problems Associated with Poor Project Management Performance,* Long International, Inc.
- Larson, E. W., and Gray, C. F., 2011, *Project Management, the managerial process,* fifth edition, by The McGraw-Hill Companies.
- Larson-Hall, J., 2010, *A guide to Doing Statistics in second language using SPSS,* 1st Edition, by Taylor and Francis.
- Lester, A., 2006, *Project Management, planning and control*, fifth edition.
- Martin, P., and Tate, K., 2001, *Getting Started in Project Management,* Published by John Wiley & Sons, Inc.
- Meredith, J. R., and Mantel, S. J., 2000, *Project Management: A Managerial Approach 4/e,* Published by John Wiley & Sons, Inc., Presentation prepared by RTBM Web Group Copyright © 2000.
- Ozmen, H., 2006, *Brainstorming, www.brainstorming.co.uk/extra/productservices.html.*
- Pinto, J. K., and Slevin, D. P., 1987, *Critical Success Factors in Effective Project Implementation.*
- PMBOK, 2013, *A Guide to the Project Management Body of Knowledge*.
- Portny, S. E., 2010, *Project Management for Dummies,* 3rd Edition.
- Rad, P. F., 2002, *Project Estimating and Cost Management.*
- Richman, L., 2011, *Successful Project Management,* Third Edition.
- Sears, S. K., Sears, G. A., and Clough, R. H., 2008, *Construction Project Management. A Practical Guide to Field Construction Management.*

NOMENCLATURE

α = significance level (Probability of error), takes values (0.05, 0.01, and 0.000).

df = degree of freedom. It is the number of changeable values in the calculation of the statistical property.

Table 1. The characteristics of participants in brainstorming, (researcher).

Sector	Specializations					
	Management	Planning	Executant	Supervisor	Statutory	Financial
Public Sector	1	1	1	1	1	1
Private Sector	1		1			
University Degree		Number	Actual service		Number	
BSc		6	15-20		5	
MSc		2	21-25		2	
			More than 25		1	

Table 2. The characteristics of questionnaire respondents, (researcher).

Variables	Categories	Number	Ratio
Academic degree	PhD	7	8.04%
	MSc	12	13.80%
	BSc	68	78.16%
Type of work	Civil	58	66.67%
	Electricity	11	12.64%
	Architect	8	9.19%
	Mechanical	6	6.90%
	Oil	3	3.45%
	Chemical	1	1.15%
Experience (year)	15-20	25	28.73%
	21-24	17	19.54
	25-29	24	27.59
	30 & more	21	24.14
Gender	Male	73	83.91%
	Female	14	16.09%
Sector	Public	64	73.6%
	Private	23	26.4%

Table 3. Test of normality, (researcher).

Items	Kolmogorov-Smirnov			Shapiro-Wilk		
	Statistic	df	Sig.	Statistic	df	Sig.
First	.236	87	0.000	.866	87	0.000
Second	.259	87	0.000	.834	87	0.000
Third	.208	87	0.000	.857	87	0.000
Fourth	.267	87	0.000	.883	87	0.000

Table 4. Likert scale quintet weights, **Abdel Fattah, 2008**.

opinion	weight	Weighted Mean
Completely disagree	1	1-1.8
Disagree	2	1.81-2.60
Neutral	3	2.61-3.40
agree	4	3.41-4.20
Completely agree	5	4.21-5.00

Table 5. The reasons of mismanagement and their mean, (researcher).

Rank	Factor cause execution phase mismanagement	Mean
1	Inability of company to meet project requirements, because it's specialized and / or large project	4.68
2	Inefficient and non- professional supervision committees	4.66
3	Inadequate planning	4.62
4	Relying on manager only to control the project	4.53
5	Unrealistic project plan	4.51
6	Inaccurate estimation of cost	4.48
7	Lack of control to time of the project or predict the date of its end	4.45
8	Lack of funds for archiving, investigations, and data collection	4.41
9	Poor performance of project managers	4.39
10	Neglect the role of supervisors in the planning process	4.37
11	Delayed cash flows by owners	4.37
12	Inefficient executive manager of project	4.32
13	Non-completion of the plan in exact time	4.31
14	Lack of experience in creating and preparing project documents	4.29
15	Lack of funds for training and continuous development	4.28
16	Absence of an organizational structure for the company	4.25
17	Poor performance of the contractor	4.14
18	Randomness and lack of vision in the selection of projects	4.11

19	Bureaucracy in bidding / tendering method	4.05
20	Inappropriate contractual procedures of subcontracting	3.98
21	Time period of the execution	3.95
22	Inability of using measures of performance evaluation	3.91
23	Inefficient decision making process.	3.9
24	Multiple sources of decision and overlap in powers	3.89
25	The negative impact of people in the project area	3.71
26	Random and individual work	3.53

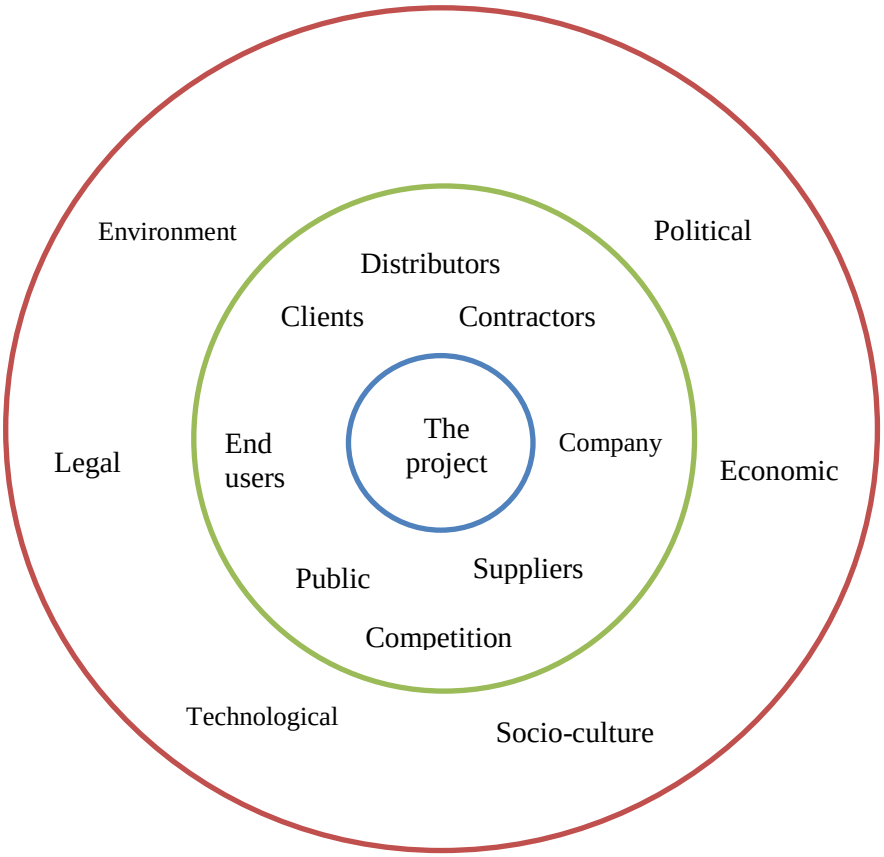

Figure 1. Project context (environment). **Lester, 2006**

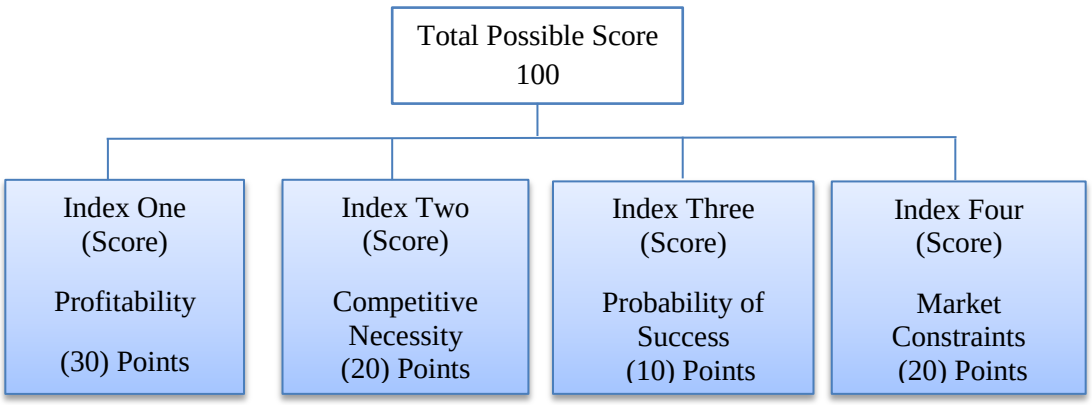

Figure 2. 100 Points project scoring system-maximum points possible (project selection model). **Rad, 2002.**

Application of Building Information Modeling (3D and 4D) in Construction Sector in Iraq

Kadhim Raheem Erzaij
Assistant Professor
Collage of Engineering-University Of Baghdad
E-mail: kadhim1969@yahoo.com

Ayad Abbas Obaid
MSc student
Collage of Engineering-University Of Baghdad
E-mail:eng.ayad89@gmail.com

ABSTRACT

Building Information Modeling (BIM) is becoming a great known established collaboration process in Architecture, Engineering, and Construction (AEC) industry. In various cases in many countries, potential benefits and competitive advantages have been reported. However, despite the potentials and benefits of BIM technologies, it is not applied in the construction sector in Iraq just like many other countries of the world.

The purpose of this research is to understand the uses and benefits of BIM for construction projects in Iraq. This purpose has been done by establishing a framework to application of BIM and identifying the benefits of this technology that would convince stakeholders for adopting BIM in the construction sector in Iraq.

Through this research, the use of this technology has been clarified by using the proposed framework (application Revit software and linking it with the MS Project and Navisworks Manage software on the case study) to identify the important benefits to be the beginning to apply the Building Information Modeling technology in the construction sector in Iraq.

The research results indicated that such proposed framework can greatly improve the performance of the current state of project management through improving the project quality, cost saving and time-saving.

Keywords: Building information modeling, Architectural Engineering and Construction (AEC) industry, BIM knowledge, BIM benefits, The construction sector in Iraq.

تطبيق نمذجة معلومات البناء (3D و4D) في قطاع الانشاء في العراق

د. كاظم رحيم ارزيج
استاذ مساعد
كلية الهندسة-جامعة بغداد

اياد عباس عبيد
طالب ماجستير
كلية الهندسة-جامعة بغداد

الخلاصة

أصبحت نمذجة معلومات البناء (BIM) وسيلة تعاون بين أعضاء الفريق الهندسي في صناعة التصميم وتشييد البناء (AEC) في عدة بلدان، وتم معرفة الفوائد المحتملة والمزايا التنافسية. ومع ذلك وعلى الرغم من إمكانيات وفوائد تكنولوجيا نمذجة معلومات البناء، لا يتم تطبيقها في قطاع البناء والتشييد في العراق مثل العديد من البلدان الأخرى.

ان الغرض من هذا البحث هو فهم استخدامات وفوائد نمذجة معلومات البناء للمشاريع الانشائية في العراق، وقد تم ذلك الغرض من خلال انشاء إطار عمل لتطبيق نمذجة معلومات البناء والتعرف على فوائد هذه التكنولوجيا التي من شانها ان تقنع أصحاب المصلحة من اجل اعتماد نمذجة معلومات البناء في قطاع البناء والتشييد في العراق.

وقد تم توضيح استخدام هذه التكنولوجيا (بتطبيق برنامج (Revit) على حالة دراسية لتكوين نموذج ثلاثي الابعاد وربطه مع الجدول الزمني المتولد من (MS Project) في برنامج (Navisworks Manage). للتعرف على الفوائد المهمة لتكون بداية لتطبيق تكنولوجيا نمذجة معلومات البناء في قطاع البناء والتشييد في العراق.

وأشارت نتائج البحث ان إطار العمل المقترح يمكن ان يحسن كثيرا من أداء الوضع الحالي لإدارة المشروع من خلال تحسين نوعية المشروع، توفير الوقت والتكاليف.

1. INTRODUCTION

1.1 General

The benefits of Building Information Modeling (BIM) are being realized by construction firms around the world. However, in Iraq it is not applied until now. The Researcher will explore how the engineers in construction sector can take advantage of the benefits that BIM allows. BIM is more than just a process; it paves the way to a new form of project procurement and delivery. To realize the full potential of BIM and work with the models in the most productive way it needs to have the correct tools and knowledge.

BIM is a technological system to conveying and storing information for the buildings, with an ability to visually display buildings parts in a 3-D view. The 3-D capability is enhanced by the parametric modeling engine, which automatically interrelates building objects to other objects and coordinates changes and revisions across the project deliverables, Rundell **and Stowe, 2005.** For instance, a change to the length of a wall in a building drawing is automatically reflected in the walls that connect to it. The idea is that the BIM produces a faster, cheaper, more accurate, and better-coordinated project experience during design, construction, and future use. With the growth of information technologies in the field of construction industry over the last years, numerical building information modeling and process simulation has evolved to a fully accepted and widely used tool for the project life circle management. Building information is present through the whole life cycle of the engineering and construction phases. Due to the long time and the numerous contractors, the phenomena of mass information and information attenuation occur throughout the life cycle. The traditional methods of information exchange cannot meet the mass information processing requirements of modern large-scale construction projects, **Ding, L. and X. Xu, 2014.**

1.2 Definitions

Due to the different perceptions, overview and experiences of researchers and professionals in the AEC industry, they can define BIM in different ways **Khosrowshahi and Arayici, 2012**. For example, **Gu and London, 2010** said that BIM is an information technology (IT) enabled approach that involves applying and maintaining an integral digital representation of all building information for different phases of the project lifecycle in the form of a data repository. On the other hand, **Eastman et al., 2008** emphasized that BIM is not only a tool, but also a process that allows project team members to have an unprecedented ability to collaborate over the course of a project, from early design to occupancy. **Stebbins, 2009** agreed that BIM is a process rather than a piece of software. He clearly identified BIM as a business and management decision. BIM implementation is strongly related to managerial aspects of professional practices for different working styles and cultures, **Ahmad et al., 2012**. BIM has a broad range of applications cross the design; construction; and operation process ,**Baldwin, 2012**. BIM is important to develop the design process by managing the changes in the design. It is efficient in checking and updating all the views (plans, sections and elevations) when any changes occur, **CRC construction innovation, 2007**. BIM is a new way of approaching the design and documentation of building projects.

1.3 Objective

The aim of this research is to develop a clear understanding about BIM for identifying the different factors that provide useful information to consider adopting BIM technology in projects by practitioners in the construction sector in Iraq. In achieving this aim, two main objectives have been outlined as follows:

A. To identify the BIM system.

B. To identify the top BIM benefits that would convince professionals for adopting BIM in the construction sector in Iraq.

2. UNDERSTANDING OF BIM CONCEPT

BIM has been in use internationally for several years, and its use continues to grow. It is one of the most promising developments in the Architecture, Engineering, Construction (AEC) industry and it has the potential to become the information backbone of a whole new AEC industry **Stanley and Thurnell, 2014**. BIM is continuously developing as a concept because the boundaries of its capabilities continue to expand as technological advances are made, **Joannides et al., 2012**. BIM is now considered the ultimate in project delivery within the AEC industry. It is motivating an extraordinary shift in the way the construction industry functions. This fundamental change involves using digital modeling software to more effectively design, build and manage projects, **Azhar et al., 2008**.

3. TYPES OF BIM

Many new terms, concepts and BIM applications have been developed such as 4D; 5D; six-dimensional (6D); and seven-dimensional (7D). The (D) in the term of 3D BIM means "dimensional" and it has many different purposes for the construction industry. **Wang, 2011** explained BIM types as the following:

- 3D: three-dimensional means the height, length and width.
- 4D: 3D plus time for construction planning and project scheduling.
- 5D: 4D plus cost estimation.

Recent advances in BIM have disseminated the utilization of multidimensional nD CAD information in the construction industry. In addition to the parametric properties of 3D BIM, the technology also has 4D and 5D capabilities. Recent advancements in software have allowed contractors to add the parameters of cost and scheduling to models to facilitate value engineering studies; estimating and quantity take offs; and even simulate project phasing.

4. DIFFERENCES BETWEEN BIM AND CAD

The differences between BIM and computer-aided design (CAD) is that a traditional CAD system uses many separate (usually 2D) documents to explain a building. CAD output is essentially a collection of lines, numbers and text on a page. Because CAD documents are created separately, there is little to no correlation or intelligent connection among them. For example, a door is represented as a line or a curve, without a detailed understanding of its basic attributes and without any inherent understanding. A wall in a plan view is represented by two parallel lines, with no understanding that those lines which represent the same wall in a section. The possibility of uncoordinated data in a CAD based work environment is very high, **Eastman et al., 2008.**

BIM takes a different approach in comparison with CAD. The BIM model serves as a central database, by collecting all information into one location and cross-linking that data among associated objects, **Azhar et al., 2008**.

All documents within the BIM model are interdependent and share intelligence. A change anywhere in the BIM model is propagated throughout all relevant views and documents for the project. The BIM application has an intelligent understanding of the fact that objects created by users represent real-world components of building such as windows, walls, doors and roofs. Thus, BIM objects have characteristics similar to their real-world counterparts such as windows, which can only exist in a wall, and walls always have a thickness attribute. Use of such intelligent objects distinguishes the geometry created by BIM from a 3D model, **Joannides et al., 2012.**

5. AWARENESS LEVEL OF BIM

There is a pressing demand for improved awareness and understanding of BIM across the AEC industry, according to many studies related to BIM. Lack of knowledge regarding BIM has led to a slow uptake of this technology and ineffective management of adoption, **Mitchell and Lambert, 2013**.

In general, many studies, such as **Arayici et al., 2009**, **Khosrowshahi and Arayici 2012** and **Elmualim and Gilder, 2013** who concluded that there are a lack in the awareness of BIM and its benefits in the field of construction industry as well as the business value of BIM from a financial perspective. More precisely, there is a large lack in understanding of BIM (the core concepts of BIM) and its practical applications throughout the life of projects. In addition, there is a lack in technical skills that professionals need to have for using the BIM software as well as lack in knowledge of how to implement the BIM software to be helpful in construction processes, **Azhar et al., 2008.**

6. DEVELOPMENT AND IMPLEMENTATION OF THE BIM MODEL

The researcher selected a case study to describe the results obtained from using the software's. The case study chosen is State Company for Industrial Design and Implementation (SCIDC)/ Ministry of Industry and Minerals because the researcher has cooperation contract with this organization and because of the ability to access data necessary.

This section will illustrate the benefits of BIM tools for construction projects through applying these tools on a project completed by using AutoCAD software. The project sample is the project named "Administration Building for the industrial compound at Dhi-Qar" province in southern Iraq, which is one of many projects the State Company for Industrial Design and Implementation executes over the country (Iraq), and it was completed by the company in November (2012). The total area of the building is 1840 m^2 with (11 m) height.

6.1 The proposed framework to Create BIM model (3D and 4D)

The proposed framework to create 3-D and 4-D by using BIM tools can be described as shown in **Fig.1**

6.2 Evaluation of the proposed framework

The researcher gave a training course about the application of Building Information Modeling by taking the administration building of industrial complex in Dhi-Qar

province in southern Iraq as a case study to evaluate the proposed framework. Participated in this course 31 engineers with different managerial positions and experiences belonging to State Company for Industrial Design and Implementation from the various disciplines. The aim of the training course is to evaluate the efficiency of the BIM technology through its impact on quality, cost and time of the project. After the end of the training course was evaluated the benefits of BIM system by engineers through the questions set. **Figure 2** and **Fig.3** show the engineering fields and years of experience respectively.

As for the result, the researcher has concluded by using simple statistics for each item of evaluation form that are distributed after interviewing to get the most important results as shown in **Table 1** the percentage regarding evaluating BIM system as shown in **Table 2**.

According to the analysis and results of the evaluation which are presented in the researcher's conclusions that the use of the BIM system is high useful for engineers in the construction sector and will help them to make their mission easier, faster and more accurate.

7. CONCLUSIONS

The extensive review of the literature was conducted to achieve the object of the study. The object of this study was to improve a clear understanding about Building Information Modeling system for finding the different factors that provide suitable information to consider utilizing BIM tools in projects by a stockholder in the construction sector in Iraq. The research leads to the following conclusions:

1. The study shows that the awareness level of BIM system is low and not satisfactory. This is because of many reasons, for instance:
   a. The lack of education for Building Information Modeling and programs to implement it in universities and organizations.
   b. The lack of adequate training for the application of the Building Information Modeling in the construction projects.
   c. The lack of demand for this system by the customer or the government.
   d. The lack of publicity and awareness for this system.
   e. Lack of clarity of the benefits of BIM system.
   f. The cost of staff training for BIM system.
   g. The lack of standards and clear guidelines for the application of this system.
2. It is required to improve the knowledge level of engineers with respect to BIM software.
3. According to the study, the proposed framework can improve and develop the performance of project management through the many solutions, benefits and features the proposed framework provides, for instance:
   a. Achieving integration, cooperation, and communication between the work teams.
   b. Submission designs without error.
   c. Improving productivity of the work.
   d. Improving the quality of the work.
   e. Improving information of security management.
   f. Facilitating the preparation and management of documents and consolidated.
   g. Reducing the risks for the project.
   h. Generating drawings and construction details with high accuracy.

i. Improving communication between different parties of the project.
j. Improving accounts of the necessary quantities of materials.
k. Cost savings.
l. Reducing waste of materials.
m. Reducing change orders.
n. Reducing the need to re-work of the design.
o. Time saving.
p. Improving logistics.
q. Early involvement of the owner to make quick decisions.
r. The arrangement of needs for off-site prefabrication.

4. Adopting such system does not mean moving completely and immediately from the current state to the new state, but the process should happen gradually to ensure integrating the system with the operations and procedures in the organizations and projects and in order for the employees and project members to be familiar with the new system.
5. The information that is extracted from Revit software requires skill in the management and understanding of databases for the program, optimum management for databases within the program Revit to fit with any other project, all information entered to configure the model in BIM Revit is available for use in Navis work manage.

8. RECOMMENDATIONS

Based on the achieved purposes of this study as stated earlier, the recommendations below were drawn as a result of the research findings. The recommendations are as follow:

1. Education And Training To Increase BIM Awareness And Interest

a. The use of BIM system should be encouraged through educational and training courses to get the precision and clarity, speed and a high standard in the construction industry and to implement the terms of the sustainability of access to green building.
b. Academic institutions and universities must take the lead to highlight new ways to engage BIM in the construction industry.
c. Improving and developing the cooperation, coordination, and interaction between the construction organizations and scientific and research organizations largely.

2. Government support to apply this system

The government agencies must take progressive steps to apply BIM in the construction sector in Iraq such as:

a. Through developing a guide to BIM that will be a reference for all parties involved in the construction sector in Iraq.
b. Providing legal benchmarks for business improvement, where the absence of standard BIM contract documents is preventing people from adopting and utilizing BIM with security in the construction sector.
c. Supporting and developing incentives and rewards systems.
d. Supporting and developing incentives and rewards systems for the effective employee.

REFERENCES

- Ahmad A. M, Demian P and Price A.D.F, 2012, *BIM implementation plans: A comparative analysis In: Smith, S.D (Ed) Procs 28th Annual ARCOM Conference, 3-5 September 2012*, Edinburgh, UK, Association of Researchers in Construction Management, 33-42.
- Arayici, Y., Khosrowshahi, F., Ponting, A. M., and Mihindu, S., 2009, *Towards implementation of building information modelling in the construction industry*, Proceedings of the Fifth International Conference on Construction in the 21st Century "collaboration and integration in Engineering, Management and Technology". Istanbul, Turkey: Middle East Technical University and Florida International University, PP. 1342-1351.

- Azhar, S., M. Hein, and B. Sketo, 2008, *Building Information Modeling (BIM): Benefits*, Risks and Challenges. McWhorter School of Building Science. Auburn University. Auburn. Alabama, AL.

- Baldwin, M., 2012, *BIM implementation & execution plans, BIM Journal*, Vol. 3, No. 35, PP. 73-76.

- CRC for Construction Innovation, 2007, *Adopting bim for facilities management: solutions for managing the Sydney opera house*, Brisbane, Australia: Cooperative Research Centre for Construction Innovation, Icon.Net Pty Ltd.

- Ding, L. and X. Xu, 2014, *Application of Cloud Storage on BIM Life-cycle Management*, International Journal of Advanced Robotics Systems, 11, PP. 129.

- Eastman, C., Teicholz, P., Sacks, R., and Liston, K., 2008, *BIM handbook " a guide to building information modeling for owners, managers*, designers, engineers, and contractors". Hoboken, New Jersey: John Wiley & Sons, Inc.

- Elmualim, A., and Gilder, J., 2013, *BIM: innovation in design management, influence and challenges of implementation*. Architectural Engineering and Design Management, Vol. 10, No. 1080, PP. 1745-2007.

- Gu, N. and K. London, 2010, *Understanding and facilitating BIM adoption in the AEC industry, Automation in construction*, Vol. 19, No. 8, PP. 988-999.

- Joannides, M. M., Olbina, S., and Issa, R. R., 2012, *Implementation of building information modeling into accredited programs in architecture and construction education*, International Journal of Construction Education and Research, Vol. 8, No. 2, PP. 83-100.

- Khosrowshahi, F. and Y. Arayici, 2012, *Roadmap for implementation of BIM in the UK construction industry. Engineering*, Construction and Architectural Management, Vol. 19, No.6, PP. 610-635.

- Mitchell, D., and Lambert, S., 2013, *BIM: rules of engagement. CIB World Building Congress (Cib Bc13)*, Brisbane, Australia: Cibwbc, PP. 1-5.

- Rundell, R. and Stowe, K., 2005, *Building Information Modeling and Integrated Project Delivery-Design-Build Synergy in Action*, Design-Build Dateline, June 2005: 20-23.

- Stanley , R., & Thurnell, D., 2014, *The benefits of, and barriers to, implementation of 5d BIM for quantity surveying in new Zealand*, Australasian Journal of Construction Economics and Building, Vol. 14, No. 1, PP. 105-117.

- Stebbins. J, 2009, *Successful BIM Implementation: Transition from 2D to 3D BIM*, "Digital Vision Automation".
- Wang, M. 2011. *Building information modeling (BIM): site-building interoperability methods. MSc Thesis*, Interdisciplinary Construction Project Management, Faculty of the Worcester Polytechnic Institute, U.S.A.

List of abbreviations

Abbreviation	*The interpretation of the abbreviation*
BIM =	building Information Modeling
AEC =	architecture, Engineering, and Construction
MEP =	mechanical, Electrical and Plumbing
OM =	operation and Maintenance
D =	dimensional
2D =	two dimensions: x, y
3D =	three-dimensional: x, y, z (the height, length and width)
4D =	four-dimensional; 3D model connected to a time line
5D =	five-dimensional; 4D model connected to cost estimations
6D =	six-dimensional; 6D model which is 5D plus site
7D =	seven-dimensional; 7D model: BIM for life cycle facility management
nD =	a term that covers any other information
CAD =	computer Aided Design

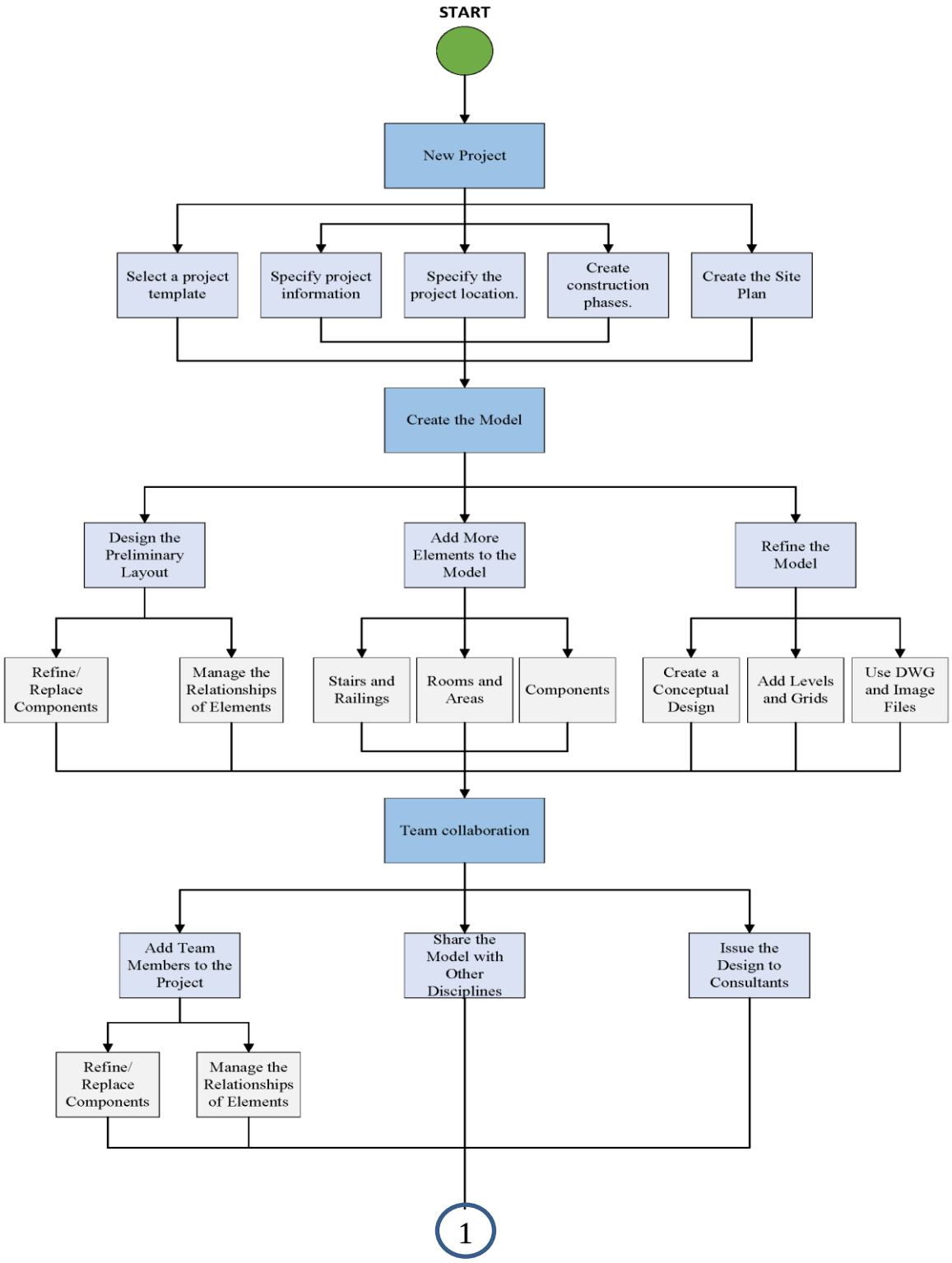

Figure 1. Flowchart of The proposed framework (by researcher).

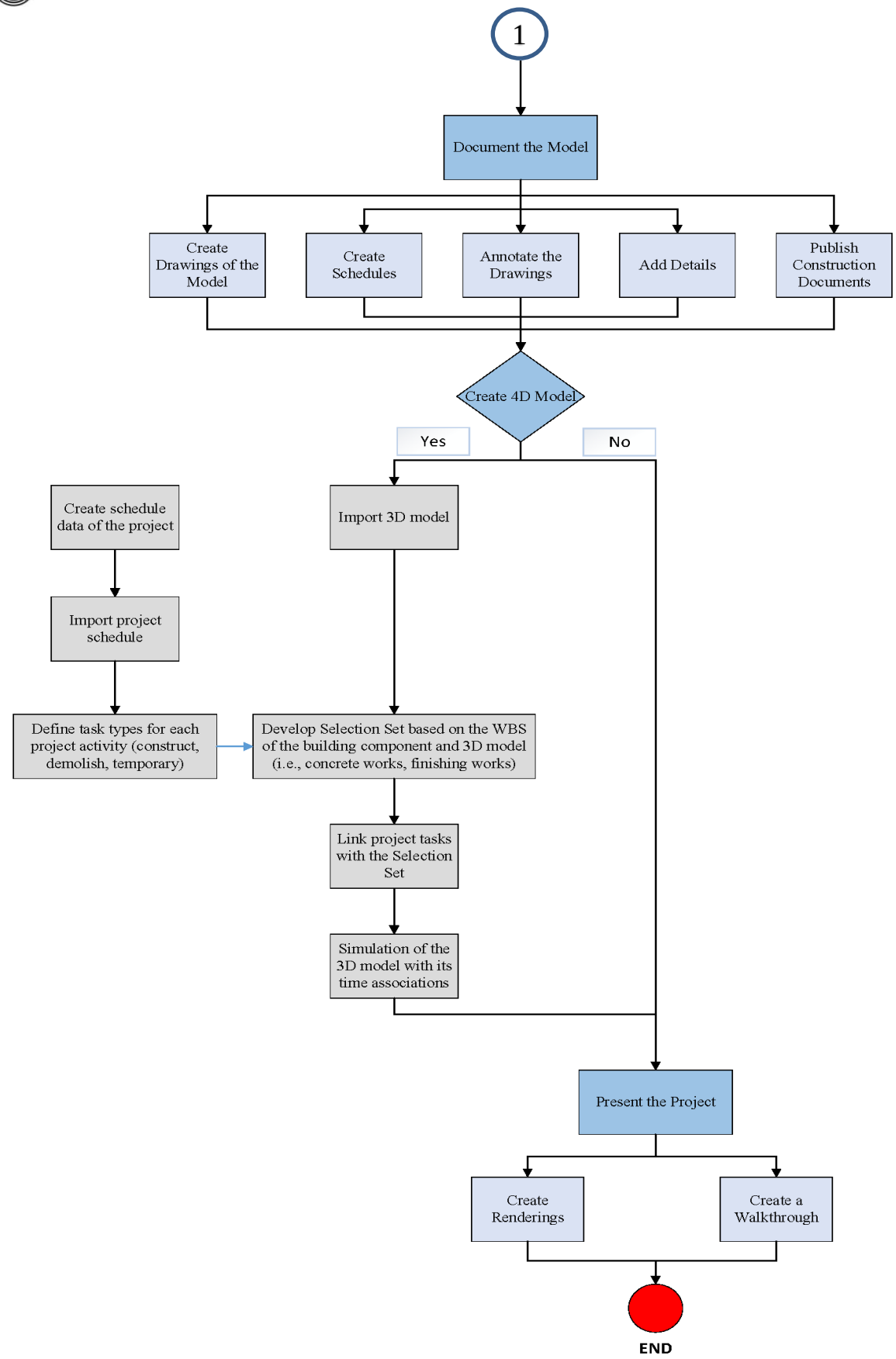

Figure 2. Continued.

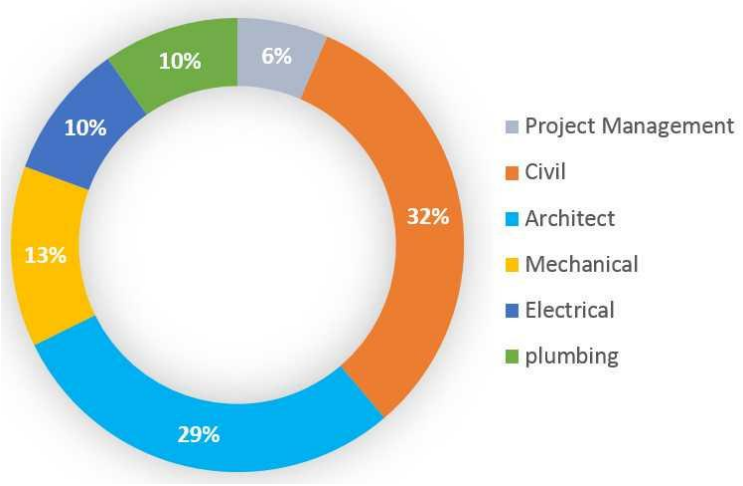

Figure 3. Engineering Fields**.**

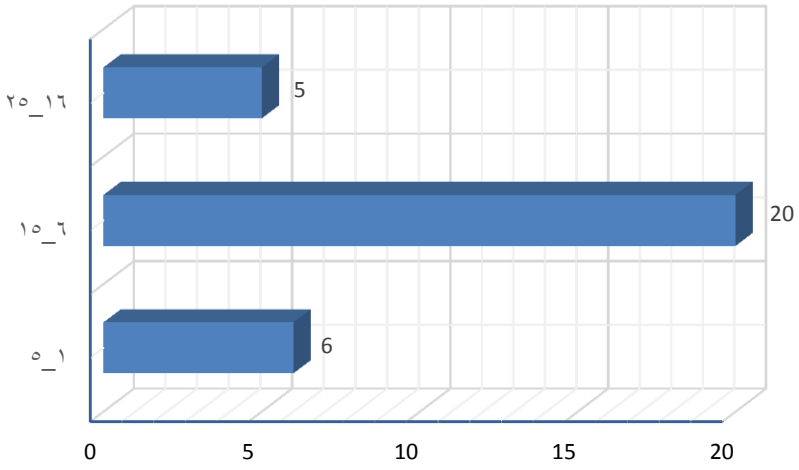

Figure 4. Years of experience**.**

Table 1. The answers regarding evaluating BIM system**.**

Firstly	Impact on project quality	Excellent	Very Good	Good	Medium	Acceptable
1	Achieve Integration and cooperation and communication between the work teams	20	8	3	0	0
2	Submission designs without error	21	7	3	0	0
3	Improve productivity of the work	20	9	2	0	0
4	Improve the quality of the work	21	7	3	0	0
5	Improving information security management	25	4	2	0	0

6	Facilitate the Preparation and management of documents and consolidated	24	6	1	0	0
7	Reduce the risks for the project	22	7	2	0	0
8	Generate drawings and construction details with high accuracy	23	7	1	0	0
9	Improve communication between different parties of the project	23	6	2	0	0
Secondly	Impact on project cost	Excellent	Very Good	Good	Medium	Acceptable
1	Improve accounts of the necessary quantities of materials	18	10	3	0	0
2	Cost savings	22	8	1	0	0
3	Reduce waste of materials	18	12	1	0	0
4	Reduce change orders	23	8	0	0	0
Thirdly	Impact on project time	Excellent	Very Good	Good	Medium	Acceptable
1	Reduce the need to re-work of the design	23	8	0	0	0
2	time saving	25	5	1	0	0
3	Improving logistics	13	12	6	0	0
4	Early involvement of the owner to make quick decisions	22	9	0	0	0
5	the arrangement of needs for off-site prefabrication	17	11	3	0	0

Table 2. The answers percentage regarding evaluating BIM system.

Firstly	Impact on project quality	Excellent	Very Good	Good	Medium	Acceptable
1	Achieve Integration and cooperation and communication between the work teams	64.5%	25.8%	9.7%	0	0
2	Submission designs without error	67.7%	22.6%	9.7%	0	0
3	Improve productivity of the work	64.5%	29%	6.5%	0	0
4	Improve the quality of the work	67.7%	22.6%	9.7%	0	0
5	Improving information security management	80.6%	12.9%	6.5%	0	0
6	Facilitate the Preparation and management of documents and consolidated	77.4%	19.4%	3.2%	0	0
7	Reduce the risks for the project	71%	22.6%	6.5%	0	0
8	Generate drawings and construction details with high accuracy	74.2%	22.6%	3.2%	0	0
9	Improve communication between different parties of the project	74.2%	19.4%	6.5%	0	0
Secondly	Impact on project cost	Excellent	Very Good	Good	Medium	Acceptable
1	Improve accounts of the necessary quantities of materials	58.1%	32.3%	9.7%	0	0

2	Cost savings	71%	25.8%	3.2%	0	0
3	Reduce waste of materials	58.1%	38.7%	3.2%	0	0
4	Reduce change orders	74.2%	25.8%	0	0	0
Thirdly	Impact on project time	Excellent	Very Good	Good	Medium	Acceptable
1	Reduce the need to re-work of the design	74.2%	25.8%	0	0	0
2	time saving	80.9%	16.1%	3.2%	0	0
3	Improving logistics	41.9%	38.7%	19.4%	0	0
4	Early involvement of the owner to make quick decisions	71%	29%	0	0	0
5	the arrangement of needs for off-site prefabrication	54.8%	35.5%	9.7%	0	0

Improvement of Gypseous Soil Using Cutback Asphalt

Zainab Hassan Shakir
Assistant Lecturer
Building and Construction Engineering Department, University of Technology/ Baghdad
Zainab.h46@yahoo.com

ABSTRACT

Gypseous soils are widely distributed and especially in Iraq where arid area of hot climatic is present. These soils are considered as problematic soils; therefore this work attends to improve the geotechnical properties of such soil and reduce the dangers of collapse due to wetting process. In this research, undisturbed soil sample of 30 % gypsum content from Karbala city is used. The Single Oedometer collapse test is used in order to investigate the collapse characteristics of natural soil and after treatment with 3%, 6%, 9%, 12% and 15% of Cutback Asphalt. Moreover, two selected additive percentages (9% and 12%) are used to evaluate the suitability of using the Cutback Asphalt for improvement of the bearing capacity of gypseous soils. A steel model box is used for this purpose, the treatment depth is equal to one and twice the footing width. The tests results showed that the total settlement of 25 mm of treated soil with (MC-30) material can be achieved at vertical stress lower than that value required for natural soil. Also, thickness of treated layer with (MC-30) material below the proposed foundation has a significant effect on the value of bearing capacity of the soil. The rate of salt dissolved (C.V) is extremely decreased especially at all percentages of Cutback Asphalt. The best bearing improvement ratio is found at 9% asphalt and at a depth equal to foundation width. However, the Cutback Asphalt can be successfully used by 12% for collapse potential treatment while it is not suitable for improvement of the bearing capacity of gypseous soils.

Key words: gypsum soil, cutback asphalt, collapse potential.

تثبيت التربة الجبسية بأستخدام الاسفلت السائل

زينب حسن شاكر
مدرس مساعد
قسم هندسة ألبناء وألانشاءات،ألجامعه ألتكنولوجيه/ بغداد

ألخلاصه

تنتشر الترب الجبسية بمناطق محددة من العالم بشكل عام وبالعراق على وجه الخصوص حيث تتواجد المناطق القاحلة ذات المناخ الحار.

تعتبر هذه الترب من الترب ذات المشاكل الهندسية الانهيارية لذلك يهدف هذا البحث الى محاولة تحسين خصائص هذه التربة وتقليل خطر الانهيار عند تعرضها للترطيب .

في هذا البحث تم استخدام نموذج التربة من محافظة كربلاء بنسبه جبس30% وتم التحري عن الطاقة الانهيارية للتربة باستخدام فحص الاودوميتر المفرد .

الدراسة اقترحت معالجة مشكلة الانهيار في هذه التربة باستخدام مادة (Cutback Asphalt) (MC-30) بنسبة 3%,6%,9%,12%,15% وباعماق مساوية لعرض الاساس وضعف عرض الاساس .نتائج المعالجة بينت تصنيف الترب الجبسية بانها تربة ذات مشكلة هندسية من النوع الخطر بسبب ارتفاع قيمة طاقة الانهيار الى 10%. أوضحت النتائج انه يمكن استخدام ماده الاسفلت نوع (MC-30) بنجاح في تحسين خصائص الانهيار للترب الجبسية ولغاية محتوى امثل للاسفلت في التربة وبنسبة 12% . بناء على ذلك فانه تنخفض قابلية التحمل للتربة الجبسية بزيادة نسبه الاسفلت المضاف بصورة تدريجية . لقد اظهرت نتائج الفحص ان التربة المعالجة بمادة الاسفلت (MC-30) تصل الى الهبوط الكلي البالغ 25 mm تحت اجهاد عمودي اقل من قيمة الاجهاد العمودي المطلوب للحصول على نفس مقدار الهبوط للتربة الطبيعية . كما ان سمك الطبقة المعالجة بماده الاسفلت (MC-30) تحت الاساس لها تاثير كبير على مقدار قابلية التحمل للترب الجبسية .ان معدل ذوبان

الاملاح ينخفض كثيرا بصورة خاصة عند زيادة نسبة الاسفلت المضاف. من خلال دراسة النتائج وجد ان احسن نسبة لتحسين في قابلية التحمل هي 9%من مادة الاسفلت عل عمق مساوي الى عرض الاساس. بينت نتائج الفحوص ايضا بأن مادة الاسفلت نجحت بشكل كبير في تحسين خصائص الانهيار لكنها غير ملائمة لتحسين قابلية التحمل للترب الجبسية.

1. INTRODUCTION

Gypseous soils are of the most complex materials that challenge the geotechnical engineers. It is a well-known fact that gypseous soils demonstrate high bearing capacity and very low compressibility when they are in the dry state. Conversely sudden collapsible disposal was reported when the gypseous soils are exposed to water. The collapsibility of gypseous soils scores from the direct contact of water. The rate of dissolution of gypsum depends primarily on environmental changes in moisture content generating from fluctuation of ground water table and/or surface water, permeability and state of flow conditions in addition to the type and content of gypsum**, Al-Saoudi et.al, 2013.** The dissolution of gypsum particles within the soil mass due to wetting can cause many problems to the engineering structures and road network the structure of gypseous soil can be transformed from stable condition to unstable when undergo to increase in moisture content. The gypseous soil is defined as soil that contains sufficient quantities of gypsum (calcium sulphate)**, FAO, 1990.** This soil is commonly formed at dry state particularly due to the cementation of the soil particles by gypsum, but the issue turnoff intricate when the water flow through the gypseous soils causing nominate and reasonable collapse behavior in the soil structure. Many studies have been conducted on gypseous soils in Iraq because they are covering a wide area of nearly 31.7% of the surface sediments of Iraq with gypsum content ranging between 10-70%**, Ismail, 1994,** and are 0.6% of the world**, Alphen and Romero, 1971.** Gypsiferous soils have been studied in the past within the classical framework of soil mechanics that is related to saturated condition. As such, they are characterized as collapsible, problematic soils that suffer large settlement and have significant loss of strength under long term of flooding**, Khalid, 2013.** When salt firmness soils are undergoing softening due to raising in moisture content can cause degeneration of same gypsum. Practically softening can occur in various ways like local shallow wetting, deep local wetting. Many problems have been notified on damages happened to structures supported on gypseous soils like cracks, overturning of structures. These problems are very dangerous, thus improvement of gypseous soils are urgently necessary. On the other hand, asphalt material can be used as improvement material for the problematic soils where the main function of asphalt is to reduce the effect of water on gypsum particles and to increase the strength parameters of the soil**, Al-Obaydi et.al, 2007.** In Iraq, asphalt is a cheap and available material; it can be easily used to improve the properties of gypseous soil. Many forms of asphalt are available such as asphaltic bitumen, tars, Cutback Asphalt and emulsion asphalt or bitumen can be added to the base soil of roads, Kadhim**, 2014.**

The Cutback Asphalt is most common and economical type of asphaltic materials used for soil stabilization especially medium-curing types where it's produced from the refineries**, Transport and Road Research Laboratory, 1987**. Moreover, **Jasim, 2015** assessed the durability of asphalt stabilized gypseous soil by using emulsion asphalt. It was stated that after exposing the specimens to cycles of (heating – cooling), the undrained shear strength increased up to 10 cycles then decreased with further increased number of cycles. The dissolution of gypsum due to

distillation, irrigation and hail water or from other provenance is a risky case in gypseous soil age. This process will command to on undue and sometimes tragic settlement. Shear strength of soil will minimize as a result of this process. The safety and good execution of the foundation of structures particularly in hydraulic structures and earth structure like embankments and dams will be administered by the changes in the properties of these soils.

2. PREVIOUS EXPERIENCES

The behavior of gypseous soils and its improvements attempts were carried out by many research works which can be outlined as follows:

Al-Rawi, 1971 suggested that both cutback and emulsion asphalt could be used to stabilize Iraqi soils.

Epps et.al, 1971 studied the mixture of sandy soil with asphalt and found that 4-5% is the optimum cutback percent for maximum stability.

Al-Kawaaz, 1990 studied the behavior of sandy gypesous soil asphalt mix in Oedometer test; the main conclusion is the increase in binder content.

Al-Shakayree, 2003 showed that, in sandy soil the maximum dry unit weight decreases, and the optimum water content increases with the increase in gypsum content result in increase in rebound strain.

Al-Obaidi, 2003 used two materials in order to improve the collapsibility characteristics of sandy gypseous soil with gypsum content of 70% from Al-Ramady city west of Iraq. The first material was Glass sand as a natural residual material, and the second was powder of destroyed ceramic as a residual of industrial material. Both materials succeeded to improve the collapse deformation of gypseous soil with more than 50%, where the collapse potential reduced from about 10% to 4.5%.

Al-Harbawy and Al-Khashab, 2004 reported the effect of stabilizing gypseous soil using liquid asphalt types such as cutback and emulsion on its behavior of shear strength is considerably observed. Addition of liquid asphalt provides cohesion strength to the soil mass and also acts as a waterproofing agent. Cutback Asphalt increases the resistance of gypseous soil to permeability, such resistance increases as void ratio increases.

Al-Saidi et.al, 2011 demonstrated that the stabilizing of gypseous soil using the optimum fluid content of 16% (5%Cutback Asphalt+11% water) led to improve the unconfined compressive strength, compressibility, and rebound consolidation. The additive acts as waterproofing of gypseous soil. While under absorbed condition, lime-cutback mixture was used in order to satisfy the base course construction requirements.

Aziz, 2011 showed that fuel oil is a good material to modify the basic properties of the gypseous soil such as collapsibility and permeability, which are the main problems of this soil. The fuel oil

provides an appropriate amount of the cohesion in the soil which is suitable for carrying the loads from the structure.

3. MATERIALS

3.1 Gypseous Soil

The soil samples were taken from Eaan Tamur city, Karbala governorate, south west of Iraq. From a depth of 3m up to 6m below the natural ground level. The samples are packed in a double nylon bags and transported to the soil mechanics laboratory at University of Technology in Baghdad for testing.

3.2 Asphalt

The type of asphalt used in this research is medium curing cutback (MC-30) liquid asphalt which is used in maintenance of surface layers of asphalt produced by Al- Dora Refinery in Baghdad Governorate. This type is fabricated by one step:

91.2 % [(40-50) asphalt cement] + 8.8% [kerosene] → (MC-30) (1)

Properties of Cutback Asphalt (MC-30) used are given in **Table 1.**

4. PROPERTIES OF GYPSEOUS SOILS

4.1 Physical Properties

The summary of the physical tests results are shown in **Table 2.**

4.1.1 Grain size distribution

The grain size distribution was determined according to **(ASTM D422- 63, (2007))** using dry sieving. The grain size distribution curve of the soil is clarified in **Fig.1.**

4.1.2 Specific gravity

The specific gravity was determined according to BS 1377: 1975, Test No.6 (B). Kerosene was used instead of distilled water because of the dissolving action of gypsum by water**, Head, 1980.**

4.1.3 Water content

This was determined in accordance to BS 1377:1975, Test (A).The oven dry temperature was kept at 45˚C due to dehydration of gypsum.

4.1.4 Compaction test

Standard compaction tests are carried out on soil sample to determine the water content –unit weight relationship according to**, ASTM D698, 2000**.

4.2 Chemical Properties

The gypsum content is determined according to the method presented by**, Al-Mufty and Nashat, 2000**. This method consists of oven drying the soil at 45˚C until the weight of the sample becomes constant. The weight of the sample at 45 ˚C is recorded, then the same sample is dried at 110˚C for 24 hrs and the weight is recorded again. The gypsum content is then calculated according to the following equation:

$$X\ (\%) = \frac{[\![w_{45^\circ c} - w_{110^\circ c}]\!]}{w_{45^\circ c}}\ x4.778x100 \quad (2)$$

Where:

x= gypsum content (%).

$w_{45^\circ c}$ = weigth of the sample at 45 ˚C.

$w_{110^\circ c}$ = weigth of the sample at 110˚C.

4.3 Geotechnical Properties

4.3.1 Collapsibility

Gypseous soils exhibits collapse behavior as results of volume change upon wetting. The term of "collapse"commonly refers to the deformation of the soil mass due to reduction in its volume when exposed to water. **Jennings and Knight, 1957** proposed a single Oedometer collapse test to predict the collapsibility of the soil under the foundation. The collapse potential C.P is defined as:

$$C.P = \frac{\Delta e}{1+e_\circ} \quad (3)$$

Where:

Δe = the difference in void ratio of the sample at a specific stress.

$e_\circ$ = the natural void ratio.

The severity of collapse according to the collapse potential is shown in **Table 3**.

It was found that, the value of collapse potential for the natural soil is (10%), and according to the specification listed in **Table.3** the case of severity is classified as trouble to severe, and hence the soil needs to be treated.

5. EXPERIMENTAL PROGRAM

The experimental program in this study can be categorized into the following groups:

Group (A): Consisting of five mixtures which were prepared from various percentages of Cutback Asphalt and added to the natural gypseous soil samples in order to perform the testing program. The percentages of Cutback Asphalt are 3%, 6%, 9%, 12%, and 15% and expressed as binder content (%) these values were chosen depending on numerous references that stated and specified. The range of the binder content used by**, Kadhim, 2014** who employed percentages of binder was equal 2%, 4%, 6%, 8%, 10%. The mixed samples were tested by single Oedometer collapse test, the sample was prepared in Oedometer ring with initial condition unit weight equal 12.5 $\frac{kN}{m^3}$ .The loading sequence of single Oedometer collapse test is 25, 50, 100, 200 and 400 kPa, and the loading interval is 1 hour for each vertical stress. However, the loading duration for the collapse stress of 200 kPa is 24 hours for both unsaturated (drying) and saturated (soaking)

conditions. The loading sequence of single Oedometer test is according to **Jennings and Knight, 1957 and ASTM D5333, 2003**.

Group (B): The geotechnical model tests of this group were conducted in proposed steel model box with dimensions of 30 cm in length, 30 cm in width and 35 cm in depth. The filter layer of fine gravel material was placed to a depth of 5cm from the bottom of steel box. The soil was prepared at the same properties used in group A. The soil strata extend to the depth of 2B from the surface filter where B is the footing width. The model is soaked with water by means of flexible pipe connected at the container bottom. Two values of collapse potential (6.2% and 2.6%) were chosen to be treated, which are corresponding to asphalt contents of (9% and 12%) respectively. These values of asphalt contents represented the best treatment percentages, which succeeded to obtain significant reduction in collapse potential from single Oedometer collapse test. This treatment can be induced to a depth of 6 cm and 12 cm under model foundation. A square footing of dimension 6 × 6 cm was placed on the surface of the treated soil layer and subjected to vertical static loading where the loads are applied at regular time intervals of (4-15) min according to **ASTM D1194, 1994** for each load increments. One dial gauge was used and the vertical settlement of the footing for each increment of load was recorded.

6. DISCUSSION OF TEST RESULTS

6.1 Collapse Test

The results of single Oedometer collapse test can be shown in **Table 4.** and **Fig.2** The reduction in collapse potential of gypsum soil is clearly observed as a result of adding the Cutback Asphalt material (MC-30) as shown in **Fig.2**. The collapse potential (C.P) is considerably decreased from 10% to 2.6% with the increase in the percentage of (MC-30) to 12%. This behavior is attributed to the action of asphalt material as water proofing for gypsum particles, in other words the (MC-30) film fill the air voids in soil mass as well as covering the gypsum grain and reduce its ability to dissolve by water. The improvement results showed that 12% of Cutback Asphalt additive is the optimum value for collapse reduction. Adding (MC-30) material such as 15% leads to a reverse behavior where the deformation of the soil mass increased dramatically as shown in **Fig.2** The increasing of soil deformation with high percentage of (MC-30) asphalt can be related to two reasons, the first reason is the lubricant action of (MC-30) layer which causes sliding of soil particles each one on other during loading. The second one can be related to the increase of the total volume and liquidity of the soil mass with the increase of (MC-30) content which may cause direct decrease in the value of dry density and increases the collapse potential.

6.2 Effect of Cutback Additive on the Coefficient of Salt Dissolved

Firstly, the material of Cutback Asphalt additive tries to reduce the water accessibility to the gypsum particles. Then, the presence of Cutback Asphalt as a thin layer surrounded the soil particle also leads to decreasing the interaction between the water and gypsum subsequently, the reaction between them would be slow. Thus, the salts dissolution need more time to be significantly settled. It is worthy mentioned, that (C.V) is expressed as the rate of settlement of soil or by other words represents the coefficient of salt dissolved during soaking.

The addition of Cutback Asphalt to the gypseous soil shows a good reduction in settlement value so that the asphalt percentage has a proportional relation with the time required for collapse to occur. **Table 5** presents the variation the coefficient of salt dissolved with different amounts of asphalt ranging from 0 to 15%. It is noticed that, adding (0%, 3%, 6%, 9%, 12%, and 15%) asphalt require to (8, 11, 13, 15, 31, and 33) minutes to achieve 90% of total dissolve of salts. However, the test results indicated the high suitability of Cutback Asphalt to be used as improvement material for collapsibility of gypseous soils. The results also demonstrate an excellent indication on the asphalt efficiency to be used in reducing the gypsum soil collapse. The effect of asphalt content on the coefficient of salt dissolved can be displayed in **Fig.3 to 8.** From the **Fig.3 to 8** it was observed that, the irregular shapes of curves upon loading are attributed to the addition of asphalt to the gypseous soil reduce the amount of dissolved gypseous and coefficient of salt dissolved (C.V).

6.3 Bearing Capacity Test

The bearing capacity of gypseous soil after treatment with 9% and 12% of (MC-30) asphalt was investigated using proposed foundation model with treatment depth of 6 cm and 12 cm. The results of load-settlement relationship shown in **Fig.11** indicate that, the bearing capacity decreases after treatment with (MC-30) material. The total settlement of 25 mm of treated soil can be achieved at vertical stress lower than those value required for natural soil. Moreover, treatment of gypseous soil to a depth deeper than 1B (i.e. 6 cm) causes more reduction in the value of bearing capacity of the soil. This behavior can be attributed to decreasing of the shear strength of the soil with adding of (MC-30) material as a result of decrease in angle of internal friction. Moreover, the load distribution under proposed foundation extends normally to a depth of 2B, therefore in this case study it can be observed that the bearing capacity in the first case of treatment (i.e. to a depth 2B of 12 cm) is lower than the first case of treatment (i.e. to a depth 1B of 6 cm). That is clearly shown in **Fig.13.**

On the other hand at a depth equivalent to foundation width, it was noted that the bearing improvement ratio (B.I.R) increased from 136% to 192% when the asphalt amount in soil decreased from 12% to 9% respectively. This could be explained that the best percent of improvement was gained when the amount of asphalt is 9%. In other words, any increase in asphalt percent could lead to a negative effect on the bearing capacity. This could be attributed to the amount of asphalt existed in the soil at 12% which causes increasing the soil compressibility and reducing the shear strength at this percent more than its effect on soil collapse; hence, reducing the bearing capacity and increasing the settlement value. This is clear in **Fig.11.** When the depth of soil-asphalt mixture equals to double foundation width, the asphalt presence at any percent at this depth reduces significantly the bearing capacity because: a large area of influence zone beneath the foundation would be increased in terms of compressibility and decreased in terms of modulus of elasticity. Thus, the shear properties (C and φ) would considerably reduce and this explains the reduction in (B.I.R) value with respect to asphalt percent. **Fig.13** clarifies the result.

In sequence the settlement values after using the admixture was less than their corresponding values without admixture. The value of settlement reduction ratio (S.R.R) decreased to 0.52 and 0.68 at an admixture ratio of 12% and 9% respectively. Therefore, the best percent in reducing the settlement at depth (asphalt + soil) equal to foundation width was 9%, as clearly is shown in **Fig. 11.**

Regarding the stabilized soil with asphalt at a depth of double value of foundation width, it was found that, the settlement in both cases of asphalt 9% and 12% increases the settlement with respect to that calculated from the untreated soils. Thus, stabilizing at a depth of 2B at any admixture percent would has a negative effect on the settlement values. This is clearly shown in **Fig.13.**

7. CONCLUSIONS

1. The Cutback Asphalt (MC-30) material can be used successfully to improve the collapsibility characteristics of gypseous soil and the optimum (MC-30) asphalt recommended is 12 %.
2. The bearing capacity of the soil decreases after treatment with (MC-30) asphalt. Thus this additive is not suitable for improvement of the bearing capacity of gypseous soils.
3. The total settlement of 25 mm of treated soil with (MC-30) material can be achieved at vertical stress lower than that value required for natural soil.
4. The thickness of treated layer with Cutback Asphalt material below the proposed foundation has a significant effect on the value of bearing capacity of the footing.
5. The rate of collapse (C.V) extremely decreases using all the percentages of Cutback Asphalt.
6. The best percent of bearing improvement ratio (B.I.R) and settlement reduction ratio (S.R.R) are acquired at a depth equal to foundation width, and when the asphalt content is 9%.

REFERENCES

- Al-Harbawy, A.F.Q., Al-Khashab, M.N., 2004, *The Effect of Emulsified Asphalt Addition on Some of the Engineering Properties of Expansive Clayey Soils*, Eng. And Technology, Vol.2, No. 23, PP.51-71.

- Al-Kawaaz, N., 1990, *Characteristics of Soil Asphalt Mixture*, M.Sc. Thesis, College of Engineering, University of Baghdad.
- Al-Mufty, A. A, and Nashat, E. H., 2000, *Gypsum Content Determination in Gypseous Soil and Rock*, Proceedings of the 3^{th} Jordanian International Mining Conference Amman, Vol.2, PP.485-492.

- Al-Obaydi, A. A. H., Mohmmed, Y. T., and Omar, M. E. T., 2007, *The Use of Liquid Asphalt to Improve Gypseous Soils*, internet reference www.iasj.net/iasj.

- Al-Obaidi, Q.A.J., 2003, *Studies in Geotechnical and Collapsible Characteristics of Gypseous soil*, M.Sc. Thesis, Civil Engineering Department, College of Engineering, Al-Mustansiriyah University, Baghdad, Iraq.

- Alphen, J.G.V., and Romero, F.D.E., 1971, *Gypsiferou Soils*, Bulletin-21, Int., Inst. for Land Reclamation and Improvement, Wegeningen, Holland.

- Al-Rawi N., 1971, *Prospects of Using Asphalt to Stabilize Iraqi Soils*, AL-Muhandis, Vol.15, No.3, Baghdad, Iraq.

- Al-Saoudi, N. K. S., Al-Khafaji, A. N., and Al-Mosawi, M. J., 2013, *Challening Problems of Gypseous Soils in Iraq*, Proceeding of the18^{th}International Conference on Soil Mechanics and Geotechnical Engineering.

- Al-Shakayree, T.K.K., 2003, *Improvement of Gypseous Soil below Foundation Using Quick Lime*, M. Sc. Thesis, Department of Building and Construction, University of Technology.

- Al-Saidi, Aamal. A., Ban, H. Al-Khayat, and Saad, I. Sarasam, 2011, *Implementation of Gypseous Soil- Asphalt Stabilization Technique for Base Course Construction*, Journal of Engineering, Vol.5, and PP.1.

- Aziz, H. Y., 2011, *Gypseous Soil Improvement Using Fuel Oil*, International Journal of Civil, Environmental, structural, Construction and Architectural Engineering, Vol.5, No.3.

- ASTM D5333, 2003, *Standard Test Method for Measurement of Collapse Potential of Soil*, Annual Book of ASTM Standards, Vol.04.08,

- ASTM D1194, 1994, *Standard Test Method for Bearing Capacity of Soil for Static Load and Spread Footing.*

- ASTM D422 -63, 2007, *Standard Test Method for Particle- Size Analysis of Soils.*

- ASTM D698, 2000, *Standard Test Method for Laboratory Compaction Characteristics of Soil Using Standard Effort (600*$\frac{KN-M}{m^3}$*).*

- British Standard Institution BS 1377, 1975, *Method of Testing Soils for Civil Engineering Purposes*, London.

- Department of the Environmental, Transport and Road Research Laboratory, 1987, *Soil Mechanics for Road Engineering*, London.

- Kadhim, A.J., 2014, S*tabilization of Gypseous Soil by Cutback Asphalt for Roads Construction*, Journal of Engineering and Development, Vol. 18, No.1, ISSN 1813-7822.

- Epps J.A., Dun lap W.A., Gallaway B.M., and Currin D., 1971, *Soil Stabilization*, HRB-HRR No.351.

- FAO, 1990, *Management of Gypseous Soils*, Soil Resources, Management and Conservation Service, FAO Land and Water Development Division.

- Head, K.H., 1980, *Manual of Soil Laboratory Testing*, Vol. 1, Prentch Press, London.

- Ismail, H.N., 1994, *The Use of Gypseous Soils, Symposium on the Gypseous Soils and Their Effect on Strength*, NCCL, Baghdad.

- Jasim .A. L., 2015, *Assessing the Durability of Asphalt Stabilized Gypseous Soil Embankment*, M. Sc. Thesis, Department of Civil Engineering, University of Baghdad.

- Jennings J.E., and Knight K., 1957, *The Additional Settlement of Foundation Sandy Subsoil on Wetting*, Proceeding 4th Int. Conf. Soil mechanics and foundation engineering, Vol.1, PP.316-319.

- Khalid, I. A., 2013, *Effect of Gypsum on The Hydro Mechanical Characteristics of Partially Saturated Sandy Soil*, Ph.D Thesis, College of Cardiff School of Engineering, Cardiff University, British.

NOMENCLATURE

Cc = coefficient of curvature.
Cu = coefficient of uniformly.
C.P = collapse potential (%).
C.V = coefficient of salt dissolve.
$e_\circ$ = is the natural void ratio.
Gs = specific gravity.
X = gypsum content (%).
$w_{45^\circ c}$ = weigth of the sample at 45 °C.
$w_{110^\circ c}$ = weigth of the sample at 110°C.
$\emptyset$ = angle of internal friction.
Δe = is the difference in void ratio of the sample at a specific stress.

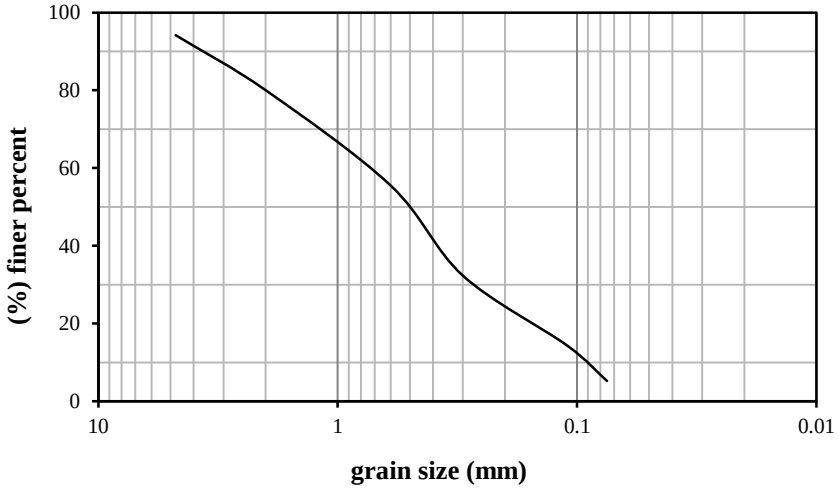

Figure 1. Grain size distribution of soil.

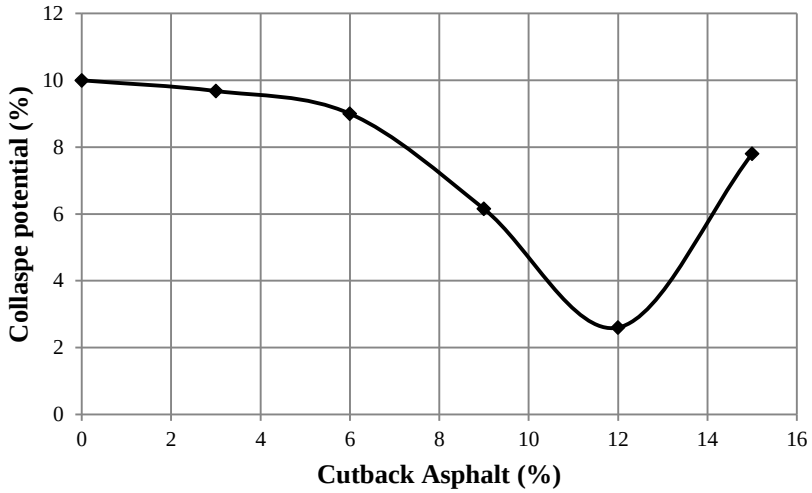

Figure 2. Variation of collapse potential with respected to percentage of Cutback Asphalt**.**

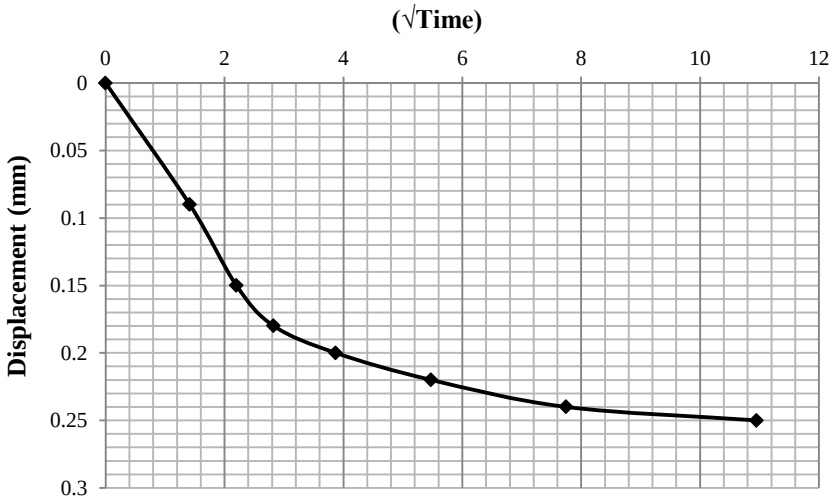

Figure 3. Relationship between displacement vs. time for (the natural case).

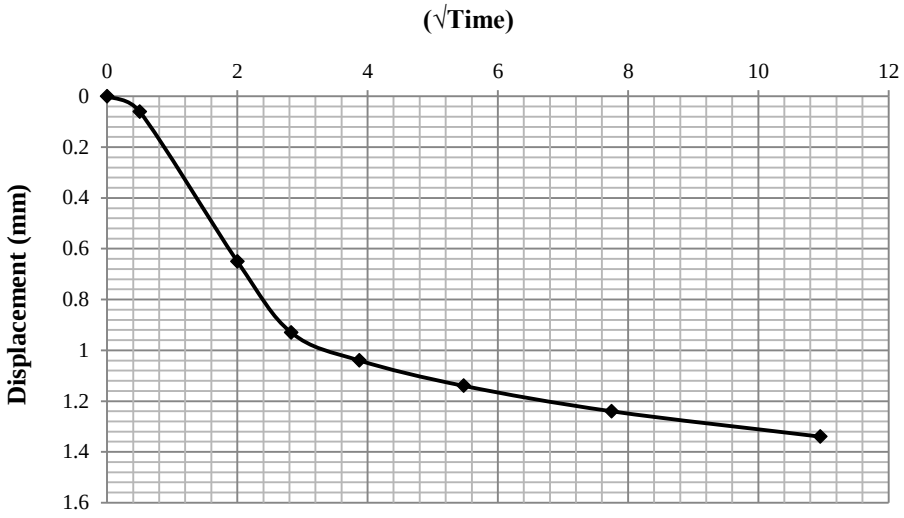

Figure 4. Relationship between displacement vs. time for (3% Cutback Asphalt).

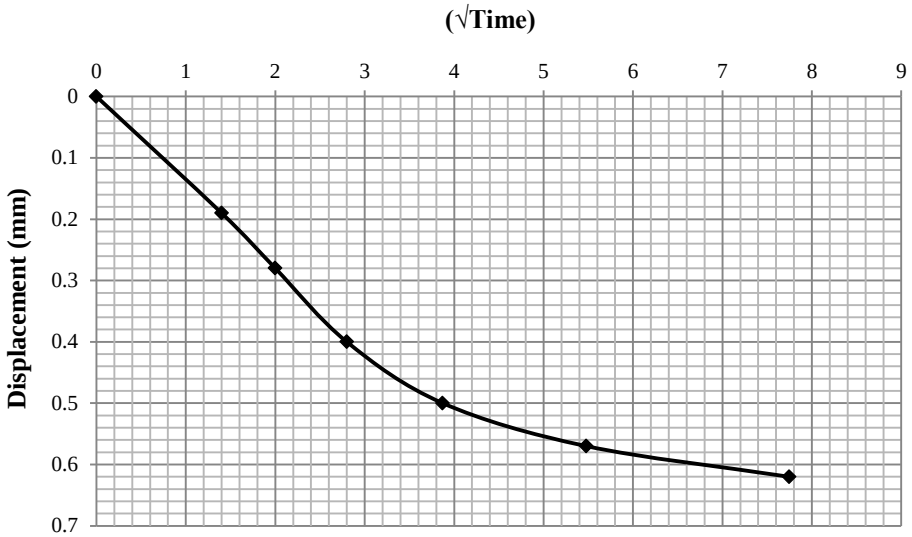

Figure 5. Relationship between displacement vs. time for (6% Cutback Asphalt).

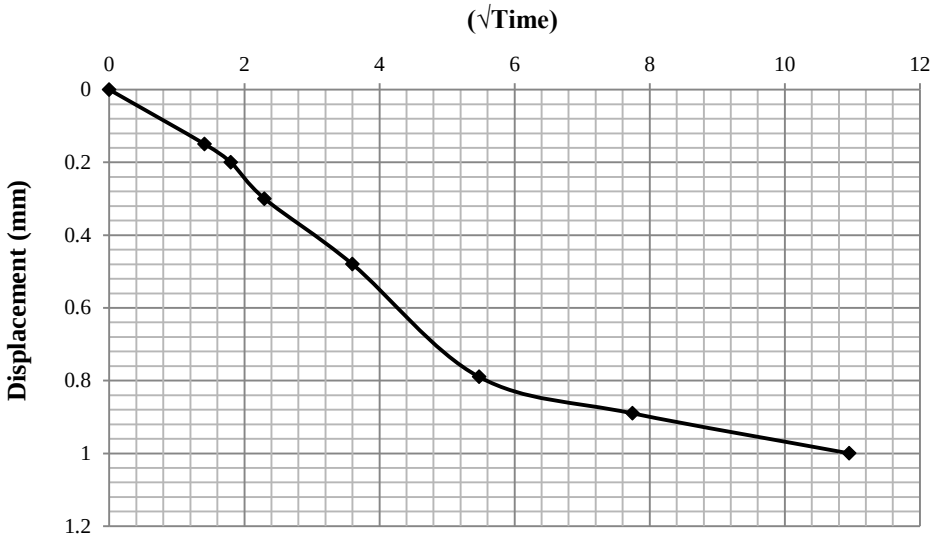

Figure 6. Relationship between displacement vs. time for (9% Cutback Asphalt).

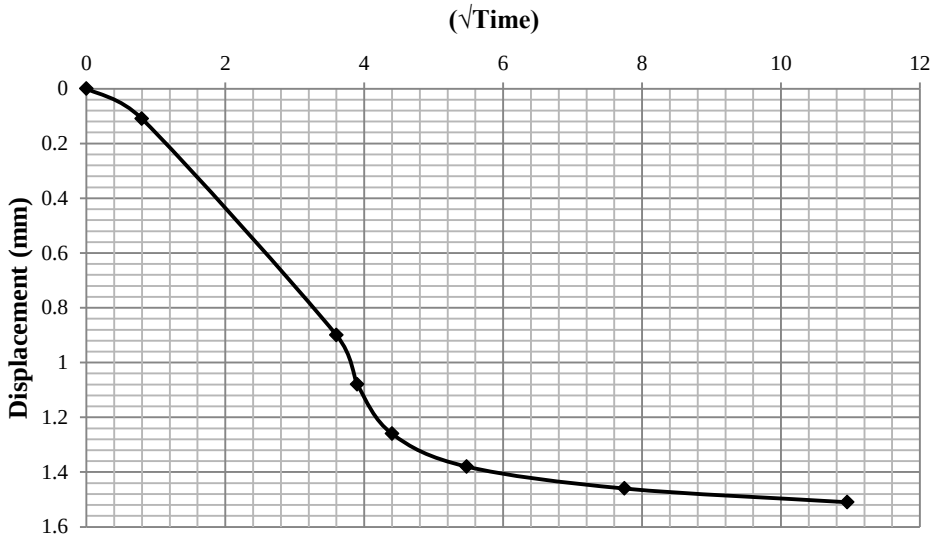

Figure 7. Relationship between displacement vs. time for (12% Cutback Asphalt).

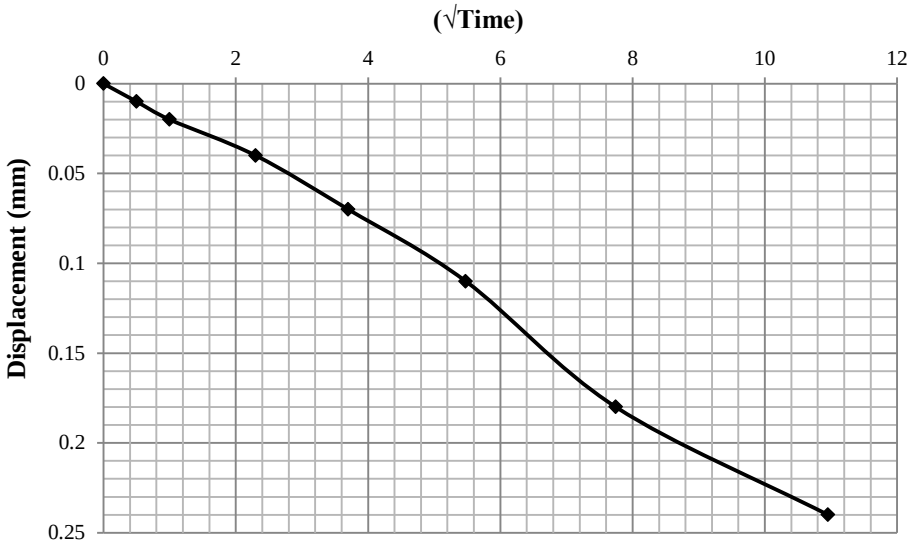

Figure 8. Relationship between displacement vs. time for (15% Cutback Asphalt).

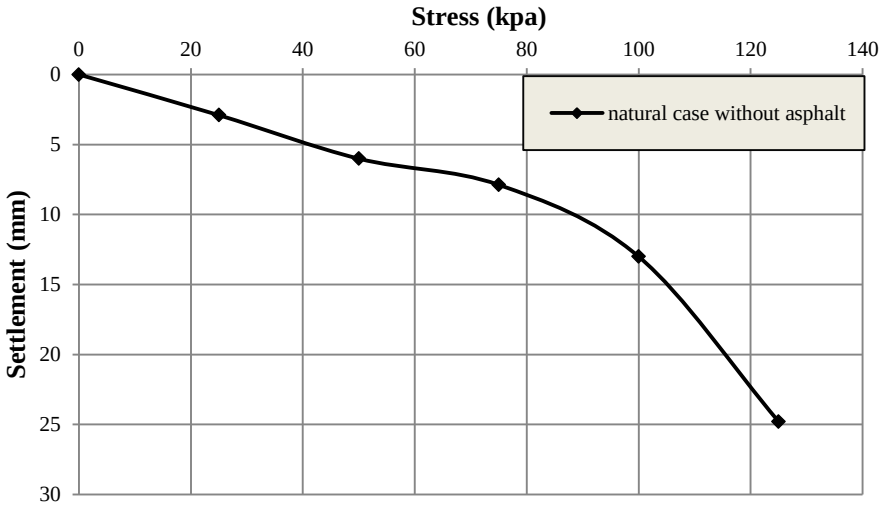

Figure 9. Stress-settlement curve for untreated soil.

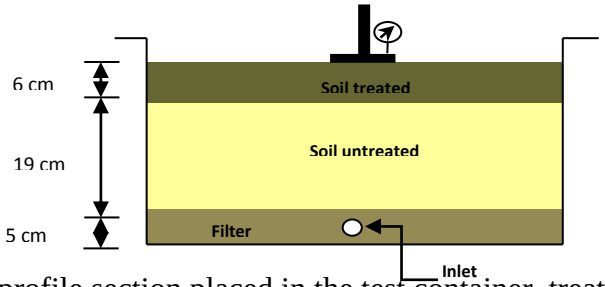

Figure 10. Soil profile section placed in the test container, treated layer equal to footing width(B).

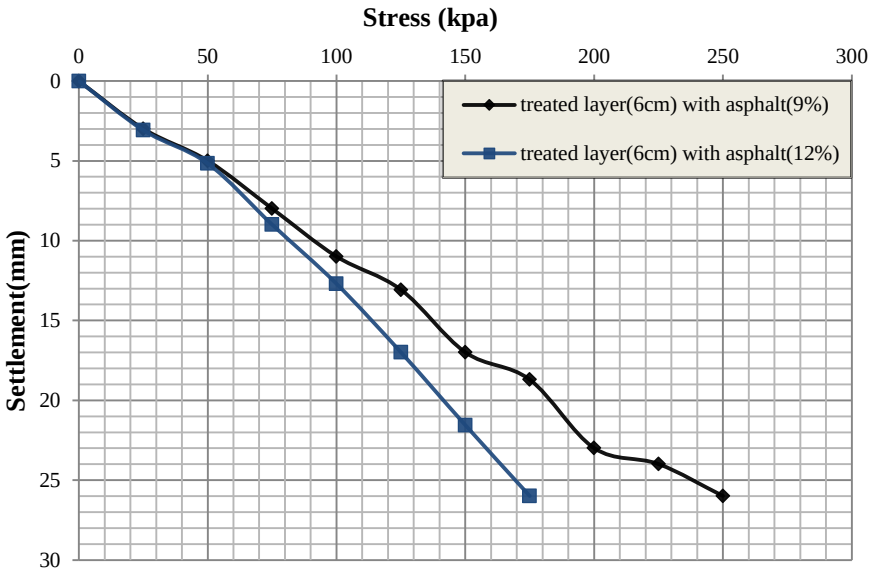

Figure 11. Stress- Settlement curve for soil treated with 9 %and 12% of the asphalt content at a depth equal to footing width.

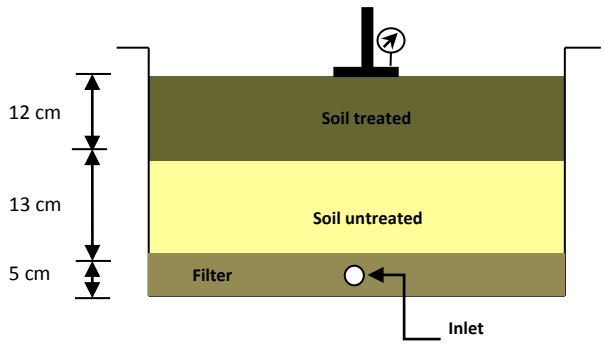

Figure 12. Soil profile section placed in the test container, treated layer equal to footing double width (2B).

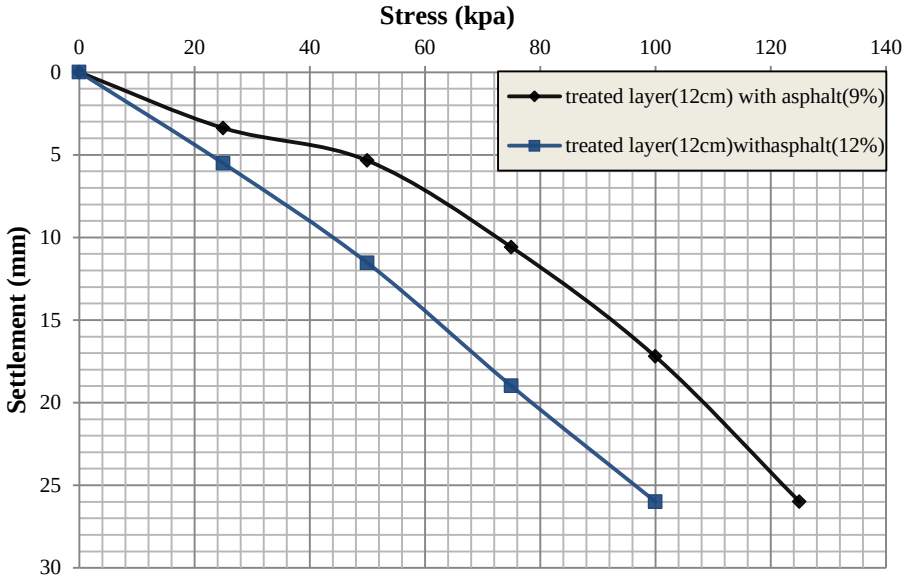

Figure 13. Stress- Settlement curve for soil treated with 9% and 12% of the asphalt content at a depth equal to double footing width.

Table 1. Properties of Cutback Asphalt (as tested by Al-Dora refinery lab).

Properties	Grades
Type	Medium curing cutback languid asphalt (MC-30)
Specific gravity	0.99
Test on residue from distillation penetration at 25°c (100g, 5 sec) Ductility at 25°c Solubility in CCL_4,%weight	120-300 100minimum 99.5 minimum
Kinematics viscosity at 60°c	75-150

Table 2. Summary of the physical properties of the soil**.**

Soil properties	Result value
***Gypsum content (%)	30
Specific gravity (Gs)	2.54
Initial void ratio (e_o)	1.03
Initial water content (%)	12.4
Maximum dry unit weight ($\frac{kN}{m^3}$)	18.1
Optimum water content (%)	13.5
Angle of internal friction ($\emptyset^\circ$)	30
Gravel (G) (%)	5.84
Sand (S) (%)	89.36
Silt (M) + Clay (C) (%)	4.8
Soil classification according to (unified soil classification system)	SW
Coefficient of uniformly (Cu)	8.1
Coefficient of curvature (Cc)	1.3

*Gypsum content is determined according to equation (2) section (4.2)

Table 3. Collapse identification (after Jennings and Knight, 1957)**.**

Severity	No problem	Moderate	Trouble	Severe	Very severe
C.P (%)	0-1	1-5	5-10	10-20	20

Table 4. Results of collapse potential.

Cutback Asphalt (%)	Collapse potential (%)
0	10
3	11.2
6	9
9	6.2
12	2.6
15	7.8

Table 5. The coefficient of salt dissolve results with respect to asphalt percentages**.**

Asphalt content (%)	T_{90}	C.V
0	8	0.432
3	11	0.3
6	13	0.26
9	15	0.2301
12	31	0.108
15	33	0.102

Optimization of Surface Roughness For Al-alloy in Electro-chemical Machining (ECM) Using Taguchi Method

Mostafa Adel Abdullah
Dept. of Production Engineering and Metallurgy
University of Technology/Baghdad. Iraq
Email mostafa_ad_87@yahoo.com

Dr. Shukry Hammed Aghdeab
Assistant Prof
Dept. of Production Engineering and Metallurgy
University of Technology/Baghdad. Iraq
Email shukry_hammed@yahoo.com

Safaa Kadhim Ghazi
Assistant Lecturer
Dept. of Production Engineering and Metallurgy
University of Technology/Baghdad. Iraq
Email Safaa_kadhim1988@yahoo.com

ABSTRACT

Electro-chemical Machining is significant process to remove metal with using anodic dissolution. Electro-chemical machining use to removed metal workpiece from (7025) aluminum alloy using Potassium chloride (KCl) solution .The tool used was made from copper. In this present the optimize processes input parameter use are (current, gap and electrolyte concentration) and surface roughness (Ra) as output. The experiments on electro-chemical machining with use current (30, 50, 70)A, gap (1.00, 1.25, 1.50) mm and electrolyte concentration (100, 200, 300) (g/L). The method (ANOVA) was used to limited the large influence factors affected on surface roughness and found the current was the large influence factors with (72.17%) . The results of the optimization of comparison of experimental and prediction conditions current at level-1(30 A), gap at level-1 (1.00mm) and electrolyte concentration at level-1(100(g/L)) shown the average experiments and prediction surface roughness (1.352 μm) and (1.399 μm) respectively..

Keywords: Electro-chemical machining, surface roughness, optimization, taguchi, ANOVA.

امثلية الخشونة السطحيةلسبيكة الالمنيوم في التشغيل الكهروكيمياوي باستخدام طريقة تاكوشي

مصطفى عادل عبد الله
مدرس مساعد
هندسة الانتاج والمعادن /الجامعة التكنولوجية /العراق بغداد

د. شكري حميد غضيب
استاذ مساعد
هندسة الانتاج والمعادن /الجامعة التكنولوجية /العراق بغداد

صفاء كاظم غازي
مدرس مساعد
هندسة الانتاج والمعادن /الجامعة التكنولوجية /العراق بغداد

الخلاصة

التشغيل الكهروكيمياوي هي طريقة مؤثرة لإزالة المعادن باستخدام محلول انحلال . في هذا البحث التشغيل الكهروكيمياوي يستعمل لإزالة معدن المشغولة المكون من سبائك الألومنيوم (7025) باستخدام محلول من ملح (كلوريد البوتاسيوم) و الأداة المستخدمة مصنوعه من النحاس. تم في هذه العملية تحديدالمتغيرات المدخلة باستعمال التيار، الفجوة وتركيز المحلول. وباستخدام أسلوب تاكوشي لتصميم وتحليل التجارب للحصول على الأمثل.وتكون خشونة السطح كمخرج لسبكة الألومنيوم نوع (7024). التجارب اجريت التشغيل الكهروكيمياوي باستعمال قيم تيار (30، 50، 70)امبير وهناك فجوة (1.00، 1.25، 1.50) ملم وتركيز المحلول (100، 200، 300) (غرام / لتر). تم استخدام أسلوب (أنوفا) لتحديد اي

العوامل يكون كبير التأثير على خشونة السطح . وجد أن التيار كان من اكبر العوامل تأثيرا بنسبة (72.17٪). نتائج الاستغلال الأمثل والمقارنة بين مستويات الظروف التجريبية باستعمال التيار المستوى الاول (30)امبير، الفجوة في المستوى الاول (1.00) ملم وتركيز المحلول في المستوى الاول (100)(غرام/لتر) أظهر متوسط التجارب والتنبؤ للخشونة السطح هي (1.352)مايكرون و (1.399) مايكرون على التوالي.
الكلمات الرئيسية : التشغيل الكهروكيمياوي،الخشونة السطحية ،الامثلية ،تاكوشي،انوفا.

1. INTRODUCTION

Electro-chemical machining (ECM) is a non-conventional process that depends on the removal of workpiece atoms by electro-chemical dissolution process, **Al-Hofy, 2005.**The removal process of use anodic dissolution, where anode is workpiece and tool is cathode. To dissolve metal from the work piece, electrolyte is push on the gap between metal and electrode, while the current is passed on the cell ,**Hiba, 2011,** focused on the effect of the change in current , gap on surface roughness of . The results obtained show that, increasing of the gap size between the tool and the workpiece from (1mm) to (3mm) leads to increase of (46%) in the surface roughness of the workpiece, increasing of the current density from (2.4485 Amp/cm^2) to (3.6728 Amp/cm^2) leads the to decrease in surface roughness of the workpiece by approximately (31%). Used the Statistical Package for the Social Sciences (SPSS) software to prediction the results. **Babar, et al, 2013,** discuss the effect and condition optimization of ECM process used titanium based alloy. The condition of process that use are applied voltage, electrolyte concentration sodium chloride (NaCl) and feed ,which optimization according to material removal rate (MRR) as output. Analysis of variation contribution to performance characteristics. The results shown that the large influnance condition is voltage and then the electrolyte concentration and feed. The raise material removal rate (MRR) lead to raise in electrolyte concentration and voltage. The optimum values of process parameters are (electrolyte concentration (15 wt%), applied voltage (20 V)), tool feed rate (0.32mm/min).

Mohanty, et al., 2014, studied the effect of process parameter (voltage, electrolytic concentration and feed rate) on performance characteristics such as roughness average (Ra) affecting the surface roughness. The surface roughness initially increases with concentration, but it decreases at maximum concentration. The optimal condition for SR was found to be at (30 g/l) concentration of when electro-chemical machining used a tool of copper in an aqueous sodium chloride (NaCl). ANOVA were used to study the effect of parameters on cutting machining. It was observed that an increase in voltage where is roughness average (Ra) decreased. Voltage was found to be significantly electrolyte, (15V) voltage and (0.2 mm/min) feed rate. **Habib, 2014,** studied the effect of (ECM) cutting condition (voltage, electrode feed, and current) on the surface roughness. Taguchi method and analysis of variance (ANOVA) are used to optimization the electro-chemical machining process. The results show that maximum factor effect on surface roughness are current with (53%)then feed with (21%), voltage (11.5%). The optimum parameter(30V) voltage, (1 mm/min) feed rate used to get better roughness average (Ra=3.218 μm).

2. THEORY OF TAGUCHI

Taguchi discovers a novel conception for the quality control method named as (Taguchi parameter design). The method stated that the quality of manufactured part must be computed by the deviation amount from the required value. He takes into consideration not only the

operation mean, but also the variation magnitude or (noise) created with manipulating the inputs parameters or operation variables. The technique is focus on two major groups; a unique matrix type called orthogonal array (OA), all the columns include number of experiment depending on the level number for the control factor, in addition to (signal to noise ratio) S/N **Abbas,2009 .**

$$S/N = -10\log\left[\frac{1}{n}\sum_{i=1}^{n}(y_i^{\,2})\right] \quad ; \qquad i=1, 2,\ldots\ldots \quad \ldots\ldots\ldots\ldots\ldots(1)$$

The formula is utilized to calculating signal to noise ratio are given Eq(2):

$$S/N = -10\log\left[\frac{1}{n}\sum_{i=1}^{n}(1/y_i^{\,2})\right] \quad ; \qquad i=1,2,\ldots\ldots\ldots \quad \ldots\ldots\ldots\ldots\ldots(2)$$

Where, y_i the measurements of output , and n is the measurements of input.

The final design of input parameter for work done according to MINITAB16 software as follow:

STAT ⟶ DOE ⟶ Taguchi ⟶ Create Taguchi Design

3. ANALYSIS OF VARIANCE

The results using (ANOVA) to explain the effect of machining condition on the roughness average (Ra) depend on machining condition current, gap and electrolyte construct while others are independent variables., F- ratio refer to mean square error and (%) percent is refer to influence rate of operation variables to (Ra), **Mohammed,2016.**

4. EXPERIMENTAL WORK

In electro-chemical machining design using drilling machine and other parts accessories with workpiece (7024)Aluminum alloy .The percentages of chemical composition is given in **Table 1.** with anode workpiece dimension (40x 30) mm and thickness (20) mm as shown in **Fig 1**,with using nine simple with change in machining parameter and constant machining time(5)min and different depth of hole.

4.1 The ECM machine

The ECM cell used in these experiments is shown in **Fig 2**. It consists of : The drilling machine, workpiece fixture, electrolyte pump and power supply.

The drilling machine Provides a rigid base and good control of the tool feeding with manual controlling to maintain the gap size between tool and workpiece. workpiece fixture is made from cast iron. Pumps the electrolyte in the reaction chamber to gap between tool and workpiece. The used power supply in the experiment is a (D.C) welding machine with current (5 A/10 V-400 A/36V) type CEBORA .

4.2 Cathode Tool

In this paper, copper tool used with purity is (99.9%). The reason for using copper metals is because they are (easy to machine, have high electric conductivity and high corrosion resistance). with diameter (10 mm) , length (5 cm) and roughness average (Ra) (0.475 μm) as shown in **Fig 3.**

4.3 Electrolyte

The electrolyte use to creates appropriate conditions for anodic dissolution (workpiece), conducts the current and removes the waste from the gap. In this work as KCl as electrolyte with compost, listed in **Table 2.**

4.4 Design of Experiments

The total of experiments machining is (nine experiments) with (3) levels (3) parameters as (3^3). A partial factorial design was done use (9)to study the effect of parameter on surface roughness (Ra). The cutting parameters used (current, gap and electrolyte construct). The levels of cutting parameters are listed in **Table 3.**

4.5 Surface Roughness measurements

The Pocket Surf gauge is portable surface measurements use ,with selectable traverse length (1, 3 or 5)mm as shown in **Fig 4 .**

5. RESULTS AND DISCUSSION

The experiments work using the design parameter array **Table 4**. as shown in **Fig 5.** The complete response data to get minimize surface roughness. The Signal-to-Noise ratio (S/N) should be as small as possible, because the quality characteristic "smaller is better" was used. S/N values were calculated from Eq.(1), and the results have been arranged in the last column of array in **Table 4.** The results were analyzed by using main effects for both surface roughness values and signal-to-noise ratio, and ANOVA analyses. Then the estimate results which obtained checked experimentally to insure the estimate value. In terms of the average effects, the average value of surface roughness for each parameter (A, B and C) listed in **Table 4.**

5.1 Analysis of Variance

The results are analyzed by using (ANOVA) method to find the effect of machining condition on the surface roughness, surface roughness as the output, current, gap and electrolyte concentration as input. Therefore, the most influential parameter is the current (72.17%), gap (17.81%) and minimize effect electrolyte concentration (5.63%) as shown in **Table 5.**

5.2 Optimal Design Conditions For Surface Roughness

The main effects figure used to find the better design parameter to get the better surface roughness and to select the better machining parameters using **Fig 6.** which shows the main effect figure conditions for minimum surface roughness were: current at level-1 (30 A), gap at level-1 (1.00 mm and electrolyte concentration at level-1(100(g/L)).

The **Fig 6**.and **Fig 7.** depending on data in **Table 4.** Because of using "smaller is better" quality characteristic in this study, The difference (max-min) parameter of three levels for each parameter indicates that the current has the highest effect on the surface roughness followed by a gap and electrolyte concentration.

6. CONCLUSION

This research used Taguchi's design (minimum number of experiments can use this method)for get optimum parameter with lowest surface roughness,.

- The Maximum surface roughness when current (70 A) , gap (1.50 mm) and electrolyte concentration (300(g/L)).
- Through ANOVA method , found current is very important factor influnes (72.17%) on surface roughness.
- The compare of experimental and prediction conditions levels (A1B1C1) (current at level-1(30 A), gap at level-1 (1.00 mm) and electrolyte concentration at level-1(100(g/L)). shown the average experiments measure and prediction surface roughness from Taguchi (1.352 μm) and (1.399 μm) respectively .

REFERENCES

- Al-Hofy. H,2005, *Advanced Machining Process, Nontraditional and Hybrid Machining Process*, Mcgraw-Hill Company, Egypt.
- Hiba. H. Alwan , 2011,*Study of Some Electrochemical Machining Characteristics Of Steel Ck35,* M.Sc Thesis University Of Technology, Iraq.
- - Babar.P. D, B. R. Jadhav ,2013,*Experimental Study On Parametric Optimization Of Titanium Based Alloys (Ti-6al-4v) In Electrochemical Machining Process,* International Journal Of Innovations In Engineering And Technology , Vol. 2, pp.171-175,India.
- Mohanty. A, Gangadharudu Talla, S. Dewangan, S.Gangopadhyay,2014 ,*Experimental Study of Material Removal Rate, Surface Roughness & Microstructure In Electrochemical Machining Of Inconel 825*, International & All India Manufacturing Technology, India.
- Habib. S. S,2014 , *Experimental Investigation of Electrochemical Machining Process Using Taguchi Approach,* International Journal of Scientific Research In Chemical Engineering ,Vol.1,No. 6, Pp. 93-105, Egypt, .

- Abbas Khammas,*2009, Optimization of Cyclic Oxidation Parameters in Steel-T21 for Aluminization Coating Using Taguchi-ANOVA analysis by MINITAB13,* Eng.& Tech. Journal, Vol. 27, No.12 .
- Mohammed , Atheer R, Abdullah , Mostafa A, Abdulwahhab , Ahmed B,2016 ,*Effect of Cutting Parameter on Material Removal Rate and Surface Roughness in Deep Drilling Process,* Arab Journal of Science and Research, Vol.2- Issue (5), PP.274-285.

Table 1. Chemical composition of Aluminum (7024).

Element	Cu%	Mg%	Si%	Fe%	Mn%	Cr%	Ni%
Percentage(%)	2.14	1.55	0.163	0.422	0.216	0.090	0.012
Element	Ga%	Pb%	Zn%	Ti%	V%	Other%	AL%
Percentage(%)	0.010	0.071	4.93	0.038	0.007	0.132	90.219

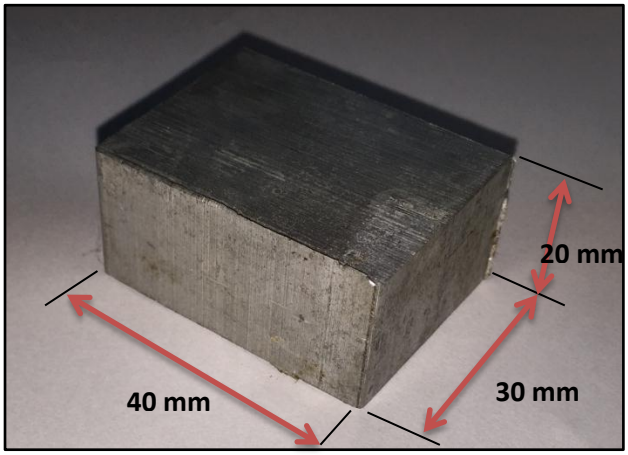

Figure 1.Workpiece dimension.

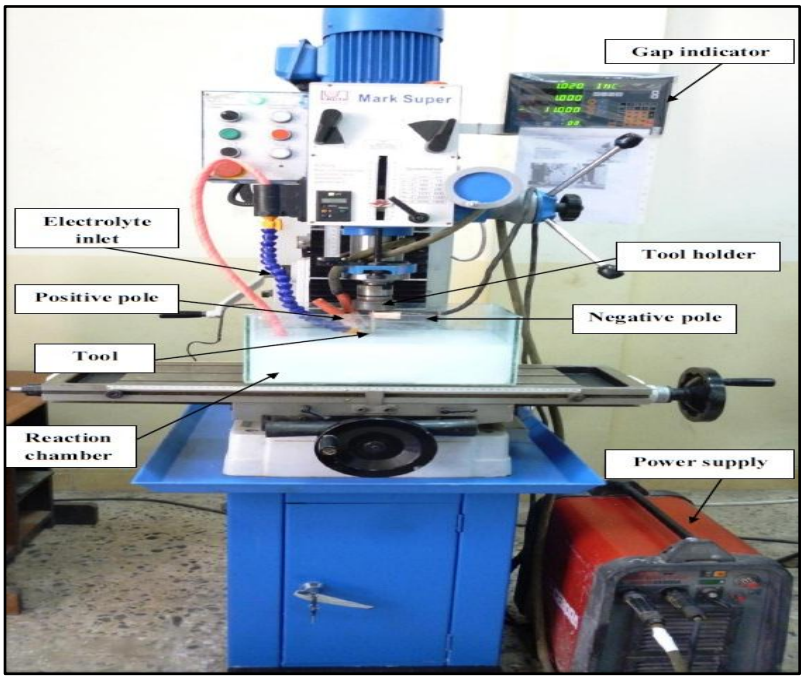

Figure 2.ECM machine model .

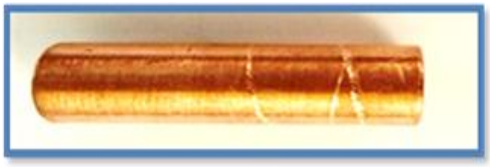

Figure 3. Cathode copper tool.

Table 2. The chemical composition (KCl).

Element	Ca%	SO_4%	Fe%	Br%	Mg%	Na%
Percentage(%)	0.001	0.003	0.0002	0.01	0.0005	0.02
Element	Gu%	Pb%	Ba%	PO_4%	N%	I%
Percentage(%)	0.0002	0.0002	0.001	0.0005	0.001	0.002

Table 3. Cutting conditions.

No	Parameter	Level 1	Level 2	Level 3	Units
1	Current	30	50	70	A
2	Gap	1.00	1.25	1.50	mm
3	Electrolyte concentration	100	200	300	g/L

Figure 4.The portable surface roughness measurements .

Table 4. The ECM conditions of experiments and S/N results.

No	Current(A)	Gap(mm)	Electrolyte concentration (g/L)	Surface roughness (Ra) (μm)			Average Ra (μm)	S/N ratio
	A	B	C	Ra_1	Ra_2	Ra_3		
1	30	1.00	100	1.37	1.11	1.21	1.23000	-1.83089
2	30	1.25	200	2.10	2.14	1.80	2.01333	-6.10291
3	30	1.50	300	2.56	2.32	2.34	2.40667	-7.63717
4	50	1.00	200	2.51	2.42	2.35	2.42667	-7.70336
5	50	1.25	300	2.71	2.68	2.76	2.71667	-8.68137
6	50	1.50	100	2.79	2.90	2.85	2.84667	-9.08782
7	70	1.00	300	3.08	3.00	2.88	2.98667	-9.50702
8	70	1.25	100	3.07	3.00	3.03	3.03333	-9.63879
9	70	1.50	200	3.11	3.23	3.10	3.14667	-9.95854

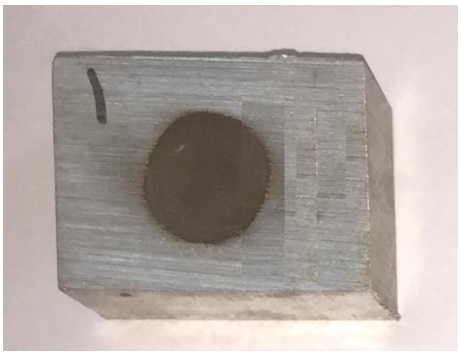

Current=30 ,Gap =1,00
Electrolyte =100

Figure 5.The sample of work use .

Table 5. Analyses ANOVA for surface roughness.

Source of variance	DOF	Sum of squares	Variance, V	F ratio	P (%)
current	2	2.136	1.068	0.5	72.17%
gap	2	0.527	0.264	0.5	17.81%
electrolyte concentration	2	0.167	0.083	0.49	5.63%
Error, e	2	0.130	0.065	-	4.36%
Total	9	2.960	-	-	100

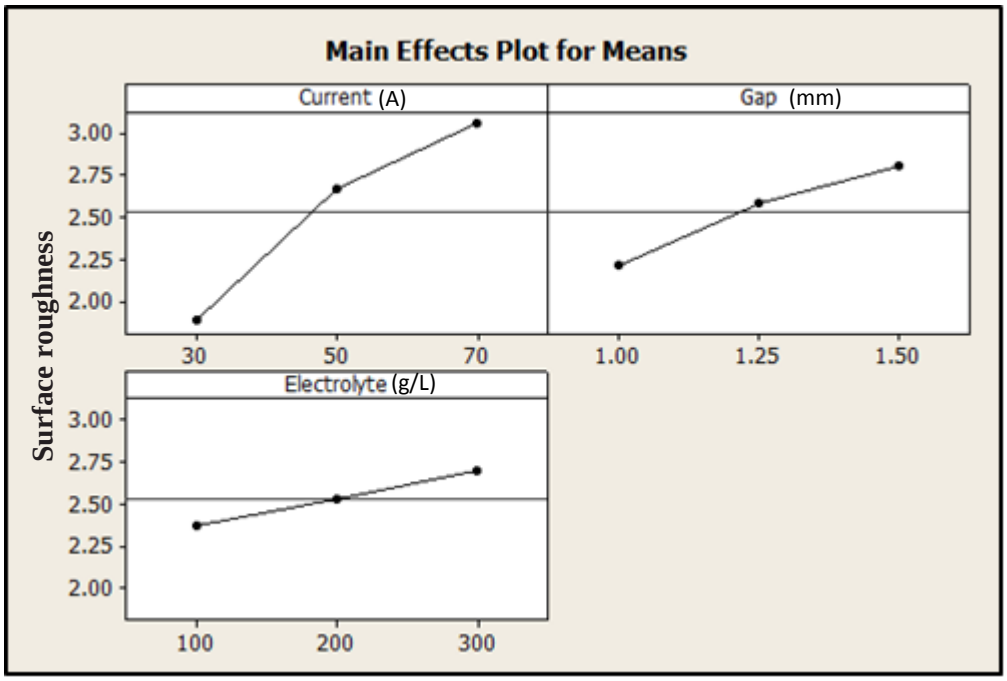

Figure 6. The main effect plot for Surface roughness.

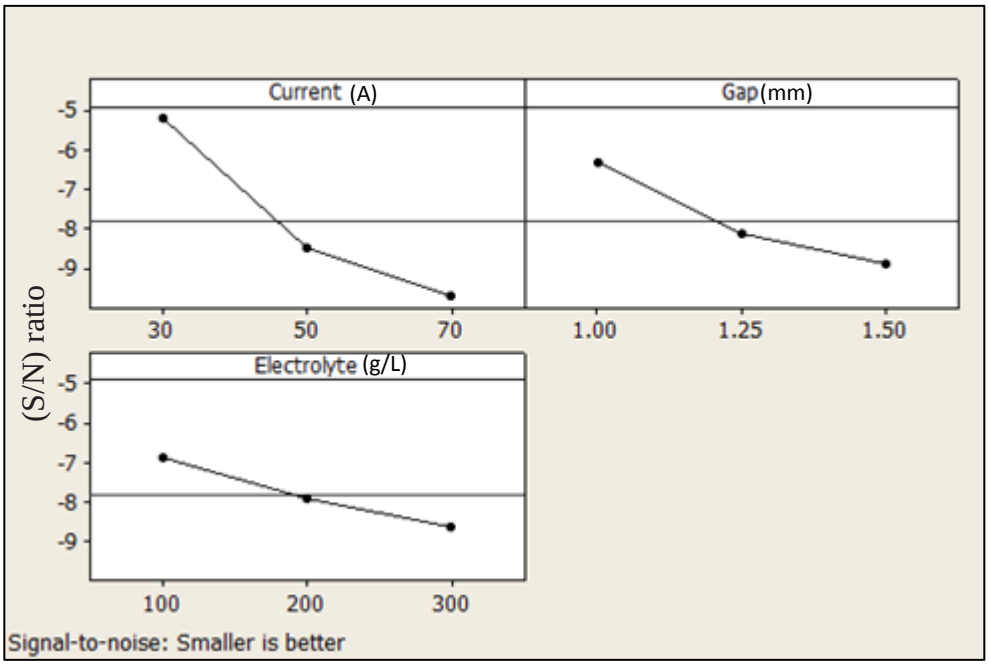

Figure 7. The main effect plot for (S/N) ratio.

Dry Sliding Wear Behavior of EN25 Steel Treated by Different Quenching Media

Bassam Ali Ahmed
Assistant Lecturer
Department of Electromechanical Engineering
University of Technology
Email: bsmty77@yahoo.com

ABSTRACT

The present investigation aims to study the effect of heat treatment by quenching in different quenching media (salt water, water and oil) following by tempering on wear resistance of EN25 steel. EN25 steel is an alloy of medium carbon low alloy steel which is used for many applications requiring high tensile strength and wear resistance such as connecting rods, adapters and in power sectors extensively. The specimens are machined to 20 mm in length and 10 mm in diameter. This study is done by two stages: The first stage is done by austenitizing EN25 steel to 850℃ for 1 hr by quenching the specimens in three different quenching media and then tempered at 300℃ in air. While the second stage is performed by wear test. Dry sliding wear test is done by using pin –on-disc technique by varying the loads as 5, 10, 15, 20 and 25 N, also varying the time as 5, 10, 15, 20, 25 and 30 min respectively. The microstructure examination, hardness and followed roughness tests are also done for the specimens before and after wear test. The results of this work showed that an improving in wear resistance and hardness for the specimen quenched by salt water more than for water and oil. At the same time the roughness decreasing for the specimen quenched by salt water more than for water and oil.

Key Word: EN25 steel, quenching heat treatment, quenching media, wear.

سلوك البلى الانزلاقي الجاف للفولاذ En 25 المعالج بأوساط تقسية مختلفة

بسام علي أحمد
مدرس مساعد
قسم الهندسة الكهروميكانيكية
الجامعة التكنولوجية

الخلاصة

يهدف البحث الحالي لدراسة تأثير المعاملة الحرارية بالتقسية في اوساط مختلفة (ماء مالح، ماء، زيت) على مقاومة البلى للفولاذ En 25 . الفولاذ En 25 هو سبيكة من فولاذ متوسط الكاربون منخفض السبائكية يستخدم في عدة تطبيقات التي تتطلب مقاومة شد ومقاومة بلى عاليتين مثل اذرع التوصيل ،المحولات وقاطعات القدرة. تم تشغيل العينات بطول 20 ملم وقطر 10 ملم . اجريت هذه الدراسة بمرحلتين: الاولى تم فيها تقسية العينات بثلاث اوساط تقسية مختلفة عند درجة حرارية 850 م^{o} ولمدة 1 ساعة، بعد ذلك تتم عملية المراجعة عند 300 م^{o} ولمدة 1 ساعة ومن ثم التبريد في في الهواء. بينما في المرحلة الثانية اجري اختبار البلى. تم اختبار البلى الانزلاقي الجاف باستخدام تقنية المسمار- على- القرص

وذلك بتغير الاحمال 5،10،15،20،25 نيوتن، كذلك تم تغير الزمن بمقدار 5،10،15،20،25،30 دقيقة على التوالي. وكذلك تم فحص البنية المجهرية واجريت اختبارات الصلادة والخشونة قبل وبعد اختبار البلى.
اظهرت نتائج البحث تحسن في مقاومة البلى والصلادة للعينة المقساة بالماء المالح اكثر مما هو عليه للعينات المقساة بالماء والزيت. وبنفس الوقت نقصان الخشونة للعينة المقساة بالماء المالح اكثر مما هو عليه للعينات المقساة بالماء والزيت.
الكلمات الرئيسية: فولاذ EN25 ، معاملة حرارية بالتقسية ، أوساط التقسية ، البلى.

1. INTRODUCTION

Today steel is an important alloy for the rapid development of technologies to obtain the best performance of service; this can be achieved by different heat treatments processes, **Murugan, and Mathews, 2013**. Heat treatment is defined as the heating of such carbon or alloying steel depending on the percentage of carbon and then cooling to change particulate characteristics of an alloy to achieve a suitable for a certain kind of application, **Fadara, et al., 2011**. Heat treatment affected on mechanical properties such as strength, hardness and ductility and also improving wear resistance. The purpose of heat treatment for the carbon steel is to alter the microstructure by using a certain heating and then cooling in a suitable quenching media to obtain the preferred characteristics, **Ismail, et al., 2016**. Wear is defined as surface phenomena including an important three mechanisms acting simultaneously, such as adhesive wear, abrasive wear, and erosive wear. Thus the heat treatment is important to reduce the wear of machinery components at minimum level, **Naveena, et al., 2015**. Many researchers were worked about heat treatment of steel such as **Jasiwal, et al. 2015**, they studied the effect of different quenching media such as cold water, hot water and vegetable oil on the microstructure and hardness of AISI 1050 carbon steel. While **Motagi**, **and Bhosle**, **2012**, studied the effect of heat treatment by quenching and tempering on mechanical properties and microstructure of two different steel alloys with and without copper. Whilst **Alabi, et al., 2012**, studied the effect of the temperature of the water as a quenchant on mechanical properties of two different medium carbon steel containing 0.33 wt.%C and 0.4 wt. %C. Whilst **Tukur**, **et al., 2014,** were studied the effect of quenching heat treatment at $900C^{o}$for 45min and then tempering at aurous tempering temperature $250C^{o}$, $350C^{o}$, $450C^{o}$ and $550C^{o}$ on mechanical properties (tensile strength, hardness) of medium carbon steel. The results of this work showed that increasing the hardness, yield strength, ductility and the optimum values of the mechanical properties attained at temperature of $250C^{o}$, while **Karthikeyan, et al., 2014**, studied the effect of subzero treatment on hardness, toughness and the amount of retained austenite present in the structure of EN24 steel alloy. They are using two different heat treatments in this work, the conventional heat treatment (CHT) and shallow cryogenic treatment (SCT). The results of this investigation reveals that the amount of the retained austenite for heat treatment (SCT) less than 2%, but for heat treatment (CHT) about 15%, at the sometime increasing in toughness and ductility.

2. EXPERIMENTAL PROCEDURE

2.1. Material Used

The selected material for this work is EN25. Table 1 and Table 2 show the chemical composition and mechanical properties of EN25 steel respectively, **Funda**, **2012**.

2.2. Preparation of The Specimens

The EN25 steel specimens have been prepared by machining them to suitable dimensions, 20 mm in length and 10 mm in diameter. Then all the specimens are grinded with emery paper (320, 500 and 1000 μm) by using Al_2O_3 with 1 μm in size and polished with suitable polishing cloth by using diamond paste.

2.3. Heat Treatment

The prepared test specimens were adapted to treat by quenching. The specimens were heated at 850c^o for 1hr. in an electrical furnace. After heating, the specimens were cooled rapidly in three different quenching media (salt water, water and oil). After quenching, the specimens were tempered at 300℃ for 1 hr. and then cooling in air **Senthilkumar**, **and Ajiboye**, **2012**. The electrical furnace used in this work as shown in **Fig.1**.

2.4. Hardness Test

The hardness values of all the specimens before and after hardening by quenching were measured by Vickers method using 20 Kg for 15 Sec. Vickers hardness number can be calculated by using the following formula, **Bolton, 1988**. For each specimen three readings were taken to define the average value of the hardness.

$$V.H.N = 1.8544 \times F/d_{ave.}^2 \qquad (1)$$

3. WEAR TEST

Wear test is carried out by using pin-on-disc technique to define the wear rate for all the specimens before and after heat treatment by quenching in the different quenchants (salt water, water and oil). **Fig.2** shows the setup of wear test.

The specimens of this project are machined to suitable dimensions 20mm in height and 10mm in diameter. Specimens for wear test are grinded and polished before and after treatment by quenching, wear test is done by fixing the specimen against the hardened disc (45 HRC) rotating at 750 r.p.m.

Wear test was done by changing the vertical applied loads as 5, 10, 15, 20 and 25 N and changing the time as 5, 10, 15, 20, 25 and 30 min respectively. For each specimen before and

after heat treatment the loss in weight is computed by sensitive electronic balance with accuracy about 0.1 mg (Type Mettler AE-60- made in China).

Wear rate of all the specimens was computed by using the following formula:

$$Wear\ rate = \Delta w / 2\pi . r.n.t \quad (2)$$

$$\Delta w = w1 - w2 \quad (3)$$

4. SURFACE ROUGHNESS TEST

Table 3 shows the average values of roughness before and after wear test. Surface roughness of the specimens before and after wear test was carried out by using apparatus type Talysurf_4 products by English Taylor_Hobson company to measure roughness average (Ra), as shown in **Fig.3**.

5. RESULTS AND DISCUSION

5.1 Microstructure Evaluation

The microstructures of the specimens before heat treatment by quenching consist of ferrite and pearlite. Heat treatment by quenching is carried out at austenization temperature, and then the specimens rapidly cooling in quenching media. In this work the quenching media are salt water, water, oil respectively. Since the cooling is rapidly by the quenching, martensite phase forming immediately with some amount of the retained austenite which affected with temperature of quenching and the percentage of carbon for the steel. Since the martensite is brittle and hard, it leads to form internal stresses, **Joshua, et al., 2014**. However heat treatment by tempering must be carried out to minimize the internal stresses. Quenching by salt water leads to obtain more martensite with little retained austenite due to the cooling for salt water more rapidly than for another quechants as shown in **Fig.4**.

5.2. Effect of Different Quenchants on Hardness

The effect of different quenchants on the hardness of the specimens is shown in Table 4. From this table it is showed that the highest value of hardness obtained by cooling in salt water more than for water and oil, it is attributed to that the cooling rate for salt water more than for another quenchants, which in turn leads to form a large amount of martensite comparing with another quenchants with little amount of retained austenite as shown in **Fig.5**. The results of the hardness of the specimens treated by different quenchants are agreed with **Singh, and Mondal, 2014**.

5.3. Effect of Diffrent Quenchants on Wear Rate

Increasing the loads and the time for wear test leads to increase the wear rate for all the specimens as shown in **Fig.6** and **Fig.7.**

Since the cooling rates are different for the quenchants, therefore the wear rates are different also. It can be noted clearly from these figures that the higher wear rate is for quenching by oil and then for water and salt water respectively. It exhibits that wear rate can be minimized significantly by hardening in suitable quenchant, it is due to generation the martensite phase which leads to increasing the hardness and then decreasing wear rate, this agrees with **Hasson**, **2013**. It can be noted clearly that for salt water the wear rate less than for water and oil because of the rapidly cooling for salt water producing the hardened martensite which in turn gave highest wear resistance. Here the results agreed with **Sultana, and Islam, 2014**.

5.4. Effect of Different Quenchants on Surface Topography

Fig.8 shows the micrographs of surface topography of the specimens quenching by different quenchants. Through the wear test, there are three mechanisms observed for the treated specimens, there are adhesive, material transfer and oxidation with plowing. By changing the loads and the time many grooves were formed as a result of micro cutting of the worn surfaces without plastic deformation, which in turn lead to make the surface more roughness. Increasing the loads of wear test leads to increase the roughness, because of the formation of the grooves as a result of wear mechanism. The roughness for salt water less than for water and oil, it is attributed to that the hardness for the quenching by oil more than for water and oil and it than decreases the roughness, **Boded, et al., 2011**. The visible plowing grooves are smoother for the specimen surface quenched by salt water because of highest hardness, while the worn surfaces for the specimens quenched by water and oil have deeper grooves and parallel respectively. At the same time fine wear debris were formed as a result of the rotating between the specimens and the hardened disc, as well as forming layers of oxides. The oxidation layers obtained because of the heating occurred as a result of friction between the specimens and the rotating disc.

6. CONCLUSIONS

1- Wear rate increases with increasing the loads and time for all the specimens before and after quenching heat treatment for all the quechants.

2- Wear resistance and hardness for the specimen quenched by salt water more than for water and oil.

3- Roughness for the specimen quenched by Salt water lower than for Water and Oil.

7. REFRENCES

- Alabi, A. A., Obi A. I., Yawas, D. S., Samotu, I. A. and Stephen S. I., 2012, *Effect of Water Temperature on Mechanical Properties of Water Quenched Medium Carbon Steel*, Journal of Energy Technologies and Policy, Vol.2, No.4, pp.40-45.

- Bolton W., 1988, *Engineering Materials Technology*, Butter Worth Heinemann Oxford.

- Boded, O. R., Ojo, P. O., Ayodele, O. R., Owa, A. F. and Ajayi, O. B., 2011, *Evaluation of As-Quenched Hardness of 1.2% Carbon Steel in Different Quenching Media*, Journal of Emerging Trends in Engineering and Applied Sciences, Vol.3, No.1, pp.127-130.

- Fadara,D. A., Fadara T. G., and Akanabi, O. Y., 2011, *Effect of Heat Treatment on Mechanical Properties and Microstructure of NST 37-2 Steel*, Journal of Mineral and Materials characterization and Engineering ,Vol.10, No.3, pp.299-308.

- Funda, E., 2012, *Properties of Carbon Steel EN25 (AISI4340)*.

- Hasson, E. O., 2013, *Effect of Quenching Media on Wear Resistance of AISI 52100 Bearing Steel Alloy*, Engineering and Technology Journal, Vol.31, No.14, pp2692-2699.

- Ismail, N. M., Katif N. A., Kamil M. A., and Hanafiah, M. A., 2016, *The effect of Heat Treatment on the Hardness and the Impact properties of Medium Carbon Steel*, Material Science and Engineering,Vol.114, pp.1-8.

- Jasiwal, S. K., Sharma, T., and Rajesh, M., 2015, *Study the Effect of Heat Treatment processes on Hardness and the Microstructure of Medium Carbon Steel*, International Journal of Emerging Technology and Advanced Engineering, Vol.5, pp.229-239.

- Joshua, T. O., Alao, O.A., and Oluyori, R.T., 2014, *Effect of Various Quenching Media on the Mechanical Properties of Inter Critically Annealed 0.267%C- 0.83% Mn Steel*, International Journal of Engineering and Advanced Technology, Vol.3, Issue.6, pp.121-127.

- Karthikeyan, K.M., Raj, R.J., Dinesh, R., and Kuman, R.A., 2014, *Effect of Subzero Treatment on Microstructure and Material Properties of EN24 Steel*, International Journal of Modren Engineering Research, Vol.4, Issue.11, pp.2249-6645.

- Murugan, V. K., and Mathews, P. K., 2013, *Effect of Tempering Behavior on Heat Treated Medium Carbon (C35Mn75) steel*, International Journal of Innovative Research in Science Engineering and Technology,Vol.2, Issue 4, pp.945-950.

- Motagi, B.S., and Bhosle R., 2012 , *Effect of Heat Treatment on Microstructure and Mechanical Properties of Medium Carbon Steel*, International Journal of Engineering Research and Development, Vol.2, Issue1, pp.7-13.

- Naveena H. S., Ramesha C. M., and Harish K. R., 2015, *A study on Mechanical Properties of Heat Treated Medium Carbon Low Alloy Steels*, International Journal for Technological Research In Engineering, Vol.2, Issue11, pp.2649-2654.

- Singh, D., and Mondal, D. P., 2014, *Effect of Quenching and Tempering Process and Shoot Peening intensity on Wear Behavior of SA-6150 Steel*, International Journal of Engineering and Materials Science, Vol.21, pp.168-178.

- Senthikumar, T, and Ajiboye, T.K., 2012, *Effect of Heat Treatment Processes on the Mechanical Properties of Medium Carbon Steel*, Journal of Minerals and Materials Characterization and Engineering, Vol.11, No.2, pp. 143-152.

- Sultana, N.F., and Islam, M., 2014, *Analysis of Mechanical Properties of Mild Steel Applying Various Heat Treatment*, International Conference on Mechanical, Industrial and Energy Engineering, pp.1-4.

- Tukur, S.A., Usman, M.M., Muhammad, I., and Sulaiman, N.A., 2014, *Effect of Tempering Temperature on Mechanical Properties of Medium Carbon Steel*, International Journal of Emerging Trends and Technology, Vol.9, No.15, pp. 798-800.

NOMENCLUTURE

d_{ave} = average indenter diameter, mm.
F = applied load, Kgf.
N = number of rotating's of the hardened disc.
R = the radius of the distance from the center of the center of the disc to the center of the specimen, mm.
T = time of the test, second.
V.H.N = vickers hardness number, Kgf/mm^2.
Δw = the changing in weight, (gm).
w1, w2 = the weight of the specimen before and after wear test, (gm).

Table 1. Chemical composition of EN25 steel in (wt. %).

Steel	%C	%Si	%Mn	%Ni	%Cr	%Mo	%S	%P
Standard value	0.4	o.3	0.6	1.5	1.2	0.25	0.005	0.01
Actual value	o.42	0.79	0.58	1.35	1.0	-	0.003	0.008

Table2. Mechanical properties of EN25 steel.

Yield Strength (MPa)	Tensile Strength (MPa)	Modulus of elasticity (GPa)	Elongation %	Hardness HV
850	635	190	13	265

Table 3. Show the readings of roughness average for the tested specimens.

The specimen	Load (N)	Values of (Ra) before wear(μm)	Values of (Ra) after wear (μm)
salt water	5	0.015	0.090
	10	0.107	0.198
	15	0.110	0.205
	20	0.203	0.278
	25	0.235	0.309
water	5	0.028	0.016
	10	0.113	0.149
	15	0.130	0.274
	20	0.210	0.276
	2 5	0.257	0.301
oil	5	0.109	0.167
	10	0.183	0.201
	15	0.243	0.299
	20	0.268	0.307
	25	0.279	0.321

Table 4. Show the values of hardness for the specimens with different quenchants.

Specimen	Hardness (HV)
As- received	265
Quenching in salt water & T300C^{o}	487
Quenching in water & T300C^{o}	394
Quenching in oil & T300C^{o}	301

Figure 1. Show the electrical furnaces for heat treatment.

Figure 2. Show the setup of wear.

Figure 3. Show the setup apparatus of roughness.

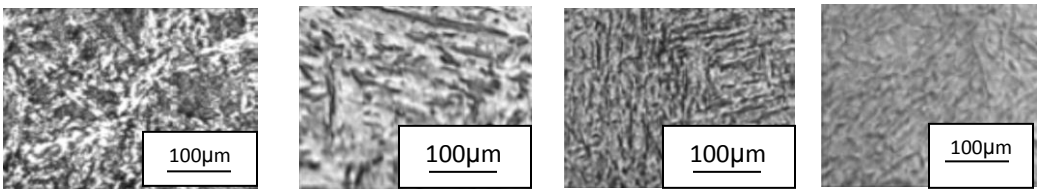

Figure 4. Photomicrographs of the specimens before and after treatment by quenching with magnification 250 X.
A-As –received.
B- Quenching by salt water.
C- Quenching by water.
D- Quenching by oil.

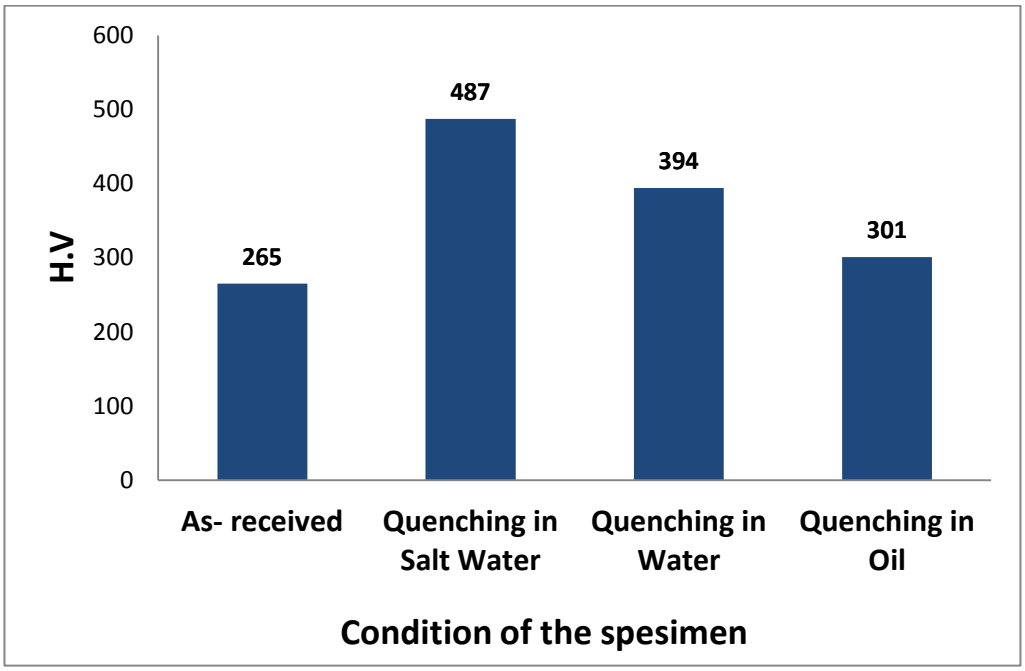

Figure 5. Show the values of hardness for the specimens with different quenchants.

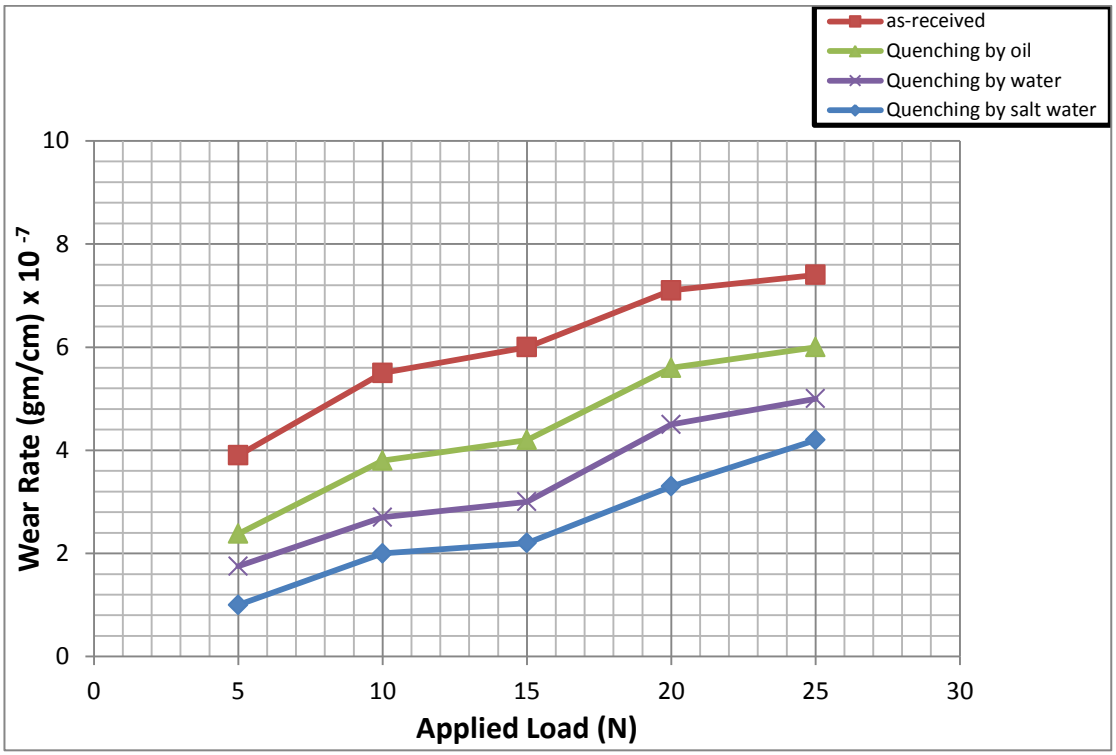

Figure 6. Relationships between wear rate and applied loads.

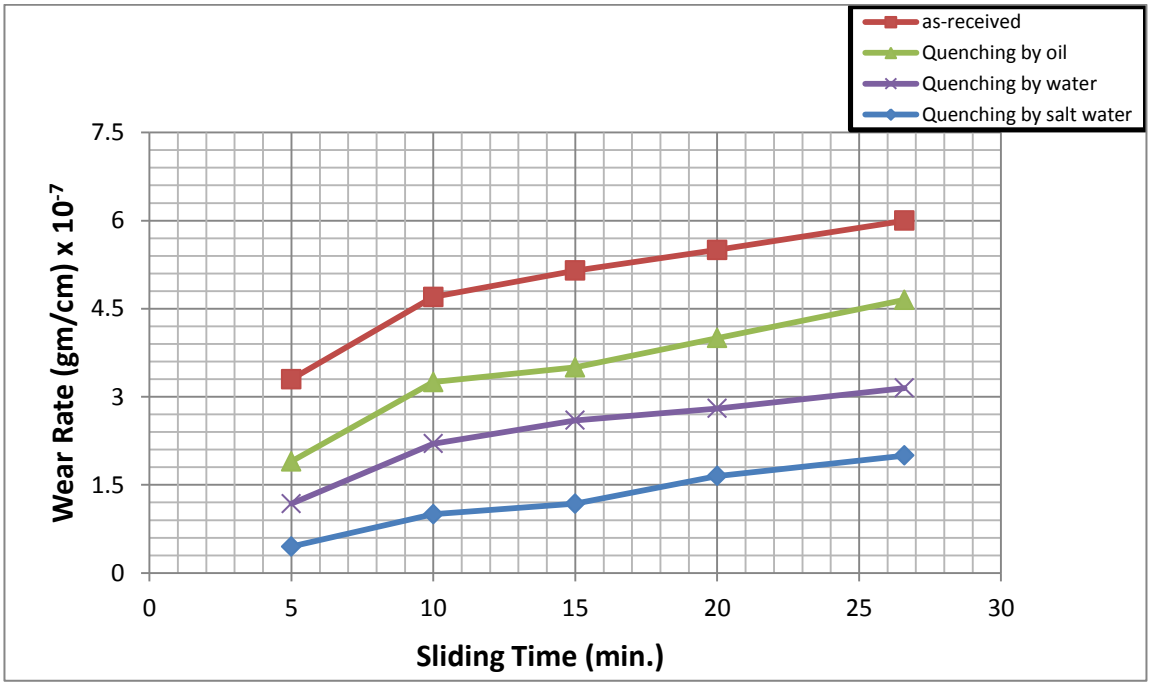

Figure 7. Relationships between wear rate and sliding time.

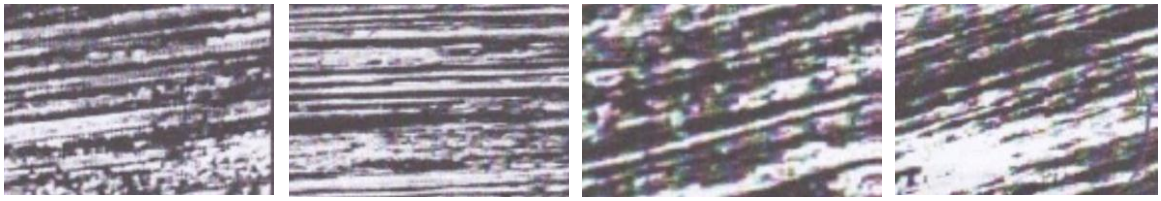

-A- -B- -C- -D-

Figure 8. Show the worn surfaces for the specimens treated by different quenchants before and after wear test at load 15N.

A. As –received.

B. Quenching by salt water.

C. Quenching by water.

D. Quenching by oil.

Comparison the Physical and Mechanical Properties of Composite Materials (Al /SiC and Al/ B_4C) Produced by Powder Technology

Khansaa Dawood Salman
Assistant Professor
Department of Electromechanical Engineering
University of Technology
E-mail: khansaadawood@yahoo.com

ABSTRACT

In this investigation, metal matrix composites (MMC_s) were manufactured by using powder technology. Aluminum 6061 is reinforced with two different ceramics particles (SiC and B_4C) with different volume fractions as (3, 6, 9 and 12 wt. %). The most important applications of particulate reinforcement of aluminum matrix are: Pistons, Connecting rods etc. The specimens were prepared by using aluminum powder with 150 µm in particle size and SiC, B_4C powder with 200 µm in particle size. The chosen powders were mixed by using planetary mixing setup at 250 rpm for 4hr.with zinc stearate as an activator material in steel ball milling. After mixing process the powders were compacted by hydraulic unidirectional press type (Leybold Harris No. 36110) at 250 Kg/cm^2 according to (ASTM-D 618). Finally the green compacts were sintered at 500 ℃ for 3 hr. by using electrical furnace with argon atmosphere. There are many examinations and tests were done for the produced metal matrix composites (MMC_S), (Al/ SiC and Al/B_4C) such as examination of the microstructure, mechanical tests (hardness and compressive strength), physical tests (density test before and after sintering, also porosity test). The results of this investigation showed that improving the physical properties (theoretical density, experimental density, porosity) and mechanical properties (Rockwell hardness and compressive strength).

Keyword: Composite materials, Powder technology, Physical Properties, Mechanical Properties.

مقارنة الخواص الفيزياوية والميكانيكية لمواد مركبة (المنيوم/ كاربيد السليكون، المنيوم/ كاربيد البورون) منتجة بطريقة تكنولوجيا المساحيق

خنساء داود سلمان
أستاذ مساعد
الجامعة التكنولوجية / قسم الهندسة الكهروميكانيكية

الخلاصة

في هذا البحث تم تصنيع مادة مركبة بطريقة تكنولوجيا المساحيق. تمت تقوية الألمنيوم 6061 بنوعين مختلفين من الدقائق السيراميكية (كاربيد السليكون ، كاربيد البورون) بنسب حجمية مختلفة 3، 6، 9، و12 % . من أهم تطبيقات التقوية بالدقائق لأرضية من الألمنيوم هي: المكابس، أذرع التوصيل . . الخ. تم تحضير العينات بأستخدام مسحوق الألمنيوم بحجم حبيبي 150 مايكرون ومساحيق كاربيد السليكون و كاربيد البورون بحجم حبيبي 200 مايكرون. تم خلط

المساحيق المستخدمة باستخدام خلاط كوكبي بسرعة 250 دورة / دقيقة لمدة 4 ساعات مع مادة سترات الزنك كمادة منشطة مع كرات طحن من الفولاذ. بعد عملية الخلط تم تدميج المساحيق بمكبس هيدروليكي أحادي الأتجاه نوع (Leybold Harris No. 36110) بمقدار 250 كغم/ سم^2 بموجب المواصفة (ASTM-D 618). أخيراً تم تلبيد المدمجات الخضراء عند درجة حرارة 500م^o لمدة 3 ساعات بأستخدام فرن كهربائي في جو من الآركون. أجريت العديد من الأختبارات والفحوصات للمواد المركبة المنتجة (ألمنيوم / كاربيد السليكون ، ألمنيوم/ كاربيد البورون) مثل فحص البنية المجهرية ، أختبارات الصلادة ومقاومة الضغط، أختبارات الكثافة قبل وبعد التلبيد، كذلك أجري أختبار المسامية. أظهرت نتائج هذا البحث تحسن واضح في الخواص الفيزياوية (الكثافة النظرية ، الكثافة التجريبية، المسامية) والخواص الميكانيكية (صلادة روكويل، مقاومة الأنضغاط).

الكلمات الرئيسية: مواد مركبة، تكنولوجيا المساحيق، خواص فيزيائية، خواص ميكانيكية.

1. INTRODUCTION

In recent years an important researches were done to enhance the mechanical properties of aluminum alloys by reinforcing them with ceramics particles such as SiC, B_4C, TiC and Al_2O_3, **Zhenga, et al., 2014**. Since the aluminum and its alloys have an attention as an important metal to obtain metal matrix composites (MMC_S) and more applications in technology. To combine the light weight, corrosion resistance with mechanical properties such as the strength, hardness and impact resistance leads to make the aluminum and its alloys important matrix materials, **Muthukrishnan, et al., 2008, Khairaldien**, **et al., 2008**, **and Ahmed, et al., 2009**. There are many reinforcement materials used for aluminum matrix because of their strength are related with their particle size, the microstructure and how they are distributed in the matrix which in turn improving the mechanical and physical properties of the producing aluminum matrix composites, **Attar**, **et al., 2015**. Powder metallurgy is an important technique using to obtain metal matrix composites with high homogeneity more than for other methods, **Nazik, et al., 2016**. There are many researches were published in this field like, **Ekiki, et al., 2010**. Investigated the effect of SiC and B_4C on the characteristics of the surface for the composites material. This study concluded that there are many factors affected on the produced composites materials such as particle size, volume fraction of the additive reinforced material. While **Nagard, et al., 2013**, studied the effect of the addition of Al_2O_3 on the mechanical and wear behavior of the composites materials of 6061 Al alloy metal matrix composites. The results of this work showed that the wear resistance of B_4C is lower than that of SiC particulate reinforcement of metal matrix composites (MMC_S). The aim of this work is to study the physical and mechanical properties of metal matrix composites reinforced by two different of particulate reinforced materials SiC and B_4C for the matrix Al – 6061 alloy.

2. EXPERIMENTAL PROCEDURE

In this work, the composite materials Al/SiC and Al/ B_4C are manufactured by using powder technology as the following stages:

2.1 Preparing the Powders

The aluminum 6061 powder at 150 μm was in particle size, while the particulate reinforcement SiC and B_4C at 200μm in particle size. Table 1 shows the characteristics of the powders used in this investigation.

2.2 Mixing the Powders

Two different composite materials were prepared by mixing the aluminum 6061 powders as a matrix at 150μm in the particle size with SiC and B_4C as a reinforcement material at 200μm in the particle size and adding zinc stearate as activator. Mixing process was carried out by using planetary mixture as shown in **Fig.1** with steel ball mill in 10 mm diameter at 250 rpm for 3 hr.

2.3 Compacting Process

Compacting process for a mixture of the powders about 30gm in uniaxial hydraulic press type (Leybold Harris No.36110), and then the mixed powders were pressed at 250 Kg/ cm^2 in punch – die set assembly as shown in **Fig.2**. Inside die wall and the surface of punch touch with the die were lubricated with graphite powder to prevent the green compacts from adhesion with die wall and don't crush during get out the die. The green compacts were weighing by accuracy balance to calculate the density of them.

2.4 Sintering Process

Sintering process was done at 500℃ for 3 hr. in electrical furnace with inert atmosphere (argon), sintering temperature increases with increasing the percentage of particulate reinforcements to obtain the composites with high strength. After sintering, it must be to calculate the density by divided the weight of the specimen to the volume.

2.5 Examinations and Tests

2.5.1 Microstructure examination

Microstructure examination of the Al/ Si and Al/ B_4C composites were done by using optical microscopy, before the examination of the microstructure, the specimens were cutting and machined by lathe, and then grinded by grinding device with emery paper (500 and 1000) μm in particle size. Following the grinding, the specimens were polished by polishing device using diamond paste at size 0.7 μm for 30 min to obtain surfaces like mirror. Final stage for preparing the composite specimens is etching them with 1% Keller reagent for 30 sec and then washing with water before the examination for the microstructure.

2.5.2 Density test

Density test was carried out for the specimen before and after sintering. The differences in values of density mean that there is porosity in the specimens. Porosity of the specimens before and after sintering was calculated by using Archimedes formula.

The theoretical densities of metal matrix composites are measured by using the following equation, **Venkatesh, and Harish, 2015.**

For Al/SiC $$\rho_c = \frac{1}{\frac{W_{Al}}{\rho_{Al}} + \frac{W_{SiC}}{\rho_{SiC}}} \quad (1)$$

For Al/B_4C $$\rho_c = \frac{1}{\frac{W_{Al}}{\rho_{Al}} + \frac{W_{B4C}}{\rho_{B4C}}} \quad (2)$$

While the actual density after the sintering was calculated by using the following equation, **Jain, et al., 2016.**

$$\rho_s = \frac{m_{a} \times \rho_w}{m_{a-} m_w} \quad (3)$$

The porosity of the specimen was calculated by the following equation:

$$Porosity\ \% = 1 - \frac{\rho s}{\rho th} \quad (4)$$

2.5.3 Hardness test

Hardness test was carried out for the specimens before and after sintering by using Rockwell hardness equipment (Wilson Hardness machine, USA Model: LM 2481 T). Composites specimens were tested by using (B) scale of Rockwell machine with hardened steel ball as an indenter of 100 Kg were used for all the specimens. For each specimen, three readings were taken at least and then determine the average of the three readings.

2.5.4 Compressive test

Compressive test was carried out for the specimens before and after sintering by using Instron Universal Tester (type Instron 1195 machine with full capacity 2.5 ton). The specimens were manufactured with 1.5 cm in height and 1 cm in diameter. All the specimens were compressed at 1 ton until the specimen were crushed. Stress – Strain curve was plotted for each composite material to obtain modulus of elasticity, yield strength and compressive strength. Compression strength is calculated by the following formula:

$$\sigma = \frac{2F}{\pi dh} \quad (5)$$

3. RESULTS AND DISCUSION

3.1 Microstructure Analysis

The morphology of the sintered metal matrix composites was done by using optical microscopy. SiC and B_4C particulates were agglomerated in small volume fractions of them, while increasing the volume fractions of SiC and B_4C lead to make the particles to distribute homogeneously in aluminum matrix and strong bonding was created between the particulate reinforcement material and matrix as shown in **Fig.3**. As a result of compacting and sintering, there are pores defects were obtained in the composites materials. During sintering the particles of the mixing powders were joining together as a result of the welding between them, also during sintering process, zinc stearate evaporated and then causes to form porosity as a substitution of it is observed from **Fig.4** that the increasing wt% of Sic and B_4C leads to increase % porosity, and then decreasing % porosity for SiC and B_4C more than 9% of them. It is perhaps at attributed to that the porosity acts as internal stresses at the interfaces between the Sic, B_4C particles and aluminum matrix.

3.2 Compacting and Sintering

The particulate reinforcement material increases the density during compacting and sintering. Condensation occurs during compacting process and the particles close together with increasing the pressing force, while during the sintering process as a result of thermal welding between the particles, and then forming the necking between them which in turn causes the shrinkage of the sintered specimens and in turn lead to improve the density which represents an important of physical property, **Khairaldien, et al., 2007**. At the same time the temperature of sintering process created a strong binding between the particulate reinforcement materials and the matrix which affected on mechanical properties such as yield strength, ultimate tensile strength and hardness because of the dispersion of particulate reinforcement materials in the matrix, which causes a higher density of dislocation and make dislocation loop around a reinforcement particles preventing them from any motion between them. **Sun, et al., 2011**, in general, the density of composite material decreases with increasing the volume fraction of the additive nanoparticles; it is attributed to that the decreasing of the wettability with increasing the volume fraction of SiC, B_4C and at the same time forming the pores at the interfaces between SiC, B_4C and the matrix, the density with SiC more than for B_4C and also higher than for the aluminum matrix. **Fig.5** shows that obviously.

3.3 Effect of SiC and B_4C on the Hardness of Composite Material

Mechanical properties of composite material dependent strongly on the volume fraction, properties of the particulate reinforcement material, size of the additive particles. Increasing the

volume of SiC and B_4C leads to increase the hardness of the manufactured of composite manufactured of composite material. The hardness of composite material with SiC higher than for composite material with B_4C, it is return to that the SiC was made strong binding with aluminum matrix higher than for B_4C, also the particles of SiC prevent the dislocations and pining them at their sites, and then increasing the hardness of the manufactured composite material. This result is agreed with that of **Jeevan, et al., 2012**. **Fig.6** shows that increasing the volume fraction of SiC and B_4C leads to increase the Rockwell hardness.

3.4 Effect of SiC and B_4C on Compressive Strength

The compressive strength of a particle reinforced metal matrix composite is extremely dependent on volume fraction of the additive particles and their sizes. Increasing the percentage of SiC and B_4C leads to increase the yield strength and compressive strength, it is attributed to that the reaction between particles and the matrix which created thermal stresses because of the differences between the melting point of SiC, B_4C and aluminum as a matrix, and then in turn increases the dislocation density. The reinforced particles obstacle the dislocation to move from one particle to another and then increases the yield strength and compressive strength. **Fig.7** shows that the increasing of volume fraction of SiC, B_4C increases the compressive strength. SiC increases the compressive strength more than B_4C for the same reasons mentioned previously. The result of this test is agreed with **Shorowordi, et al., 2003**.

4. CONCLUSIONS

Increasing the volume fractions of SiC and B_4C for 6061 Al matrix leads to improve the mechanical properties such as hardness and compressive strength.

1. Increasing the volume fractions of SiC and B_4C for 6061 Al matrix leads to improve the physical properties such as theoretical density, experimental density and porosity.

2. Small volume fractions of SiC and B_4C were agglomerated in 6061 Al matrix, while increasing the volume fractions of SiC and B_4C were distributed homogeneously in 6061 Al matrix, and the prefer percentage of SiC and B_4C is (9%).

3. Improving the mechanical properties and physical properties for SiC more than for B_4C.

5. REFRENCES

- Ahmed, A. R., Asokan, P., and Aravindan, S., 2009, *EDM of hybrid Al-SiC_P –$Glass_P$ MMC_S*, International Journal of advanced manufacturing technology, Vol.44, No.5, , pp.520-528.

- Attar, S., Nagaral, M., Reddapa, H. N., and Auradi, V., 2015, *A review on particulate reinforced aluminum metal matrix Composites*, Journal of emerging technologies and innovative research (JETIR), Vol. 2, Issue, pp.225-229.

- Callister, W. D., and JR., 2003, *Material Science and Engineering, An Introduction*, John Wiely and Sons Inc., New York.

- Ekiki, R., Apalak, M. K., Yildirim, M., and Nair, F., 2010, *Effect of random particle dispersion and size on the indentation behavior of SiC particle reinforced metal matrix composites*, Materials and Design, Vol. 31, pp. 2818-2833.

- Jain, S., Rana, R. S., and Jain, P., 2016, *Study of Microstructure and Mechanical Properties of Al-Cu matrix reinforced with B_4C particles Composite*, International research Journal of engineering and technology (IRJET), Vol.3, Issue. 1, pp 499-504.

- Jeevan, V., Rao, C.S., and Selvaraj, N., 2012, *Compaction, sintering and mechanical properties of Al-SiC_p composites*, International Journal of mechanical engineering and technology (IJMET), Vol.3, Issue.3, pp. 565-573.

- Khairaldien, W. M., Khalil, A. A., and Bayoumi, M. R., 2007, *Production of Aluminum-Silicon Carbide Composites using Powder Metallurgy at sintering temperature above the aluminum melting point*, Journal of testing and evaluation, Vol. 35, No.6, pp. 111-125.

- Khairaldien,W.M., Khalil, A.A., Bayoumi, M.R., 2007, *Production of aluminum-silicon carbide composites using powder metallurgy at sintering temperatures above the aluminum melting point*, Journal of Testing and Evaluation. 35(6)111-125.

- Muthukrishnan, N., and Murugan, M., Rao, K. P., 2008, *Machinability Issue in turning Al-SiC (10%) metal matrix Composites*, International Journal of advanced manufacturing technology, Vol.17, No.3, pp. 1220-1228.

- Nazik, C., Tarakcioglu, N., Ozkaya, S., Erdemir, F., and Canakci, A., 2016, *Determination of effect of B_4C content on Density and Tensile Strength of AA 7075/ B_4C Composite produced Via Powder Technology*, International Journal of Materials, Mechanics and Manufacturing, Vol.4, No.4, pp.251-254.

- Nagard, M., Bharath, V. and Auradi, V., 2013, *Effect of Al_2O_3 particles on mechanical and wear properties of 6061 Al alloy metal matrix composites*, Journal of Material science and Engineering, Vol. 2, No. 1, pp. 120-128.

- Sun, C., Song, M., Wang, Z., and He, Y, 2011, *Effect of Particle Size on the Microstructures and Mechanical Properties of SiC-Reinforced Pure Aluminum Composites*, Journal of Materials Engineering and Performance. 20(9) 1606-1612.
- Shorowordi, H.A., Laoui, T., Haseeb, A.S., Celis, I.P., and Froyen, L., 2003, *Microstructure and interface characteristics of B_4C, SiC and Al_2O_3 reinforced Al matrix composites: a comparative study*, Journal of materials processing technology, Vol.14, pp. 738-743.
- Venkatesh, B., and Harish, B., 2015, *Mechanical Properties of Metal Matrix Composites (Al SiC_P) particles produced by Powder Metallurgy*, International Journal of Engineering Research and General Science, Vol.3, Issue, pp. 1277-1284.
- Zhenga, R., chena, J., Zhanga, Y., and Mab, K. A., 2014, *Fabrication and characterization of hybrid structured Al alloy matrix coposites reinforced by high volume fraction of B_4C paticles*, ELSEUIER, Materials Science and Engineering Al6061, pp20-28.

NOMENCLUTURE

d: diameter of the specimen(mm).

F: applied load (N).

h: height of the specimen(mm).

m_a : weight of the specimen in air (gm).

m_w: weight of the specimen in water (gm).

WAl: weight fraction of aluminum.

W SiC: weight fraction of silicon carbide.

W B_4C: weight fraction of boron carbide.

ρc : composite density (g /cm^3).

ρAl: density of aluminum (2.7 g/ cm^3).

ρSiC: density of silicon carbide (3.1 g/ cm^3).

ρB_4C: density of boron carbide (2.51 g/ cm^3).

ρ_s: density of sintered specimen (gm/ cm^3).

ρ_w: density of water (gm/ cm^3).

ρs : density of sintered specimen (gm/cm^3).

ρth: theoretical density of the specimen(gm/ cm^3).

Table 1. Showing characteristics of the powders, **Callister, W. D., and JR., 2003**.

Specimen No.	Powder	Size (μm)	Density (gm/cm^3)
1	Al 6061	150	2.7
2	SiC	200	3.1
3	B_4C	200	2.51

Figure 1. Show the mixture for the powders.

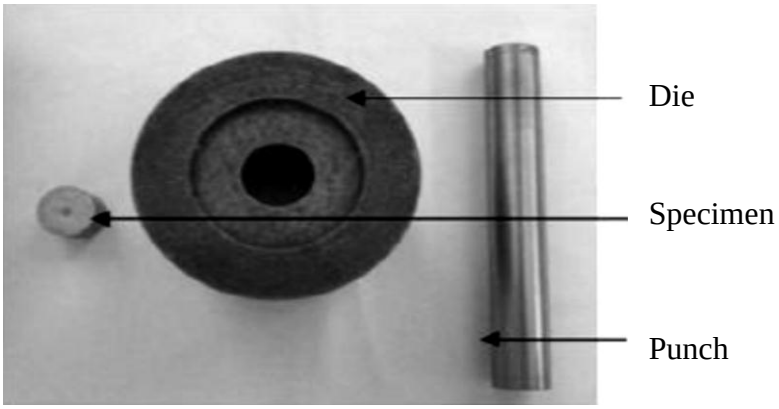

Figure 2. Show the mould for compacting process.

Without SiC and B_4C

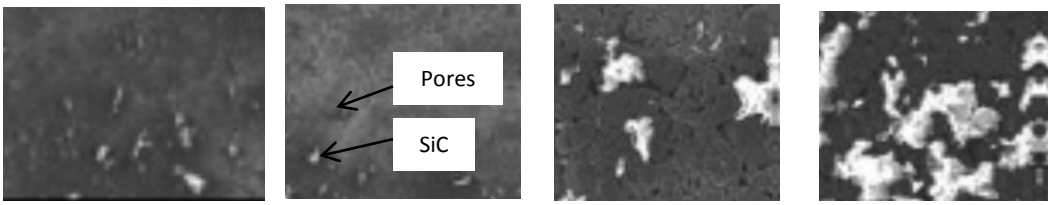

3% SiC 6% SiC 9% SiC 12% SiC

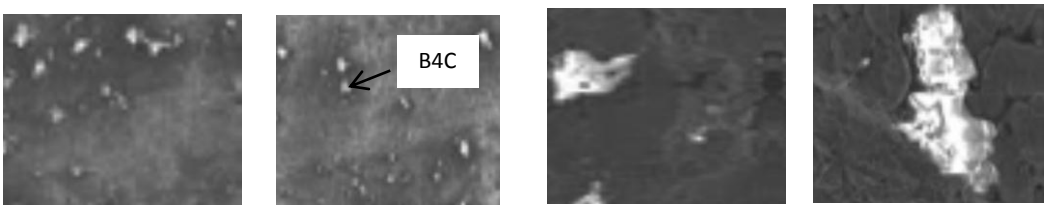

3% B_4C 6% B_4C 9% B_4C 12% B_4C

Figure 3. Showed that the micrographs of the specimens before and after adding SiC and B_4C with different weight frictions.

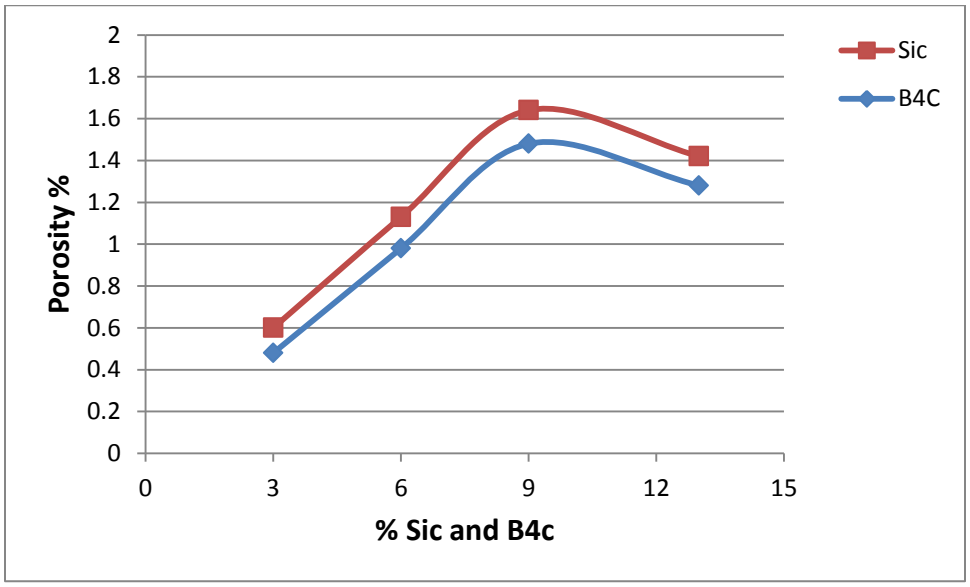

Figure 4. Showed the porosity % forming in composite materials.

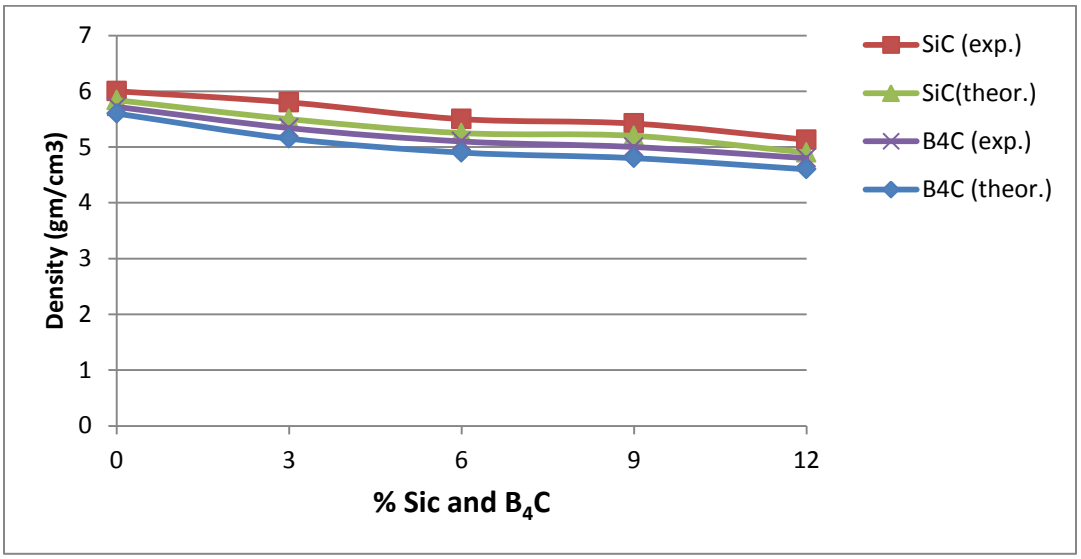

Figure 5. Showed the density forming in composite materials.

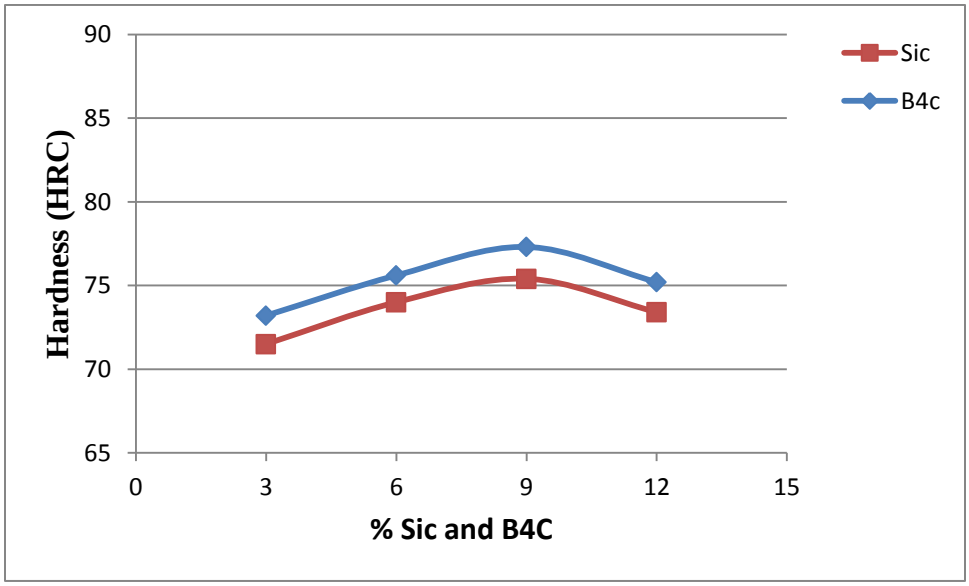

Figure 6. Showed the hardness forming in composite materials**.**

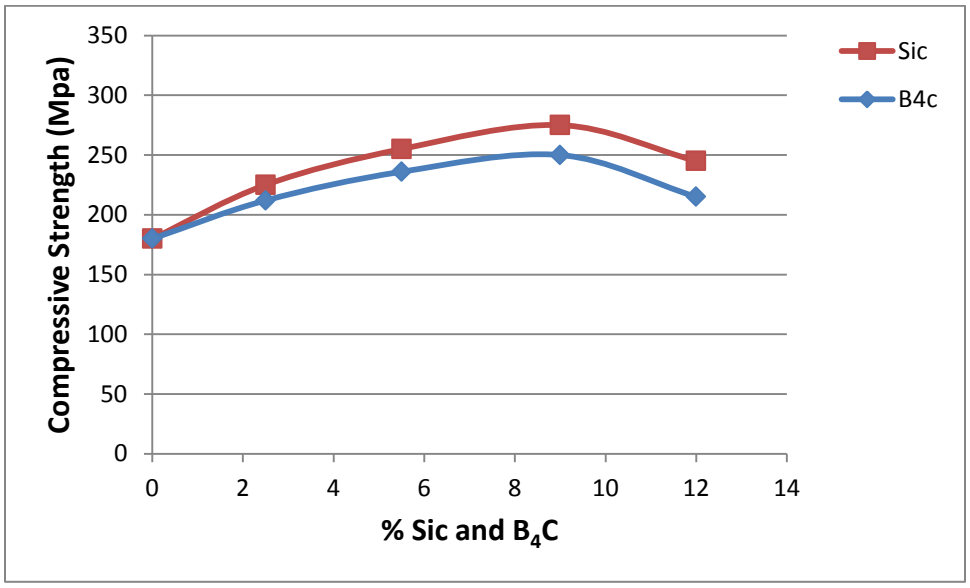

Figure 7. Showed the compressive strength forming in composite materials.

Bit Record Analysis for Bits Evaluating and Selection

Amel Habeeb Assi

Teacher assistant

College of Engineering - Baghdad University

E-mail: zahraa_z91@yahoo.com

ABSTRACT

The bit record is a part from the daily drilling report which is contain information about the type and the number of the bit that is used to drill the well, also contain data about the used weight on bit WOB ,revolution per minute RPM , rate of penetration ROP, pump pressure ,footage drilled and bit dull grade. Generally we can say that the bit record is a rich brief about the bit life in the hole. The main purpose of this research is to select the suitable bit to drill the next oil wells because the right bit selection avoid us more than one problems, on the other hand, the wrong bit selection cause more than one problem. Many methods are related to bit selection, this research is familiar with four of those methods, which they are: specific energy method, bit dullness way, cost per foot method, offset well bit record and geological information way. Five oil wells have been studied in Rumaila Oil Field in South of Iraq which they are R-531, R-548, R-536, R-544 and R-525. The wells R-531, R-536 and R-525 are vertical wells; the wells R-548 and R-544 are directional wells at angle of inclination 8.79° and 16.62° respectively.

Key words: bit record, selection, bit, rate of penetration.

تحليل سجلات الحافرة من اجل تقييم اختيار الحافرات

امل حبيب عاصي

مدرس مساعد

كليه الهندسه –جامعه بغداد

الخلاصة

سجل الحافرة عبارة عن جزء من التقرير اليومي للحفر والذي يتضمن معلومات عن نوع وعدد وحجم الحافرات المستخدمة لحفر ذلك البئر.ويتضمن سجل الحافرة ايضا معلومات مهمة اخرى مثل مقدار الوزن المسلط على الحافرة ومقدار معدل دوران عمود الحفر في الدقيقة الواحدة ومقدار معدل الاختراق وعدد الاقدام المحفورة وضغط المضخة وايضا يتضمن هذا السجل معدل تلف او تضرر الحافرة نتيجة عملية الحفر.بعبارة اخرى يمكن القول بان سجل الحافرة هو ملخص لحياة الحافرة داخل البئر اثناء عملية الحفر.الهدف الرئيسي من هذا البحث هو لاختيار الحافرات المناسبة لحفر الابار الجديدة وذلك من خلال تحليل سجل الحافرة لابار نحفورة سابقا لانه الاختيار الصحيح لحافرة يجنبنا الكثير من المشاكل اثناء الحفروالعكس صحيح.توجد اكثر من طريقة لاختيار الحافرات منها طريقة الطاقة المحددة وطريقة تلف الحافرة وطريقة كلفة حفر القدم الواحد وطريقة سجل الحافرة والمعلومات الجيلوجية. 5 ابارفي حقل الرميلة جنوبي العراق اختيرت للدراسة ثلاثة من هذه الابار عمودية والاخران موجهان بزاوييتي 8.79درجة و 16.62 درجة على التوالي. وتم حفر تلك الابار باستخدام انواع مختلفة من الحافرات منتجة من ثلاث شركات مختلفة وتم تقييم ادائية تلك الحافرات اعتمادا على اسس طرق اختيار الحافرات

الكلمات الرئيسة :سجل الحافرة،اختيار،حافرة،معدل الاختراق.

1. INTRODUCTION

All rig parts have one main purpose: to put a bit on the bottom of a hole and turn it to the right. Rig owners and operators want a bit that gives a good rate of penetration. They also want the bit to have longevity. The consideration that most affects bit selections the type of rock, or formation, the bit must drill. Even though many types of formation exit, it is not practical for rig operators to change bits every time. In this case, the rig operators would probably select a bit designed to drill medium-soft rock or medium-hard. Manufactures make bits to drill various formations hardness **Bela, 2012.**

This research shows how to get benefit of the data from bit record to select the suitable bit for drilling the next oil wells. These data belongs to five oil wells in south of Iraq**.** Since the bits that drilled those sections didn't enter to the well and get out from it without any damaging, bit dull grading is the window that from it, it can be known what happened to the bit that drilled those depths. To get most footage and fastest penetration rate, and therefore the lowest cost, the operator or contractor must choose the right bit for the job. Operators have several ways of getting information to make this decision. Dull bit records from nearby wells show wear to the bits used to drill them. For each well, the driller keeps a record of the depth, type of rock, fluids, and anything else interesting about the operation. Bit record is helpful when drilling subsequent wells in the same field**. Aswad, 1996**.

2. BIT SELECTION AND EVALUATION:

There is more than one way for choosing the best bit for drilling the oil wells, which they are:
1-specific energy way
2-bit dullness way
3- Offset well bit record and geological information way. **Allen, 1980.**
4-cost per foot way
The SE method depend on the minimum energy that is loosed at the bit to choose the bit, while bit dull grade method depending on the degree of the dull characteristic that occurred at the bit during drilling the well. A little bit damage mean good bit type and manufacturing and more bit damaging, mean bad bit manufacturing and type. Generally, not the good bit manufacturing and type effect on the bit dull grade, the drilling parameters, hydraulic and the type of formation, all of them affect in great degree on bit dull grade. This study deals with all of pervious ways **Rabia ,1982** .Depending on available data, this research is interested with the all the above ways of bit selection .

2.1 Specific Energy Method

The specific energy method gives an easy method for the suitable bits. It is defined as the demanded energy to remove one unit volume from the drilled rock.it can be taken any homogenous units. The equation of specific energy it can be derived by depending on the losses force at the bit in one minute.so,

$E=W*2* \pi r * N$ 1

Where:
E: The mechanical energy, lb.-inch.
W: Weight on bit, lb.
N: Revolution per minute, RPM.
R: Radius of bit, inch.
The equation of raised rock volume in one minute is:

V= $\pi r^2 * PR$ ……...2
Where:
PR: rate of penetration ft. /hr.
By dividing equation 1 and equation 2 to get the equation of specific energy
SE=E/V…….3
SE= W*2$\pi r * N/\pi r^2 * PR$ ……..4
Where:
SE: Specific Energy,lb-inch/inch^3
The equation of SE in lb-inch/inch^3 units is:
SE=10 WN/R*ROP……5
By using the diameter of bit D in equation 5 instead of R where R=D/2, the equation 5 Will be:
SE=20 WN/D*ROP……6
From equation 6, it's clear that any changeable in the value of WOB and N lead to change in the value of ROP, and that effect on the value of SE **Rabia ,1985**. It can be said that the SE method represent direct measurement for bit performance for the formation to be drilled, also it is an indicator to describe the interaction between the formation and the bit **Harold J., 2013**.
The value of SE don't represent an essential properties of drilled rock, it is depend in great degree on the bit design and type and manufacturing. The value of SE that result from drilling soft formation different completely from the value of SE that result from drilling hard formation, which mean the type of formation effect in great degree on the value of SE.it can be say that the SE method is accurate method to select the suitable bit type. The more economical bit (optimum bit), is the bit that give minimum value of SE **R.Harmer , 2013.**
Fig.1 shows the relation between the SE and the cumulative footage for three vertical oil wells which they are: R-525, R-531 and R-536, the value of SE is calculated by using eq.6. The columns 2, 3, 4 in **Table 1**,**Table 2** and **Table 3** represent the input data to get the column 4 in those tables by using eq.6.
For the vertical oil wells, the following points are found:

1- The smith bit of GS105BVC model is the best bit to drill 17.5 " ,R-531 from 454.2 ft. to 1862.22 ft. hole section by depending on the SE method.
2- From 1862 ft. to 4287.6 ft., 12.25" hole section .Comparing with the other two wells, the Baker H. Bit of HC606Z-PDC model in R-531 well is the best bit.
3- The Halliburton bit of SFD75H model that drilled 12.25 " hole section in R-536 well from 4287 ft. to 5874 ft. is the best bit.
4- From 5874ft to 7358ft, 8.5"hole section in well R-531. Baker H. bit of Q506X-PDC model gave the lowest value of SE.

Fig.2 Show the relation between the SE and the cumulative footage for tow directional oil wells which they are: R-544 and R-548, the value of SE is calculated by using Eq. (6) ,the column 2,3,4 in **Table 4** and **Table 5** represent the input data to get column 4 in those tables by using Eq.(6):

For directional oil wells, the following points are found:

1- From 454ft to 1862 ft., 17.5"hole section in well R-548. Baker bit of GTX-CG1 model gave the lowest SE value.
2- From 1862 ft. to 4000 ft., 12.25" hole section in well R-548. Baker bit of EP7199 model gave the lowest SE value.

3- From 4000ft to 6510 ft., 12.25" hole section in well R-544. SMITH bit of MSI616LPX model gave the lowest SE value.
4- From 6510 ft. to 7409ft 8.5" hole section in well R-544. Smith bit of MDi616LPX model gave the lowest SE value. As we can see above, by using the SE method, it can be make selection for the suitable bit to drill the next oil wells. The bits that gave the lowest values of SE is the preferred bits. **Fig. 3** show the relation between the SE and the cumulative footage for all the studied oil wells

For the all (five oil wells), the following points are found:

1- The R-548 well gave the lowest value of SE compared with the other studied oil wells for the 17.5"hole section.
2- The R-531 well gave the lowest value of SE compared with the other studied oil wells for the 12.25 "hole section.
3- The R-531 well gave the lowest value of SE compared with the other studied oil wells for the 8.5 "hole section.

2.2 Dull Bits Grading:

It is very important to grade dull bits properly. Grading a dull bit means estimating how much and where it has worn. Proper dull bit grading helps the operator and the contractor correct poor drilling practices, select the best type of bit for specific conditions, and make decisions that affect the cost of future drilling. It is a form of ongoing field testing that benefits all drilling contractors and operators **Nollely, 1986.** Roller cone bits and fixed –head (diamond) bits are both graded using an International Association of Drilling Contractor (IADC) dull bit classification system with eight categories as in **Table 6** Since fixed-head bits have no bearing, the column for bearing wear (B) always has an x in it when grading diamond bits. Roller con bits and fixed-head bits use the same dull bit grading system. They are grading on the basis of cutter wear, bearing wear (not for fixed-head), and gage wear **Glowka, 1983.**

Five wells have been studied each well consist of more than one section, the data that we have belong to 17.5",12.25" and 8.5" hole sections for each well. Five wells mean five 17.5" hole section and five 12.25" hole section and 8.5"hole section. Each section drilled by one bit or more than one bit, that depend on if that the bit is good and able to drill the planed footage .sometimes there are problems lead to use more than one bit. This study includes comparison each section in each well with the other same section size for the other wells. The comparing between those sections is about the degree of dullness to find the best bit from those bits to use it for drilling the next oil wells.

Table 7 and **Table 11** show that the 17.5"hole section in all studied wells drilled by using one bit type because this hole section is not deep and the drilled footage not more than 600ft . Also, the drilled formation in this hole section are Dibdiba, Lower Fars,Ghar,Dammam. The 17.5" hole section is drilled by using milled teeth bits in many wells. The first part from 12.25"hole section is drilled by using insert teeth bits and the second part is drilled by using PDC bits. The 8.5" hole section is drilled by using PDC bits also.

Our data show that the 12.25" is drilled by using more than one bit type because the 12.25" hole section is the longest drilled section compared with 17.5" and 8.5" hole section. From the other

hand the drilled formation in this hole section are Rus,UmmEr-Radhuma,Tayarat,Shiranish,Hartha and Sadi . In the case of directional section, the bit which drill vertical section differs from the bit which drill directional section because the directional section is drilled by using PDC bit and different BHA than those which is used in vertical section. The Roller cone bit (insert teeth bit or milled teeth bit) is just right for vertical section only, but the PDC bit is used to drill directional section and vertical section. The drilling of directional section needs special BHA like mud motor and Rotary Steerable System (RSS), PDC bit can be run with those BHA. **Table 12** and **Table 13** contain more details about the bits that was used to drill the studied oil wells.

The 12.25" hole size is drilled by using tow bit type in R-525 well and three bit in R-531well and tow bit in R-536 well and tow bit type in R-544 well and three bit in R-548 well. For the well R-525 the first bit is MDi616 bit, it was pulled due to slow ROP, Calcite stringer interbedded at top of Tayarat may have been cause of damage, the second bit MDi616E Bit was pulled at TD of 12 1/4" hole section. Bit was missing two cutters with three slightly chipped. Smith Bit of model MDI616EPX was drilled 8.5"hole section in well R-525, the bit was in relatively good condition, no chipped cutters, one nozzle lightly plugged, it can Rerun able to drill other well. This bit is used to drill the 8.5"hole section in well R-548, and as in **Table 9** Smith Bit of model MDI616EPX gave good bit dull grade, it can Rerun able to drill other well.

Depending on the degree of dull characteristic, the following points are found for vertical oil wells and as in **Tables 7, 8 and 9**:

1- From 136 ft to 1566 ft, 17.5" hole section R-536 the Halliburton bit ofEBXT08SLCmodel gave the lowest dull characteristic comparing with the others studied bits.

2- From 1696 ft to 4391 ft ,12.25" hole section R-525 Smith bit of MDi616 model gave the lowest dull characteristic comparing with the others studied bits.

3- From 4420 ft to 5723 ft ,12.25" hole section R-525 the Smith bit of MDi616Emodel gave the lowest dull characteristic comparing with the others studied bits.

4- From 5739 ft to 7327ft, 8.5" hole section R-525 the Smith bit of MDI616EPX model gave the lowest dull characteristic comparing with the others studied bits.

Depending on the degree of dull characteristic, the following points are found for directional oil wells and as in **Table 10** and **Table 11**:

1- From 136 ft. to 1566 ft., 17.5" hole section.R-544 and R-548 both of the bit have the same dull characteristic. Both of them gave good dull grade.

2- From 1696 ft. to 4391 ft ,12.25" hole section R-544 Smith bit oGFS10BVCf model gave the lowest dull characteristic comparing with the others studied bits.

3- From 4420 ft. to 5723 ft., 12.25" hole section R-544 the Smith bit of MSI616LPXmodel gave the lowest dull characteristic comparing with the others studied bits.

4- From 5739 ft. to 7327 ft,8.5" hole section R-548the Smith bit of MDi616LEPX model gave the lowest dull characteristic comparing with the others studied bits.

2.3 cost per foot method

The cost per foot method and as in Eq. depends on the cost of bit, the total drilled footage, trip time and rotating time and neglected the effect on the WOB, RPM and ROP on the bit selection.Eq.7 represent the cost per foot equation

$$CPF=C_B+C_R\,(T+tr)/F \quad \ldots\ldots (7)$$

Where:

CPF: cost per foot $/ft.

C_B: bit cost $.

C_R: Rig cost $/hr.

T: Total rotating time hr.

tr: trip time hr., t= RIH time+ POOH time……..(8)

F: Total footage drilled.

Table 14 illustrates the cost per foot for the 17.5" hole section for all the studied oil wells, from this table it's clear that the bit that drill the 17.5" hole section in R-536 Well is the best bit compared with the other studied oil wells. This bit gave the lowest CPF compared with the other studied oil wells while the bit that drill R-544 well show the biggest cost per foot. **Table 15** illustrates the cost per foot for the 8.5" hole section for all the studied oil wells, from this table it's clear that the bit that drill the 17.5" hole section in R-531 Well is the best bit compared with the other studied oil wells. This bit gave the lowest CPF compared with the other studied oil wells while the bit that drill R-548 well show the biggest cost per foot.

Note: for the 12.25" hole section, we have no accurate data concerning to the bits price and trip time, so the studying is related only for 17.5" and 8.5"hole sections.

3. COMPARISON BETWEEN THE METHODS OF BIT SELECTION

Selecting the right bits is easier when drilling additional oil wells in the field because the operator knows what formations to expect and which bit drills them best. Many methods are used for bit selection, each way of them depending on one parameter or tow and neglected the other, so it is from important to make connection between those methods for the accurate bit selection. Sometimes tow method select the same bit type. The SE method depends on the following drilling parameters: WOB, RPM and ROP but neglected the effect cost per foot and as in Eq.6. Depending on the SE method we have the following results: the bits that drill the well R-531 is the best bits compared with the other studied wells for vertical oil wells and the bits that drill the both of wells R-544 and R-548 for directional oil wells. Depending on the cost per foot method the CPF method, the Halliburton bit of EBXT08SLC model in well R-536, 17.5" hole section has the lowest CPF value compared with the other studied oil wells. Also, depending on the cost per foot method the CPF method, the bit Baker of Q506X-PDC model in well R-531, 8.5" hole section has the lowest CPF value compared with the other studied oil wells

It is from important to put describing to the bit dull characteristic that occurs through drilling the oil wells to get the benefit from it and the bit that gave low bit dull grade, is the bit that will be used to drill the next oil wells. The bit dull grade method depends on the degree of dull grade that occurred on the bit during drilling. The bits that drill the will R-525 is the best bits compared with the other studied wells for vertical oil wells. The bits that drill the will R-544 is the best bits compared with the other studied wells for directional oil wells. Generally, it should be take all the above methods in our consideration during bit selection, which will be treated with all parameters and not one parameters and that the key for the right bit selection. In other words, it should be make combination between those methods.

Table 16 and Table 17. show the comparison between SE method and bit dull grade method for vertical oil wells and directional oil wells. It's clear that each of those methods of bit selection preferred bit model differ from the other method because each method followed specific line different from the other.

4. CONCLUSIONS

1- Halliburton bit of EBXT08SLC model that drilled 17.5" hole section in well R-536 is the best bit from the studied wells(it is gave the lowest dull characteristic compared with the other studied bit in this study), is the best bit to drill 17.5"hole section in Rumaila oil field depending on the bit dull grade method . It's drilled about 501 m in 33 hr. Also. For the same section and depending on the SE method, the Smith bit of GS105BVC model in well R-531 has the lowest SE value compared with the other studied vertical oil wells.

2- For directional well, 17.5" hole section, Smith bit of well R-544 of GFS10BVC model gave the good dull characteristic, for the same section the Baker H.in well R-548 of GTX-CG1 model gave the lowest value of SE.

3- SMITH bit of MSI616LPX model which was drilled12.25" hole section (directional part) in R-548 well and the same section in R-544 well. It's drilled about 200 ft. in well R-548 and 950 ft. in well R-544 in 99.97 hr. It gave good dull grade .It is recommended to use this bit to drill 12.25"hole sections (directional part) in this field.

4- Smith Bit of model MDI616EPX which was drilled 8.5"hole section in well R-525 and the same section in well R-548,its drilled about 447 ft. in well R-548and 443ft in well R-525 ,its drilled about 980 ft. This bit gave good dull grade, it is recommended to use this bit to drill 8.5"hole sections in this field.

5- Depending on the cost per foot method the CPF method, Halliburton bit of EBXT08SLC model in well R-536, 17.5" hole section has the lowest CPF value compared with the other studied oil wells.

6- Depending on the cost per foot method the CPF method, Baker H. bit of Q506XPDC model in well R-531, 8.5" hole section has the lowest CPF value compared with the other studied oil wells.

NOMENCLATURES:

BHA= bottom hole assembly.
ROP= rate of penetration, ft. /sec.
RPM= revolution per minute, Rev. /min.
WOB= weight on bit, lb.
DMLR= daily Mud Logger Report.
POOH = pull out of hole.
PCD = polly crystalline diamond**.**
BT= broken teeth.
HC= heat checking.
CT= chipped cutter.
WT= worn teeth.
ER= erosion.
PN=plugged nozzle.
RIH=running in hole

REFRENCES

- Allen, J.H., *1980, Bit selection guidelines in vertical and directional oil wells,* Oil and Gas J., *94.*
- Aswad, Z. A. R., 1996, *Advanced Drilling Engineering,* M. Sc. Course at University of Baghdad, Petroleum Engineering Dept.
- Bela Liptak, *April 2012, Control for Drilling Oil and Gas Wells.*
- Glowka, D., Febuary.1983, *Optimization of Bit Configurations,* Soc. Pet. Eng. J. pp.21-32.
- Harold J. Flanagan, 2013, *The Effect of drilling parameters on the value of Rate of Penetration.*
- Nollely, J.P. 1986, *An Analysis of Hydrualic Factors Affecting the Rate of Penetration of Drag- Type Rotary Bits* , Drill and Prod Prac., API , Dallas 23.
- R.Harmer June 2013, *Improving Drilling Results with A real-time Performance Advisory System,* Schlumberger, World Oil.
- Rabia H."Specific energy as a csitesion for drill performance prediction" ,Int.J.Rock Mech.Min Sci.19 ,No.1 Feb.(1982)
- Rabia H."Oil well drilling engineering principles and practice" , Graham and Trotman publishing Co.,(1985)

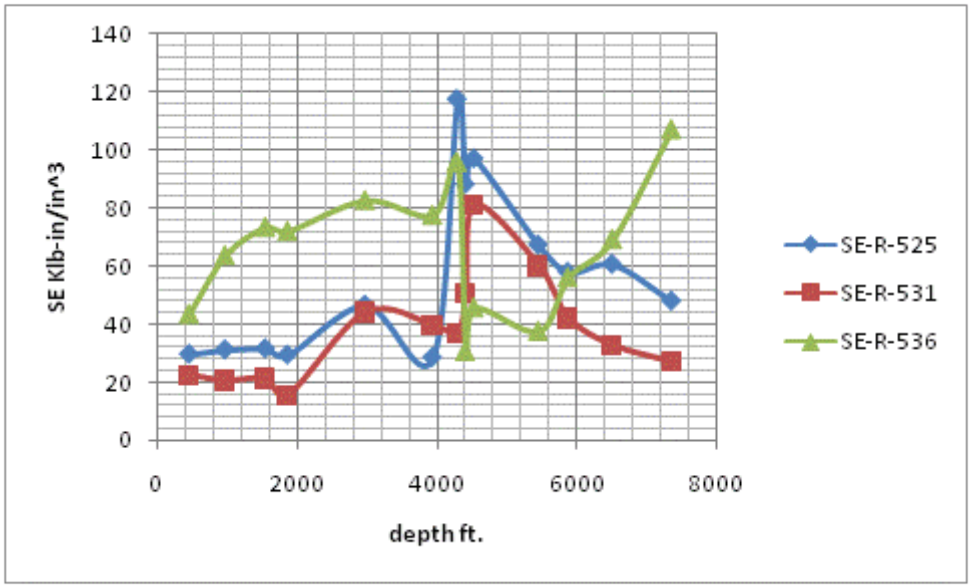

Figure 1. The relation between the SE and the cumulative footage for three vertical oil wells.

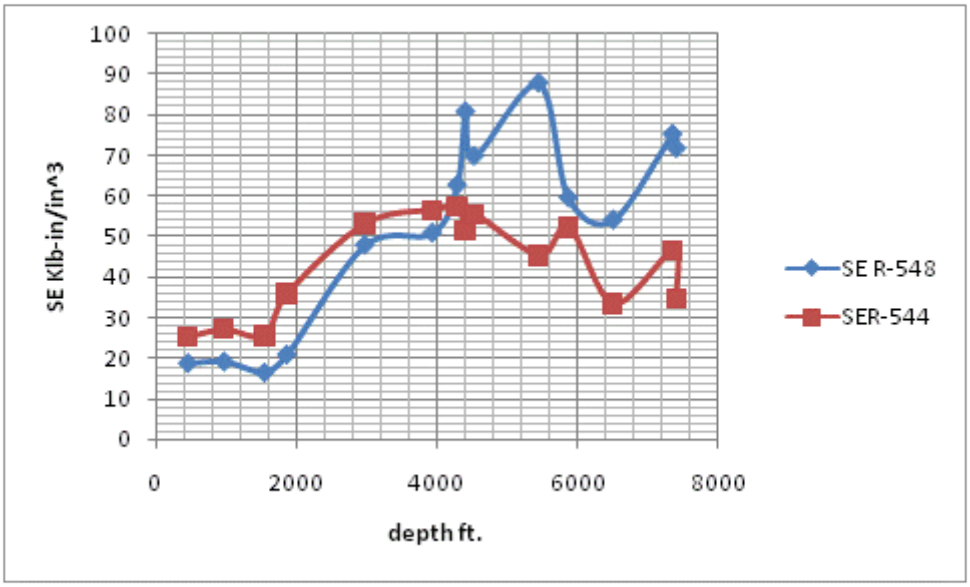

Figure 2. The relation between the SE and the cumulative footage for tow directional oil wells.

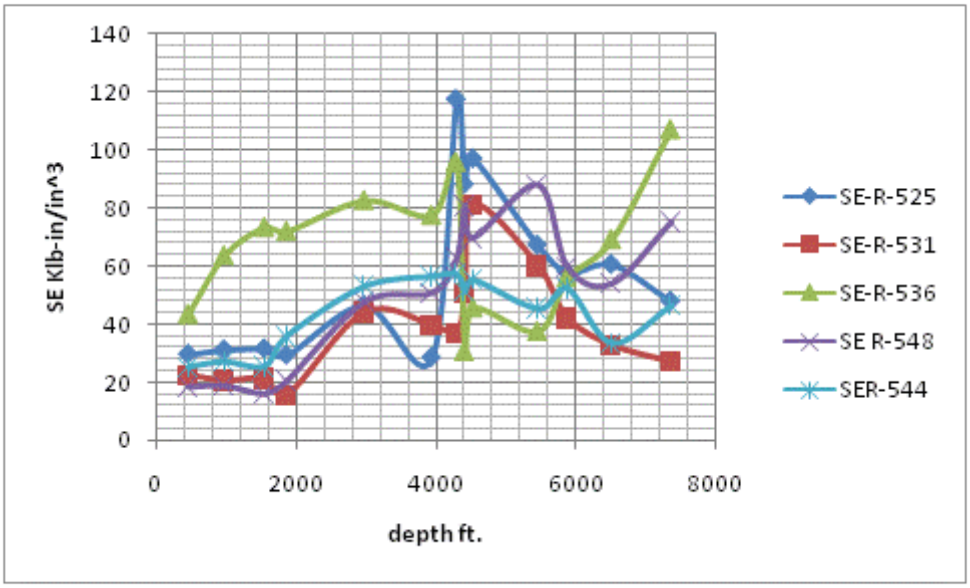

Figure 3. The relation between the SE and the cumulative footage for all the studied oil wells.

Table 1. Drilling parameter of well R-525.

cumulative footage ft.	WOB klb	RPM	ROP ft/hr.	SE klb-in/in^3	formation
454.2	13	80	40.00	29.71	Dibdiba
968.96	9.5	95	33.00	31.26	Lower Fars
1544.28	11	88	35.00	31.61	Ghar
1862.22	10	100	38.79	29.46	Dammam
2973.496	11	80	30.82	46.62	Rus
3936.4	7	90	36.00	28.57	Umm Er-Radhuma
4287.648	20	160	44.48	117.45	Tayarat
4405.74	18	120	40.00	88.16	Tayarat
4529.888	18	90	27.25	97.05	Shiranish
5450.4	12	110	32.00	67.35	Hartha
5874.32	11.5	105	34.00	57.98	Sadi
6510.2	8.5	88	29.00	60.69	Tanuma
7358.04	7	75	25.74	47.99	Mishrif

Table 2. Drilling parameter of well R-531.

cumulative footage ft.	WOB klb	RPM	ROP ft/hr.	SE klb-in/in^3
454.2	10	75	38.00	22.56
968.96	8	90	40.00	20.57
1544.28	9	80	38.50	21.37
1862.22	7.5	80	44.07	15.56
2973.496	6.4	95	22.50	44.12
3936.4	6.5	98.5	26.34	39.69
4287.648	7.5	65	21.57	36.89
4405.74	11	95	33.50	50.93
4529.888	14.5	110	32.11	81.09
5450.4	12.5	103	35.00	60.06
5874.32	10	96	37.30	42.02
6510.2	8.5	85	52.00	32.69
7358.04	9	120	65.31	27.00

Table 3. Drilling parameter of well R-536.

cumulative footage ft.	WOB (klb)	RPM	ROP ft/hr	SE klb-in/in^3
454.2	12	90	28.39	43.47
968.96	20	85	30.50	63.70
1544.28	30	75	35.00	73.47
1862.22	24	88	33.50	72.05
2973.496	18	80	28.43	82.69
3936.4	15.5	95	31.00	77.55
4287.648	19.5	110	36.50	95.95
4405.74	9.5	87	44.17	30.55
4529.888	12.5	93	41.50	45.73
5450.4	11.5	97	48.45	37.59
5874.32	13	115	43.50	56.11
6510.2	9.6	123	40.15	69.20
7358.04	14.5	131	41.70	107.18

Table 4. Drilling parameter of well R-548.

cumulative footage ft.	WOB klb	RPM	ROP ft/hr.	SE klb-in/in^3
454.2	4	77	18.80	18.72
968.96	4.5	84	22.60	19.12
1544.28	5	89	31.00	16.41
1862.22	6.8	96	35.80	20.84
2973.496	10	85	29.00	47.85
3936.4	11.6	94	35.00	50.86
4287.648	15	110	43.00	62.65
4405.74	17.4	125	44.00	80.71
4529.888	16	122	45.70	69.74
5450.4	17.7	133	43.80	87.75
5874.32	12.4	119	40.50	59.49
6510.2	9	96	37.60	54.07
7358.04	7.4	123	28.50	75.15
7409.516	6	132	26.00	71.67

Table 5. Drilling parameter of well R-544**.**

cumulative footage ft.	WOB klb	RPM	ROP ft./hr.	SE klb-in/in^3
454.2	6.6	66	19.50	25.53
968.96	7.8	75	24.50	27.29
1544.28	10	88.5	39.30	25.74
1862.22	5.5	62	15.40	36.15
2973.496	9.4	74	21.30	53.32
3936.4	6.5	155	29.00	56.72
4287.648	7	166	33.00	57.49
4405.74	6	163	31.00	51.51
4529.888	7.5	170	37.50	55.51
5450.4	7	153	38.40	45.54
5874.32	6.4	133	26.50	52.44
6510.2	5	79	27.60	33.67
7358.04	7.5	80	30.30	46.59
7409.516	5.5	78	28.90	34.93

Table 6. IADC Bit Dull Grade.

IADC : Dull Bit Grading

Cutting structure

Example of bit grading : 2, 4, BT, M, E, X, (CT,WO), DTF.

Inner	Outer	Dull Char	Location	Bearings seals	Gauge	Other dull char	Reason pulled
1	2	3	4	5	6	7	8

1 - Inner cutting structure *(All inner rows.)*

2 - Outer cutting structure *(Gauge rows only.)*

In columns 1 and 2 a linear scale of 0 ---> 8 is used to describe the condition of the cutting structure according to the following guidelines for specific bit types.

Steel toothed bits Measure of lost tooth height due to abrasion and / or damage

- 0 - No loss of tooth height
- 8 - Total loss of tooth

Insert bits Measures total cutting structure reduction of lost, worn, & or broken inserts

- 0 - No lost worn and / or broken inserts
- 8 - 0% of inserts and / or cutting structure remaining.

Fixed cutter bits Measure of lost tooth height due to abrasion and / or damage

- 0 - No lost, worn and / or broken cutting structure
- 8 - 100% of cutting structure lost, worn and / or broken

3 - Dull characteristics

Note: use only cutting structure related codes

BC - Broken cone *	LN - Lost nozzle
BF - Bond failure	LT - Lost teeth and cutters
BT - Broken teeth and cutters	OC - Off centre wear
BU - Balled up bit	PB - Pinched bit
CC - Cracked cone *	PN- Plugged nozzle or flow by areas
CD - Cone dragged *	RG - Rounded gauge
CI - Cone interference	RO - Ring out
CR - Cored	SD - Shirttail damage
CT - Chipped Teeth & cutters	SS - Shelf sharpening wear
ER - Erosion	TR - Cone tracking
FC - Flat crested wear	WO - Wash out
HC - Heat checking	WT - Worn teeth or cutters
LD - Junk damage	NO - No dull characteristics
LC - Lost cone *	* Show cone # or #'s under location 4

4 - Location

Roller cone		Fixed cutter	
N- Nose row	G - Gauge row	C - Cone	S - Shoulder
M - Middle row	A - All Rows	N - Nose	G - Guage
State cone # or #'s I.e. 1, 2, or 3.		T - Taper	A - All areas

5 - Bearings and seals

Non sealed bearings		Sealed bearings	
A linear scale estimating bearing life is used		E - Seals effective	F - Seals failed
0 = No life used ---> 8, 100% bearing life used		N - Not able to grade	X - Fixed cutter bit

6 - Gauge

X - in gauge	1/16 - 1/16" out of gauge	1/8 - 1/8" ut of gauge	3/16-3/16" out of gauge
1/4 - 1/14" out of gauge	5/16 - 5/16" out of gauge	3/8 -3/8" out of gauge	7/16 - 7/16" out of gauge
1/2 - 1/2" out of gauge	9/16 - 9/16" out of gauge	5/8 - 5/8" out of gauge	etc.

7 - Other dull characteristics

Refer to column 3 codes

8 - Reasons bit was pulled or run completed

BHA- Change bottom hol	HR - Hours on bit
DMF - Downhole motor failure	LOG - Run logs
DTF - Downhole tool failure	PP - Pump pressure
DSF - Drill string failure	PR - Penetration rate
DST - Drill stem test	Rig - Rig repair
DP - Drill Plug	TD - Total depth / casing depth
CM - Condition mud	TW - Twist off
CP - Core point	TQ - Torque
FM - Formation change	WC - Weather conditions
HP - Hole problems	
LIH - Left in hole	

Table 7. Bit record of well R-525**.**

Size (in)	Make	Type	Inner	Outer	Dull	Location	Bearing	Gauge	Other Dull	Reason
17.50	Smith	GS105BVC	2	2	BT	A	E	0	WT	TD
12.25	Smith	MDi616	3	4	WT	A	X	In Gauge	NO	PR
12.25	Smith	MDi616E	0	1	LT	T	X	In Gauge	NO	TD
8.50	Smith	MDI616EPX	0	0	PN	A	X	In Gauge	NO	TD

Table 8. Bit record ofwell R-536.

Size (in)	**Make**	**Type**	**Inner**	**Outer**	**Dull**	**Location**	**Bearing**	**Gauge**	**Other Dull**	**Reason**
17.50	Halliburton	EBXT08SLC	1	1	No	A	E	I	No	TD
12.25	Halliburton	EQH16R	6	6	B	A	8	I	BT	HR
12.25	Halliburton	SFD75H	2	3	BT	S	*	I	RR	HP
8.50	Halliburton	FX65D	2	1	No	A	X	I	No	TD

Table 9. Bit record of well R-531.

Size (in)	Make	Type	Inner	Outer	Dull	Location	Bearing	Gauge	Other Dull	Reason
17.5	Smith	GS105BVC	1	1	BT	A	E	I	Non	TD
12.25	Baker H.	VAG - 11 - TCI	2	2	WT	A	E	I	Non	BHA Change
12.25	Baker H.	HC606Z-PDC	5	2	WT	N	X	I	BT	PR
12.25	Baker H.	HC606Z	3	2	CC	N	X	I	WT	TD
8.50	Baker H.	Q506X-PDC	1	1	WT	A	X	IN	Non	TD

Table 10. Bit record of well R-544.

Size (in)	**Make**	**Type**	**Inner**	**Outer**	**Dull**	**Location**	**Bearing**	**Gauge**	**Other Dull**	**Reason**
17 1/2	Smith	XR+VE	1	1	WT	A	E	I	NO	TD
12.25	Smith	GFS10BVC	1	2	BT	G	E	I	CT	BHA
12.25	Smith	MSI616LPX	1	2	CT	A	X	I	NO	TD
8.50	Smith	MDi616LPX	1	2	CT	A	X	I	ER	TD

Table 11. Bit record of well R-548.

Size (in)	Make	Type	Inner	Outer	Dull	Location	Bearing	Gauge	Other Dull	Reason
17.50	Baker	GTX-CG1	1	1	WT	A	1	I	NO	TD
12.25	Baker	EP7199	1	2	WT	1,2	E	I	ER	BHA
12.25	Baker	HCD505z	3	4	BT	A	X	i	CT	BHA
12.25	SMITH	MSI616LPX	1	1	WT	A	X	i	NO	TD
8.50	SMITH	MDi616LEPX	1	1	BT	G	X	I	NO	TD

Table 12. The Types of Bits which is used in directional oil wells.

Bit size in	Well	Type	Manufacturing	Nozzle size 1/32"	Bit classification	Footage Drilled	Hours
17.5	R-544	XR+VE	Smith	3*18+13C	Milled	1535.196	55.69
12.25	R-544	GFS10BVC	Smith	3*16+13C	insert teeth	1577.588	105.66
12.25	R-544	MSI616LPX	Smith	6*14	PDC	2876.6	99.97
8.5	R-544	MDi616LPX	Smith	6*12	PDC	1616.952	73.31
17.5	R-548	GTX-CG1	Baker	3*18+13C	Milled	1931.864	79.00
12.25	R-548	EP7199	Baker	3*16+13C	insert teeth	1837.996	116.7
12.25	R-548	HCD505z	Baker	6*14	PDC	1517.028	102
12.25	R-548	MSI616LPX	SMITH	6*14	PDC	605.6	13
8.5	R-548	MDi616LEPX	SMITH	6*13	PDC	1350.488	70

Table 13. The Types of Bits which is used in vertical oil wells.

Bit size in	Well	Type	Manufacturing	Nozzle size 1/32"	Bit classification	Footage Drilled	Hours
17.50	R-525	GS105BVC	Smith	4*25	Milled	1862.22	48
12.25	R-525	MDi616	Smith	6*14	PDC	2425.428	53.53
12.25`	R-525	MDi616E	Smith	6*14	PDC	1698.708	36.31
8.50	R-525	MDI616EPX	Smith	6*12	PDC	1341.404	26
17.5	R-531	GS105BVC	Smith	3*18+13C	milled	1671.456	38.6
12.25	R-531	VAG - 11 - TCI	Baker H.	2*18+1*16	insert teeth	1165.78	60.46
12.25	R-531	HC606Z-PDC	Baker H.	6*14	PDC	1556.392	44
12.25	R-531	HC606Z	Baker H.	6*14	PDC	1483.72	47.04
8.5	R-531	Q506X-PDC	Baker H.	6*12	PDC	1344.432	20.95
17.50	R-536	EBXT08SLC	Halliburton	3*16+16C	insert teeth	1517.028	33.35
12.25	R-536	EQH16R	Halliburton	3*20	insert teeth	2667.668	93.82
12.25	R-536	SFD75H	Halliburton	7*14	PDC	1026.492	43.66
8.50	R-536	FX65D	Halliburton	6*12	PDC	1603.326	39.92

Table 14. Cost per foot method for 17.5" hole section for all studied oil wells.

Parameters	**R525 ,17.5 "**	**R531,17.5 "**	**R536,17.5 "**	**R-544, 17.5 "**	**R548, 17.5 "**
Bit cost ($)	35,139	36,147	31,133	35,168	30,173
Rig cost ($/hr.)	1,208	1,208	1,208	1,208	1,208
Trip time (hrs.)	13.5 hrs.	14.5 hrs.	14.0 hrs.	15.5 hrs.	16.0 hrs.
In hole time (hrs.)	48.0 hrs.	39.0 hrs.	33.0 hrs.	56.0 hrs.	79.0 hrs.
Net Footage drilled (ft.)	1862 ft.	1671 ft.	1517 ft.	1535 ft.	1932 ft.
Cost per foot	**58.8 $/ft.**	**60.3 $/ft.**	**57.9 $/ft.**	**79.2 $/ft.**	**75.0 $/ft.**

Table 15. Cost per foot method for 17.5" hole section for all studied oil wells.

Parameters	**R-525 ,8.5 "**	**R-531, 8.5 "**	**R-536, 8.5 "**	**R-544, 8.5 "**	**R-548, 8.5 "**
Bit cost ($)	53,167	52,156	50,543	53,498	53,570
Rig cost ($/hr.)	1,208	1,208	1,208	1,208	1,208
Trip time (hrs.)	38.0 hrs.	36.0 hrs.	39.0 hrs.'	35.0 hrs.	36.0 hrs.
In hole time (hrs.)	26.0 hrs.	20.0 hrs.'	40.0 hrs.	73.0 hrs.'	70.0 hrs.
Net Footage drilled (ft.)	1341 ft.	1344 ft.	1603 ft.	1617 ft.	1350 ft.
Cost per foot	**97.3 $/ft.**	**89.1 $/ft.**	**91.1 $/ft.**	**113.8 $/ft.**	**134.5 $/ft.**

Table 16. Comparison between the bit selection methods for vertical well.

Method of selection	Bit model	Bit manufacturing	Method of selection	Bit model	Bit manufacturing	Method of selection	Bit model	Bit manufacturing	Hole size"
Bit dull grade	EBXT08SLC	Halliburton in well R-536	SE	GS105BVC	Smith in well R-531	CPF	EBXT08SLC	Halliburton in well R-536	17.5
Bit dull grade	MDi616	Smith in well R-525	SE	HC606Z-PDC	Baker H. in well R-531	Non	MDi616	Non	Non
Bit dull grade	MDi616E	Smith in well R-525	SE	SFD75H	Halliburton in well R-536	Non	MDi616E	Non	Non
Bit dull grade	MDI616EPX	Smith in well R-525	SE	Q506XPDC	Baker H. in well R-531	CPF	Q506XPDC	Baker H. in well R-531	8.5

Table 17. Comparison between the SE method and bit dull grade method for directional wells.

Section	Method of selection	Bit manufacturing	Bit model	Method of selection	Bit manufacturing	Bit model
17.5	SE	Baker H.in well R-548	GTX-CG1	Bit dull grade	Smith bit of well R-544	GFS10BVC
12.25	SE	Baker in well R-548	EP7199	Bit dull grade	Smith bit of well R-544	GFS10BVCf
12.25	SE	SMITH in well R-544.	MSI616LPX	Bit dull grade	Smith bit of well R-548	MSI616LPX
8.5	SE	. Smith bit of well R-544	MDi616LPX	Bit dull grade	Smith bit of well R-548	MDi616LEPX

Strength of Reinforced Concrete Columns with Transverse Openings

Dr. Ihsan A.S. AL-Shaarbaf
Assistant Professor
Civil Engineering Department
Al-Israa University College

Dr. Abbas AbdulMajeed Allawi
Assistant Professor
Civil Engineering Department
College of Engineering
University of Baghdad
a.allawi@uobaghdad.edu.iq

Nabeel H. AlSalim
Lecturer
Civil Engineering Department
College of Engineering
Babylon University

ABSTRACT

The present work is concerned with the investigation of the behavior and ultimate capacity of axially loaded reinforced concrete columns in presence of transverse openings under axial load plus uniaxial bending. The experimental program includes testing of twenty reinforced concrete columns (150 × 150 × 700 mm) under concentric and eccentric load. Parameters considered include opening size, load eccentricity and influence of the direction of load eccentricity with respect to the longitudinal axis of the opening. Experimental results are discussed based on load – lateral mid height deflection curves, load – longitudinal shortening behavior, ultimate load and failure modes. It is found that when the direction of load eccentricity is parallel to the longitudinal axis of openings, column behavior is more pronounced when than the direction is normal to the longitudinal axis of openings.

Keywords: RC Columns, Transverse Openings, Load eccentricity, Ultimate Load.

تحمل الأعمدة الخرسانية المسلحة ذات الفتحات المستعرضة

أ.م.د .احسان علي صائب الشعرباف
قسم الهندسة المدنية
كلية الاسراء الجامعة

أ.م.د .عباس عبد المجيد علاوي
قسم الهندسة المدنية
كلية الهندسة/جامعة بغداد

م .د .نبيل حسن علي السالم
قسم الهندسة المدنية
كلية الهندسة/جامعة بابل

الخلاصة

ان البحث الخالي يتركز على دراسة السلوك الانشائي وقابلية تحمل الاعمدةالخرسانية المسلحة المحملة محوريا بوجود الفتحات مستعرض تحت تاثير الاحمال المحورية والعزوم احادية الاتجاه .يتضمن البرنامج العملي من هذا البحث فحص عشرون عموداً خرسانياً مسلحاً ذات مقطع مربع بابعاد 150×150) ملم (وبطول700) ملم .(تضمنت المتغيرات الأساسية التي جرى إعتمادها حجم الفتحة ,اللامركزية للحمل وتاثير اتجاه اللامركزية للحمل بالنسبة الى اتجاه المحور الطولي للفتحة .نوقشتْ نَتائِج الفحص على أساس سلوك الحملِ - الهطول الجانبيِ عند منتصف العمود وسلوك الحملِ - القصر الطوليِ والحمل الأقصى وأنماط الفشلِ .وجد من النتائج العملية عندما يكون لاتمركزية الحمل موازية لاتجاه المحور الطولي للفتحة يكون تصرف العمود بصورة افضل عندما يكون الاتجاه متعامد على المحور الطولي للفتحة.

الكلمات المفتاحية :الاعمدة الخرسانية المسلحة ,الفتحات المستعرضة ,لامركزية التحميل ,الحمل الاقصى.

INTRODUCTION

Transverse openings may present in reinforced concrete columns as access for services including plumbing pipes and electrical conduits. The presence of these openings results in reduction of strength and stiffness and of the columns. If the presence of such openings is negligible during the design these stage, structural damage may occurred. **Lotfy, 2013,** conducted a nonlinear finite element analysis on 21 reinforced concrete column specimens using, **ANSYS, 2010,** software version 10 to study the strength loss due to presence of transverse holes in columns. The parameters considered were dimensions, shapes and positions of the holes. A comparison between the available experimental results and finite element analysis is presented. It was found that results and conclusions may be useful for designers.

Hassan, Sarsam and **Allawi , 2013, 2015,** studied the behavior of reinforced concrete columns under uniaxial and biaxial bending. Their works deal with strengthening of columns by using carbon fiber reinforced polymer (CFRP). The experimental program includes testing of eight reinforced concrete columns (150×150×500mm) tested under several load conditions. The considered variables are the effect of both eccentricity and longitudinal reinforcement (Ø12mm or Ø6mm). Test results are discussed based on lateral and longitudinal deflection behavior, ultimate load and failure modes. The CFRP strengthening shows a complete change in the failure mode of the columns. Also, they concluded that the effect of longitudinal reinforcement in the case of uniaxial and biaxial bending is more effective for strengthened columns than for unconfined columns.

The ACI building Code ACI 318-2014 stated that "Conduits and pipes, with their fittings, embedded within a column shall not occupy more than 4% of the cross-sectional area on which strength is calculated". Experimental tests dealing with the effect of presence of transverse openings inside columns is arrived out in the present study to investigate the strength reduction for concentric and eccentric loaded columns. Also, the influence of transverse openings on the behavior and mode of failure of the tested columns is investigated.

Al-Sali , 2015, studied the behavior and the load carrying capacity of reinforced concrete short columns having different types of transverse openings. The experimental program deals with the ultimate strength of tested columns. The variables considered in the experimental work include shapes of openings having the same opening ratio of 0.133. The tested columns have been also analyzed using a nonlinear finite element model. An increase in the ultimate strength of about 2.06% is achieved when single opening of 20 mm diameter is replaced by two symmetrical openings of 10 mm diameter each. Also, a decrease in the ultimate strength of about 2.88% and 5.97% is observed when the single circular opening of 20 mm diameter is replaced by 20×20 mm square opening or 20×40 mm rectangular opening respectively.

EXPERIMENTAL PROGRAM

Column specimens having an overall height of 900 mm and a square cross section of (150 mm × 150 mm) are considered. The transverse openings are positioned at mid height of the columns as shown in **Fig. 1**. The opening ratio is calculated as the projecting area of the opening at the opening level (i.e. at mid height of column) divided by the column cross sectional area. Reinforcing steel bars provided for all columns are 4Φ10 mm longitudinal, and hence, the steel ratiois 1.4%, which lies within the ACI 318-14 Code limitations. The transverse closed bars are consisted of Φ6 mm @ 100 mm as shown in **Fig. 2.**

Test length is considered as the middle part of the column having a 700 mm height. The remaining 100 mm upper and lower parts of the column are positioned inside the upper and lower steel caps to apply the moments at the ends as shown in **Fig. 3**. This configuration is adopted to prevent possible failure at the ends. Also, the embedded ends help to stabilize the specimen throughout the testing procedure.

IDENTIFICATION OF SPECIMENS

To identify test specimens with different sizes of openings and eccentricities direction, the following designation system is suggested:

- **Group numbering:** The first character is used to identify the group number. C1 refers to specimens of group A in which the eccentricity is applied in direction parallel to the longitudinal axis of openings, and C2 refers to columns of group B in which eccentricity is applied in direction normal to the longitudinal axis of openings.
- **Opening Size:** The second character is used to identify the size of opening. Φ0 refers to columns without opening, Φ15 refers to opening of 15 mm diameter, Φ20 refers to opening of 20 mm diameter and Φ25 refers to opening of 25 mm diameter.
- **Load eccentricity:** The third character is used to specify the values of load eccentricity. E0 refers to axially loaded columns. 45 refer to 45 mm loading eccentricity and E120 refers to 120 mm loading eccentricity.

Table 1 gives specimens designation system and opening details.

MATERIALS PROPERTIES

For each group, three standard cylinders (100×200mm) were tested to obtain the compressive strength (f_c'), splitting tensile strength (f_{ct}) (ASTM standard C496) and static modulus of elasticity (E_c) at 28 days (ASTM standard C469) and at time of testing using a universal testing machine. The standard mechanical properties of hardened concrete are listed in **Table 2**.

For all columns, two sizes of steel reinforcing deformed bars were used. Bars of size (Φ10 mm) were used as longitudinal reinforcement and bars of size (Φ6 mm) were used as closed stirrups. Values for yield stress and ultimate strength are obtained according to ASTM standard A615 requirements for each bar size and are given in **Table 3**.

TESTING PROCEDURE

A. Steel Caps

According to the previous researches, a precise load eccentricity using is difficult to obtain. **Hadi , 2007,** concluded that the position of the applied load was not accurate and the columns had a tendency to break at the tested connection region. Therefore, eccentric loading was simulated by designing a new steel end caps to allow the eccentric load to be accurately positioned prior to testing of the circular columns. **Ranger** and **Bisb , 2007,** used steel collars (caps) to fix their tested columns and to ensure stability and accurate eccentric loading during testing. In the present work, new two

loading end caps were designed and implemented. In case of eccentric loading, each loading cap was consisted of four Φ20 mm holes at the base of the cap through which the threaded part of the longitudinal reinforcement is passed to ensure adequate length of development. In addition, each side of loading cap includes three M24 female threads with bolts. These bolts were used to fasten the loading cap together with the column through the available four (5×100×148 mm) steel plates. These plates were used to prevent the column from damaging when the M24 bolts are tightened to the column specimen. Another two (5×150×150mm) steel plates were used at the top and bottom of the tested column before placing the loading caps to protect the column during the test and to distribute the applied loading across column cross section. **Fig. 4** shows the steel caps and **Fig. 5** represents a schematic representation with details.

B. Measurements and Instrumentation

In case of concentrically loaded columns, axial deformation was recorded using two dial gages at two opposite sides of specimen over a length of 700 mm as shown in **Fig. 6**. While for the eccentrically loaded columns, three additional dial gages were used to monitor the lateral displacement for each specimen. The location of these dial gages were at mid height and at 320 mm above and below mid height.

The average reading of the upper and lower dial gages has been subtracted from the reading of the middle dial gage to obtain the net lateral displacement. Also, the axial deformations were recorded using three dial gages over a length of 700mm of the eccentric columns. These dial gages were fixed to the steel caps at different locations as shown in **Fig. 7**.

Also, a linear variable differential transformer (LVDT) is used to measure the axial displacement across the opening by fixing it at two points on the tension face of the specimen and the data of LVDT is recorded for each stage of loading as shown in **Fig. 8**.

C. Supporting System

The stability of the columns during testing is the main difficulty especially in case of high value of eccentricity. Therefore, a supporting system was designed to stabilize the specimens during testing. This system is consisted of four bolts located at the top and the bottom ends in touch with the caps by using steel balls located at the ends, **Fig. 9**.

The benefit of these steel balls is to assure that the supporting system does not influence the carrying capacity of the column and to prevent the possible horizontal movement of specimen at ends. In addition, this system allows movement of column inside the machine to achieve the precise eccentricity and allows the longitudinal movement of specimen to occur.

D. Loading Technique

A new loading system has been developed to apply the precise eccentric loading. This system comprised a steel shaft with half spherical hole at its end, Φ45 mm steel ball and (10×90×90 mm) square plate with a sector of spherical hole located at its middle as shown in **Fig. 10**. The steel shaft can moves vertically inside a steel ring which prevents the shaft from horizontal sliding during loading as shown in **Fig. 11**.

The location of this ring is at the center of testing machine at upper and lower bases. This technique ensures that the load has a fixed loading.

E. Testing Procedure of the Columns Specimens

The testing machine shown in **Fig. 12** has a capacity of 2000 kN. The load was gradually applied and at each increment loasing, readings were recorded. In the trial test, the column was loaded up to failure. The recorded data was analyzed to ensure the working conditions of all the instrumentation used and the safety of testing procedure. After performing the trial test, the scheduled tests were carried out.

The testing procedure is summarized as follows:

- Locating the column specimens inside the lower cap and then the upper cap was placed; All the bolts were properly fastened.
- Lifting the column to the slide steel base level then sliding it into the testing machine as shown in **Fig. 13**.
- Releasing the bolts of the loading cap.
- Applying concentric force to insure full contact between column and loading caps and tightening all the bolts, then the applied load is removed.
- By using the supporting system, the column moves horizontally until reaching the precise required eccentricity.
- The longitudinal bars were tightened to the loading caps especially in cases of eccentric loading that may undergo tension.
- Applying fixation load then all dial gages are fixed and initial reading were recorded.
- The load was gradually applied in increments. At each load increment, all readings were acquired manually.

EXPERIMENTAL RESULTS

A. Ultimate Strength Results

A.1: Group A (Load eccentricity in the direction parallel to the longitudinal axis of openings)

Foe all columns of group A, experimental ultimate strength values are shown in **Table 4**. These columns have been tested under axial compressive load or axial load with 45 mm and 120 mm eccentricity values in the direction parallel to the longitudinal axis of opening. For tested columns of this group, in which zero eccentricity and different opening ratios of (0.00%, 10.00%, 13.33%, and 16.67%) were used, a significant reduction in ultimate strength is noticed due to the significant reduction in compression area. The percentage decrease in the ultimate strength compared to column C1Φ0E0 (reference column) were 3.21%, 5.02% and 6.22% for columns C1Φ15E0, C1Φ20E0 and C1Φ25E0 respectively.

For the tested columns of this group, in which 45 mm eccentricity was exist with the same different opening ratios shown above (0.00%, 10.00%, 13.33%, and 16.67%), a significant reduction in the ultimate strength is observed since the opening area is located within the compression zone for column cross section which reduces the compression area. The low eccentricity ratio (e/h=0.3) for these columns makes the compression failure mode to be the dominant mode and no yielding of tension reinforcement was occurred. The percentage decrease in the ultimate strength compared to

column C1Φ0E45 (reference column) were 6.36%, 10.46% and 12.27% for columns C1Φ15E45, C1Φ20E45 and C1Φ25E45 respectively.

For tested columns of this group, in which 120mm eccentricity was exist and different opening ratios of (0.00%, 10.00%, 13.33%, and 16.67%),an insignificant reduction in the ultimate strength is noticed due to the large eccentricity ratio (e/h=0.8). The cracks in these columns at the tension face are formed and the effect of bending moment is more pronounced than the effect of the axial compressive load. The percentage decrease in the ultimate strength compared to column C1Φ0E120 (reference column) were 1.51, 1.51and 2.14 for columns C1Φ15E120, C1Φ20E120 and C1Φ25E120 respectively as shown in **Fig. 14**.

A.2 Group B (Load eccentricity in the direction normal to the longitudinal axis of openings)

For all columns of group B, experimental ultimate strength values are given in Table 4. These columns were tested under axial compressive load with 45 mm and 120 mm eccentricity values in the direction normal to the longitudinal axis of opening. For tested columns of this group, in which 45mm eccentricity was exist and different opening ratios of (0.00%, 10.00%, 13.33%, and 16.67%) were used, an insignificant reduction in the ultimate strength is observed since the opening area is not located within the compression zone of the column cross section as shown in **Fig. 15**.

The percentage decrease in the ultimate strength compared to column C3Φ0E45 (reference column) are 0.44, 0.85 and 1.31 for columns C2Φ15E45, C2Φ20E45 and C2Φ25E45 respectively. For tested columns of this group, in which 120mm eccentricity was exist and different opening ratios of (0.00%, 10.00%, 13.33%, and 16.67%) were used, a relatively insignificant decrease in the ultimate strength is noticed, as shown in **Fig. 14.** due to the large eccentricity ratio (e/h=0.8). The cracks in these columns at the tension face are formed and the effect of the bending moment is more pronounced than the effect of the axial compressive load.

B. Effect of Transverse Openings on the Load-Deflection Behavior

B.1: Concentrically Loaded Columns

The experimental behavior of load versus axial shortening behavior of the columns of group A, in which 0.0 mm eccentricity is used, are presented in **Fig. 16**. It can be noticed that the effect of presence of transverse openings are significant because of the total opening area lies within the column compression zonea. Also, it is evident that the increase in the opening area causes a reduction in the ultimate load and increases the deflection at the ultimate load level.

B.2 Eccentrically loaded columns

B.2.1 Load eccentricity equal to 45 mm

Figs. 17 to 22 illustrate the influence of the presence of transverse openings on the load versus vertical deflection response of the columns and lateral mid-height deflection curves of columns of group A and two in which 45 mm loading eccentricity is used. For tested columns of group A most of opening area lies within the column compression area that leads to a reduction in the ultimate load values in addition to an increase in deflection at ultimate load level. This is due to the reduction in stiffness and moment of inertia of the columns as the opening area increases. Also, one can conclude from Figs. 17 to 22 that the effect of eccentricity of loading in direction parallel to the longitudinal axis of openings (specimens of group A) is more than that of the direction when it is normal to the longitudinal axis of openings (specimens of group B). This is because the opening is existed in compression zone in case of parallel direction of opening axis and loading eccentricity while this not find in the other case.

B.2.2 Load Eccentricity Equal to 120 mm

Figs. 23 to 28 show the effect of the presence of transverse openings on the load versus vertical deflection response of the columns and lateral mid-height deflection curves of columns of group A and two in which 120 mm loading eccentricity is used. From these figures, it is clear that the increase in transverse opening size has a negligible effect on the ultimate load capacity. However, the increase in opening ratio affects deflection values at the ultimate load because the increase in opening ratio leads to a reduction in column stiffness.

C. Effect of Eccentricity on the Behavior of Reinforced Concrete Columns with Transverse Openings

To study the effect of eccentricity of loading on the response of reinforced concrete columns having transverse openings, eight columns of group A and eight columns of group B were tested with two values of e/h (0.3 and 0.8).

C.1 Group A (load eccentricity in the direction parallel to the longitudinal axis of openings)

For group A and for columns having zero opening ratio (solid columns), the behavior of specimen C1Φ0E45 is compared with that of specimen C1Φ0E120 using the load versus vertical and lateral mid-height deflections as shown in **Fig. 29** and **Fig. 30**. The ratio of ultimate capacity of column C1Φ0E120 to that of column C1Φ0E45 is 0.3.

For same group and for columns having 0.1 opening ratio, the behavior of specimen C1Φ15E45 is compared with that of specimen C1Φ15E120 using the load versus vertical and lateral mid-height deflections as shown in **Fig. 31** and **Fig. 32**. The ratio of ultimate capacity of column C1Φ15E120 to that of column C1Φ15E45 is 0.32. For columns having 0.133 opening ratio, the behavior of specimen C1Φ20E45 is compared with that of specimen C1Φ20E120 using the load versus vertical and lateral mid-height deflections as shown in **Fig. 33** and **Fig. 34**. The ratio of ultimate capacity of column C1Φ20E120 to that of column C1Φ20E45 is 0.33.

Finally, for the same group and for columns having 0.167 opening ratio, the behavior of specimen C1Φ25E45 is compared with that of specimen C1Φ25E120 using the load versus vertical and lateral mid-height deflections as shown in **Fig. 35** and **Fig. 36**. The ratio of ultimate capacity of column C1Φ25E120 to that of column C1Φ25E45 is 0.33.

C.2 Group B (load eccentricity in the direction normal to the longitudinal axis of openings)

For group B and for columns having zero opening ratio (solid section), specimen C3Φ0E45 is compared with specimen C3Φ0E120 using the load versus vertical and lateral mid-height deflections as shown in **Fig. 37** and **Fig. 38**. The ratio of ultimate capacity of column C3Φ0E120 to that of column C3Φ0E45 is 0.287.

For the same group and for columns of 0.1 opening ratio, specimen C3Φ15E45 is compared with specimen C3Φ15E120 using the load versus vertical and lateral mid-height deflections as shown in **Fig. 39** and **Fig. 40**. The ratio of ultimate capacity of column C3Φ15E120 to that of column C3Φ15E45 is 0.288.

For columns having 0.133 opening ratio, specimen C3Φ20E45 is compared with specimen C3Φ20E120 using the load versus vertical and lateral mid-height deflections as shown in **Fig. 41** and **Fig. 42**. The ratio of ultimate capacity of specimen C3Φ20E120 to that of specimen C3Φ20E45 is 0.289.

Finally, for the same group and for columns of 0.167 opening ratio specimen C3Φ25E45 is compared with specimen C3Φ25E120 using the load versus vertical and lateral mid-height deflections as shown in **Fig. 43** and **Fig. 44**. The ratio of ultimate load of column C3Φ25E120 with respect to that obtained for column C3Φ25E45 is 0.290.

TEST OBSERVATIONS

Images of selected tested concentrically and eccentrically loaded columns of groups A and B are shown through **Figs. 45 to 50**.

For all concentrically loaded columns shown in **Figs. 45 and 46**, one can noticed that the appearance of vertical cracks in concrete cover at the middle third zone of the specimen was always the first sign of failure and cracks in all specimens with opening were noticed. They were generated in a diagonal direction around the openings and growth to concur with the vertical cracks then these cracks spread rapidly after spalling of concrete cover. At this stage, the concrete core carries the applied axial load due to the coupling confinement effect of ties and longitudinal bars.

Failure is occurred in a brittle and explosive manner, where the longitudinal bars buckled and a crush occurred in concrete at section of the opening and this section was separated into two sliding surfaces. For all loaded specimens with 45mm eccentricity shown in **Figs. 47** and **48**, it can be noticed that crushing of concrete was observed on the compression face of the columns at the middle third zone of the specimen and few number of horizontal cracks in this zone initiated at the tension face of the column. Some of these cracks pass through the opening and progress starting from tension to compression faces. At later stage, the concrete cover firstly spalled off followed by buckling of the longitudinal bars and a loss of strength was immediately observed after reaching the peak load.

For all loaded columns with 120mm eccentricity shown in **Figs. 49** and **50**, one can noticed that a large number of distributed horizontal cracks occurred at the tension face along the column. Also, these cracks extended to the side faces of tested column especially at the middle third of specimen length. These cracks are wider than the cracks at loaded columns with 45mm eccentricity. At a later stage, the strength of specimen stood constant after reaching the peak value with a rapid increase in crack width at tension face. Then concrete cover spalled off at the compression face and a loss of strength was immediately observed after the peak load is reached.

CONCLUSIONS

According to the experimental tests carried out in this research work, the following conclusions can be drawn:

1. The presence of transverse openings in reinforced concrete columns reduces the ultimate load strength. For columns subjected to pure compressive axial load, the experimental results showed a reduction in ultimate strength ranging between 3.21% and 6.22%.
2. For columns in which the load eccentricity is applied in the direction parallel to the longitudinal axis of opening and tested with eccentricity equal to 45mm (e/h=0.3), the experimental results showed a reduction in strength ranging between 6.36% and 12.27%, while for eccentricity equal to 120mm (e/h=0.8), the experimental results showed that insignificant reduction in ultimate strength can occur.
3. The experimental results showed that insignificant reduction is occurred for both eccentricities 45 and 120 mm for columns in which the load eccentricity is applied in the direction normal to the

longitudinal axis of opening. Noting that, the above range of strength reduction is corresponding to opening ratios ranging between 10.0 % and 16.67%.

4. It was found that the load eccentricity has a significant effect on the load deflection curve and the ultimate strength value of the uniaxially loaded columns. The experimental results showed that when load eccentricity increases the ultimate load is considerably decreased.
5. For tested columns in which the eccentricity is applied in the direction parallel to the longitudinal axis of opening, an increase in the eccentricity from 45 mm to 120 mm causes a decrease the ultimate strength by about 70%, 68.45%, 67% and 66.54% for opening ratios of 0.0%, 10.00%, 13.33% and 16.67% respectively.
6. For tested columns in which the eccentricity is applied in the direction normal to the longitudinal axis of opening an increase in the eccentricity from 45 mm to 120 mm causes a decrease the ultimate strength by about 71.31%, 71.18%, 71.05% and 70.93% for opening ratios of 0.0%, 10.0%, 13.33% and 16.67% respectively.

REFERENCES

- Al-Salim, N. H., 2015, Behavior and Stress Analysis around Openings for Reinforced Concrete Columns, International Journal of Chemical, Environmental & Biological Sciences (IJCEBS) Vol. 3, Issue 5, ISSN 2320–4087 (Online), pp. 404 – 407.
- ASTM A615 / A615M - 16, Standard specification for deformed and plain carbon-steel bars for concrete reinforcement, Annual Book of ASTM, vol. 01.04.
- ASTM C469 / C469M – 14 Standard test method for static modulus of elasticity and poisson's ratio of concrete in compression Annual Book of ASTM, vol. 04.02.
- ASTM C496 / C496M – 11 Standard test method for splitting tensile strength of cylindrical concrete specimens Annual Book of ASTM, vol. 04.02.
- Building Code Requirements for Structural Concrete. (ACI 318-14), and Commentary (ACI 318R- 14), American Concrete Institute, Farmington Hills, Michigan 2014.
- Hadi, M.N.S. (2007), Behavior of FRP wrapped circular concrete columns under eccentric loading, University of Patas, Patas, Greece, July 16-18, pp.10.
- Hassan, R. F., Sarsam, K. F, and Allawi, A. A. 2013, Behavior of strengthened RC columns with CFRP under biaxial bending, University of Baghdad Engineering Journal, Vol. 3, No. 9, ISSN 1726 –4073, pp. 1115-1126.
- Hassan, R. F., Sarsam, K. F, and Allawi, A. A. 2015, Behavior of strengthened RC short columns with CFRP under eccentric load, THE 7TH ASIA PACIFIC YOUNG RESEARCHERS AND GRADUATES SYMPOSIUM, "Innovations in Materials and Structural Engineering Practices, Malaysia, Kuala Lumpur.
- Installation Guide 2010, ANSYS – VERSION -10, Computer Software for structural engineering.
- Lotfy, F. M., 2013, Nonlinear analysis of reinforced concrete columns with holes, International Journal of Civil and Structural Engineering, Vol. 3, No. 3, ISSN 0976-4399, pp. 655-668.
- Ranger, M., and Bisby, L., Effect of load eccentricities on circular FRP-confined reinforced concrete columns, University of Patas, Patras, Greece, July 16-18, 2007, pp.10.

Table 1. Designation of tested columns.

Group	Column designation	e/h	Opening size, mm	Opening ratio, %
A	C1Φ0E0	0.0	0.0	0.0
	C1Φ0E45	0.3	0.0	0.0
	C1Φ0E120	0.8	0.0	0.0
	C1Φ15E0	0.0	15	10
	C1Φ15E45	0.3	15	10
	C1Φ15E120	0.8	15	10
	C1Φ20E0	0.0	20	13.33
	C1Φ20E45	0.3	20	13.33
	C1Φ20E120	0.8	20	13.33
	C1Φ25E0	0.0	25	16.67
	C1Φ25E45	0.3	25	16.67
	C1Φ25E120	0.8	25	16.67
B	C3Φ0E45	0.3	0.0	0.0
	C3Φ0E120	0.8	0.0	0.0
	C3Φ15E45	0.3	15	10
	C3Φ15E120	0.8	15	10
	C3Φ20E45	0.3	20	13.33
	C3Φ20E120	0.8	20	13.33
	C3Φ25E45	0.3	25	16.67
	C3Φ25E120	0.8	25	16.67

Table 2. Mechanical properties of hardened concrete, MPa.

Test	Experimental	Standard specification	Note
Comp. strength	30.8 for group A 31.3 for group B	---	---
Splitting tensile strength	3.0 for group A 3.01 for group B	3.11 3.13	
Modulus of elasticity	25325 for group A 25703 for group B	26083 26295	

Table 3. Steel bars properties.

Nominal diameter, mm	Actual Diameter, mm	Yield Stress f_y ,MPa	Ultimate Strength f_u ,MPa	Modulus of Elasticity E_s, GPa
6	5.74	533	565	195.9
10	10.03	549	621	196.6

Table 4. Ultimate strength capacity of all tested columns.

Group	Column designation	Experimental ultimate load, kN	Reduction in ultimate strength, %
A	C1Φ0E0	1034.6	Ref. column
	C1Φ0E45	457.0	Ref. column
	C1Φ0E120	137.1	Ref. column
	C1Φ15E0	1001.4	-3.21
	C1Φ15E45	428	-6.36
	C1Φ15E120	135	-1.51
	C1Φ20E0	982.7	-5.02
	C1Φ20E45	409.5	-10.46
	C1Φ20E120	135.0	-1.51
	C1Φ25E0	970.2	-6.22
	C1Φ25E45	400	-12.27
	C1Φ25E120	134.2	-2.14
B	C3Φ0E45	477.8	Ref. column
	C3Φ0E120	137.1	Ref. column
	C3Φ15E45	475.8	-0.44
	C3Φ15E120	137.1	0.00
	C3Φ20E45	473.7	-0.85
	C3Φ20E120	137.1	0.00
	C3Φ25E45	471.6	-1.31
	C3Φ25E12	137.11	0.00

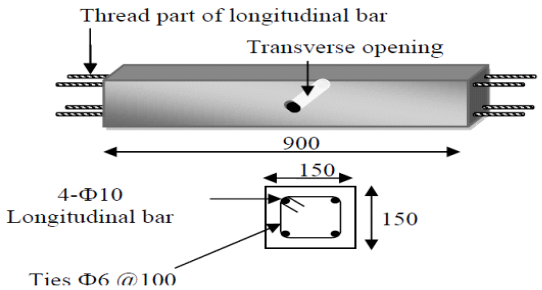

Figure 1. Dimensions and reinforcement details of column specimen.

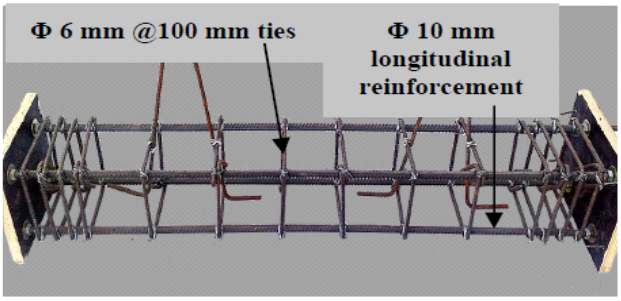

Figure 2. Details of column reinforcement

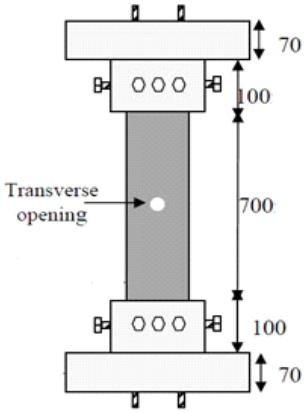

Figure 3. Specimen details and dimensions

Figure 4. Details of loading steel cap

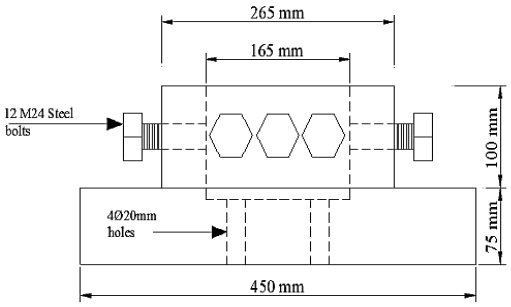

Figure 5. Schematic representation for loading steel cap

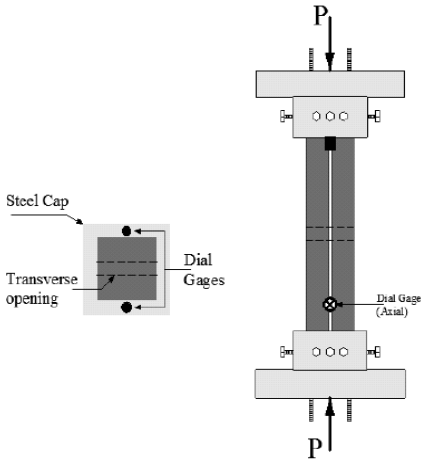

Figure 6. Schematic representation for dial gage positions mounted on concrete columns.

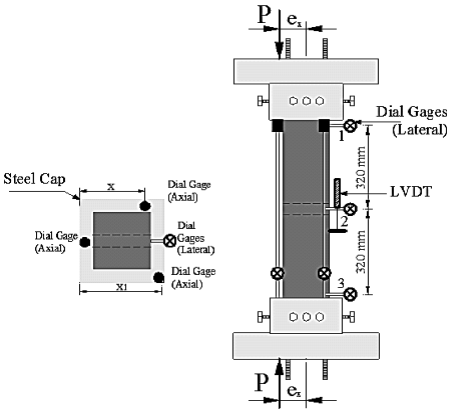

Figure 7. Schematic representation for dial gage position mounted on eccentric loaded columns.

Figure 8. LVDT use to measure axial displacement.

Figure 9. Supporting system used at columns ends.

Figure 10. Loading steel shaft details.

Figure 11. Steel shaft inside the details.

Figure 12. Testing machine used in the present work **.**

Figure 13. Lifting of tested column to the slide steel base level.

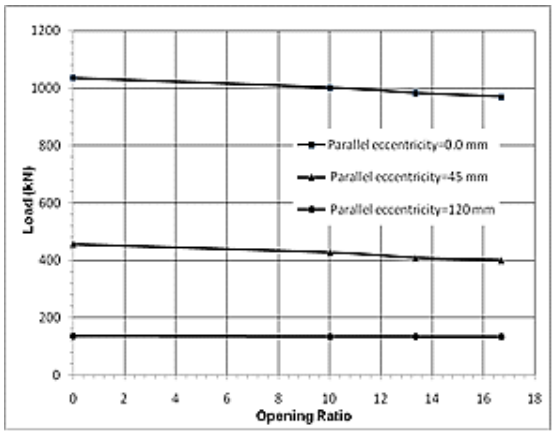

Figure 14. Effect of the opening ratio on the ultimate strength of columns of group A

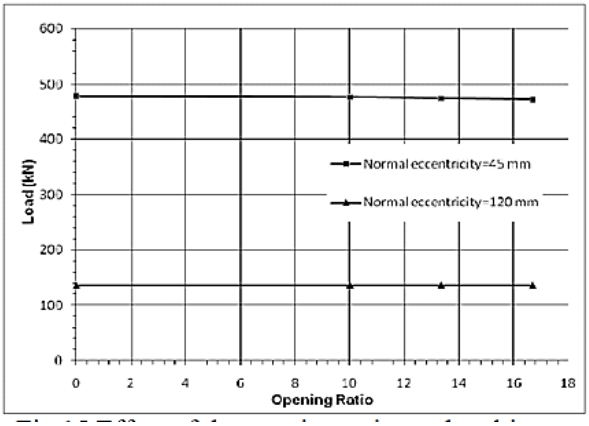

Figure 15. Effect of the opening ratio on the ultimate strength of columns of group B

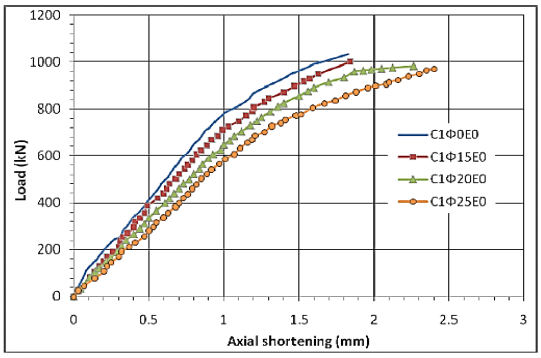

Figure 16. Load versus axial shortening for columns of group A, e = 0.0 mm

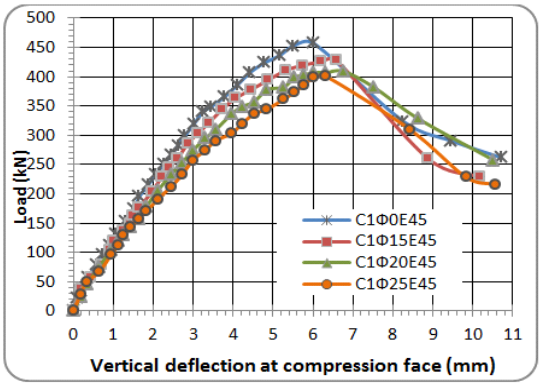

Figure 17. Load versus vertical deflection at compression face of columns of group A, e=45 mm

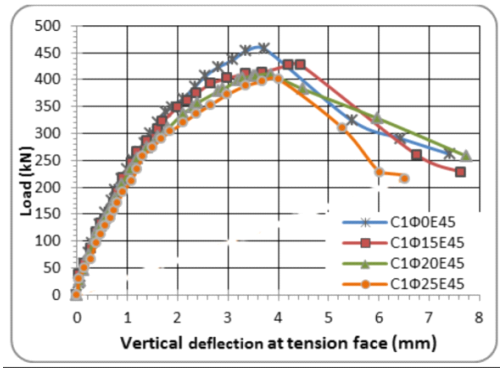

Figure 18. Load versus lateral mid height deflection of columns of group A, e=45 mm

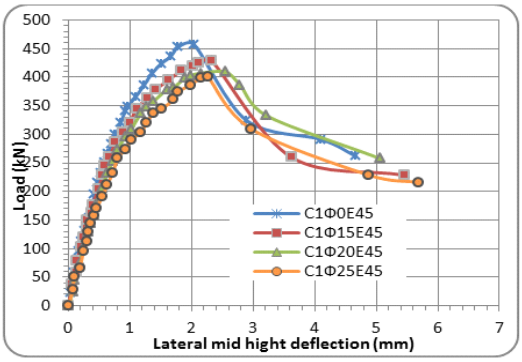

Figure 19. Load versus vertical deflection at tension face of columns of group A, e=45 mm

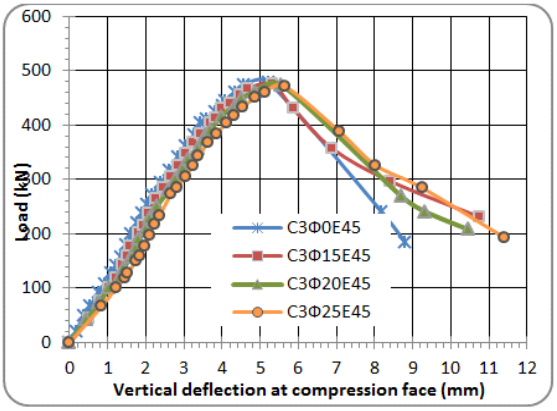

Figure 20. Load versus lateral mid height deflection of columns of group B, e=45 mm

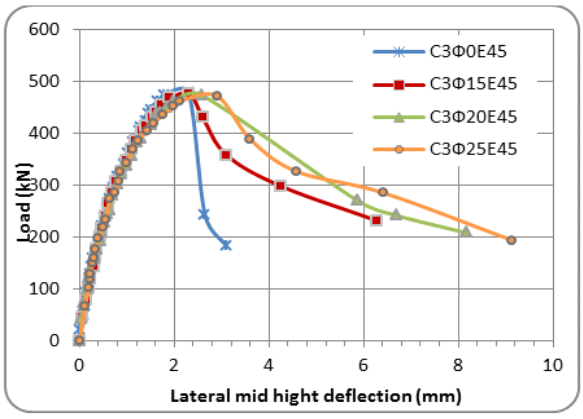

Figure 21.Load versus vertical deflection at tension face of columns of group B, e=45 mm

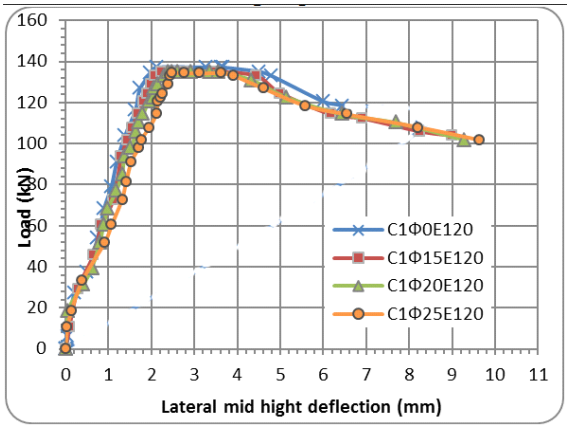

Figure 22. Load versus vertical deflection at tension face of columns of group B, e=45 mm

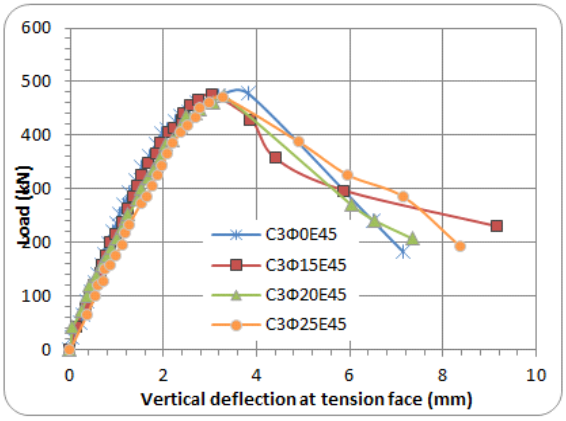

Figure 23. Load versus lateral mid height deflection of columns of group A, e=120 mm

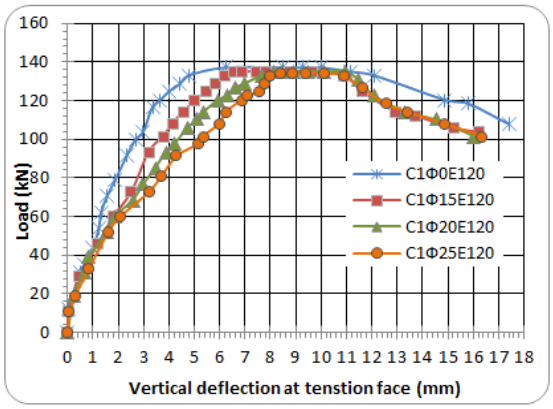

Figure 24. Load versus vertical deflection at compression face of columns of group A,e=120mm

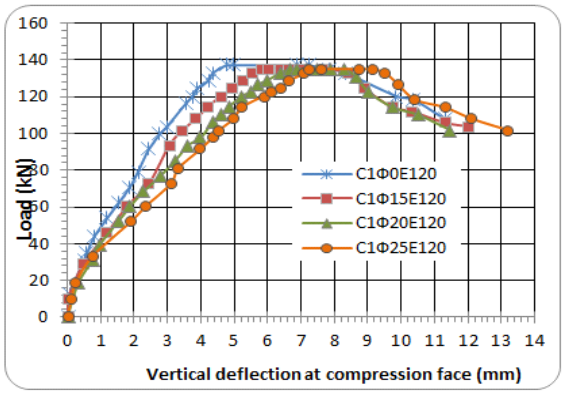

Figure 25. Load versus vertical deflection at tension face of columns of group A,e=120mm

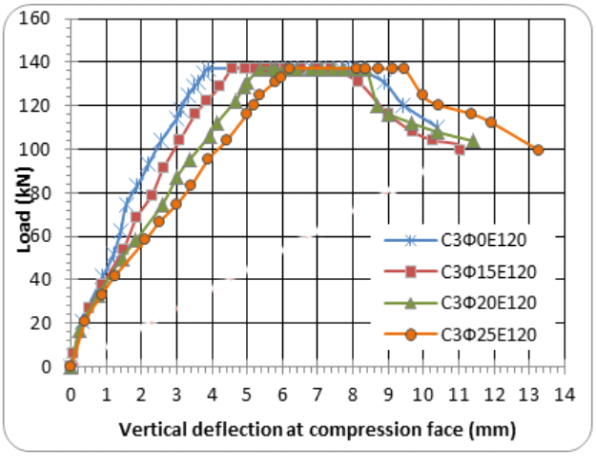

Figure 26. Load versus lateral mid height deflection of columns of group B,e=120mm

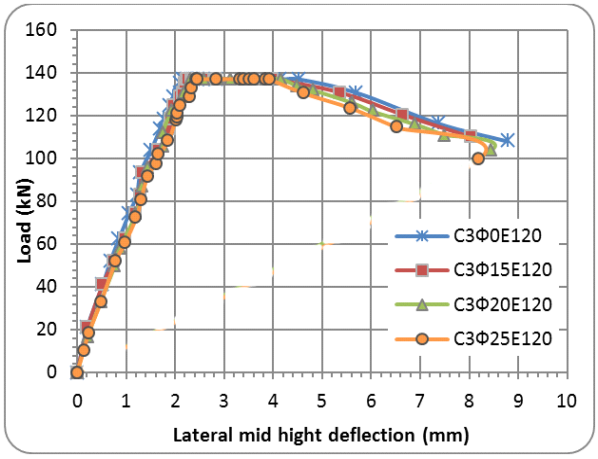

Figure 27. Load versus vertical deflection at compression face of columns of group B,e=120mm

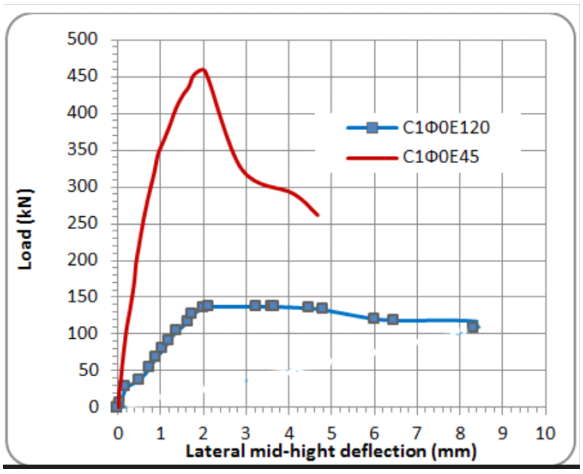

Figure 28. Load versus vertical deflection at tension face of columns of group B, e=120 mm

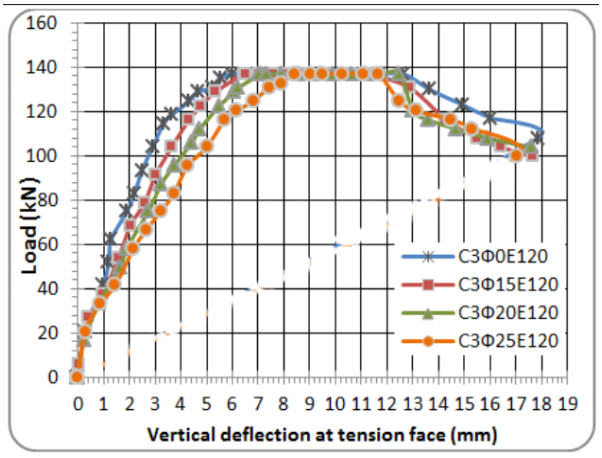

Figure 29. Load versus lateral mid-height deflection for columns C1Φ0E120 and C1Φ0E45

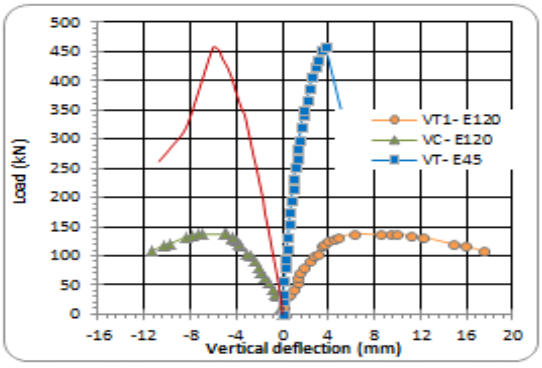

Figure 30. Load versus vertical deflection for columns C1Φ0E120 and C1Φ0E45

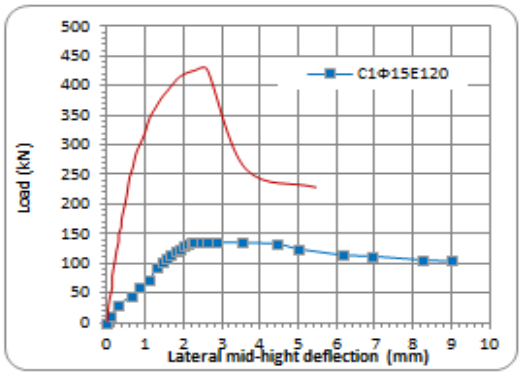

Figure 31.Load versus lateral mid-height deflection for columns C1Φ15E120 and C1Φ15E45

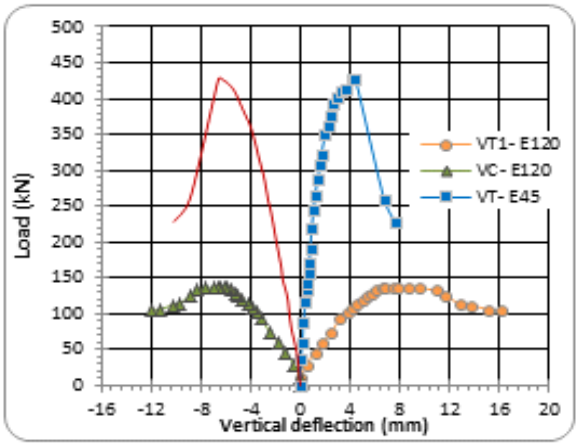

Figure 32. Load versus vertical deflection for columns C1Φ15E120 and C1Φ15E45

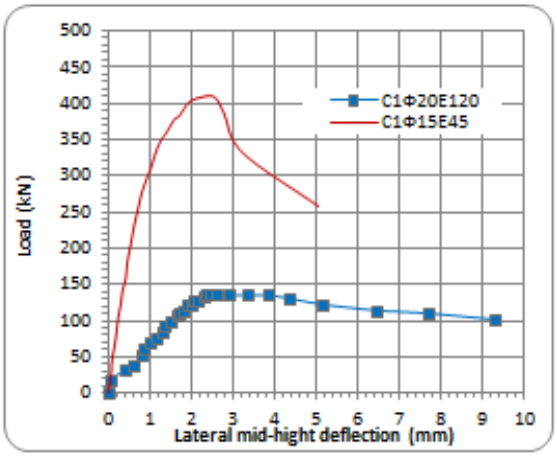

Figure 33. Load versus lateral mid-height deflection for columns C1Φ20E120 and C1Φ20E45

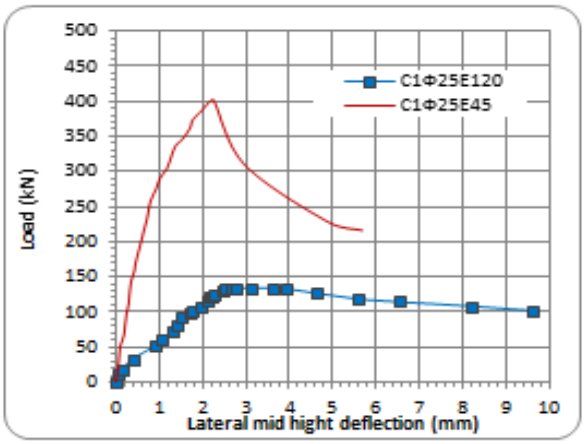

Figure 34. Load versus vertical deflection for columns C1Φ20E120 and C1Φ20E45

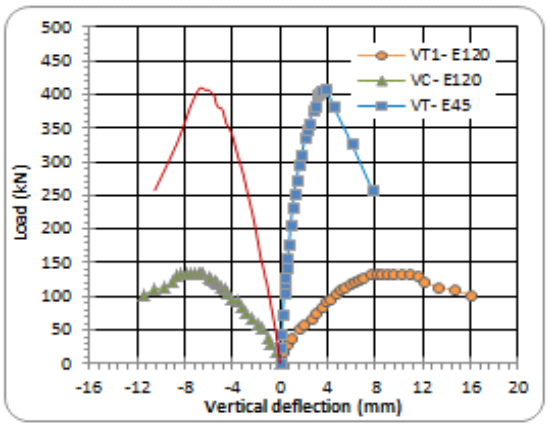

Figure 35. Load versus lateral mid-height deflection for columns C1Φ25E120 and C1Φ25E45

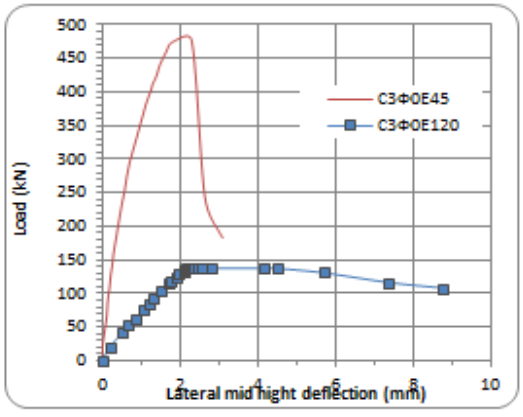

Figure 36. Load versus vertical deflection for columns C1Φ25E120 and C1Φ25E45

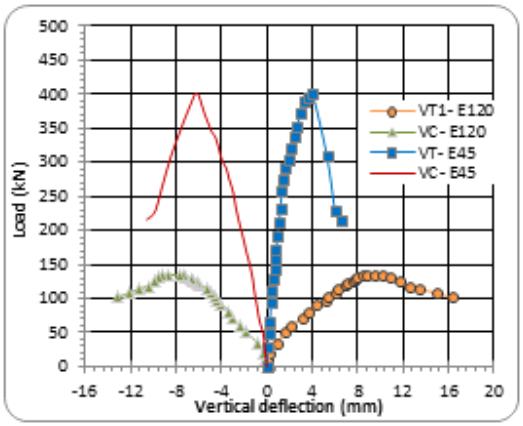

Figure 37. Load versus lateral mid-height deflection for columns C3Φ0E120 and C3Φ0E45

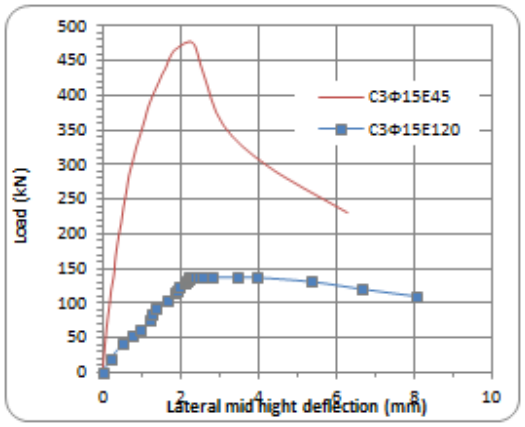

Figure 38. Load versus vertical deflection for columns C3Φ0E120 and C3Φ0E45

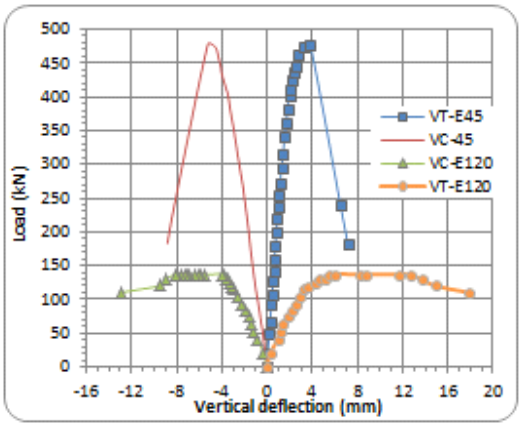

Figure 39. Load versus lateral mid-height deflection for columns C3Φ15E120 and C3Φ15E45

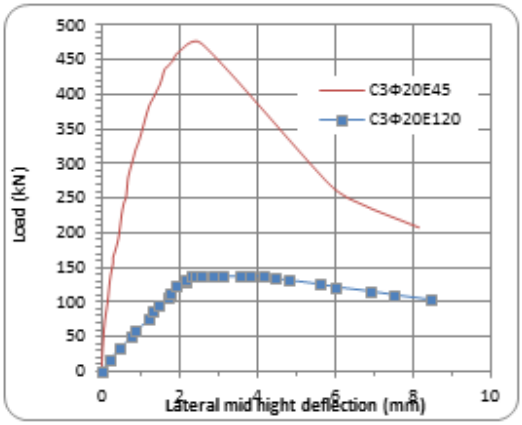

Figure 40. Load versus vertical deflection for columns C3Φ15E120 and C3Φ15E45

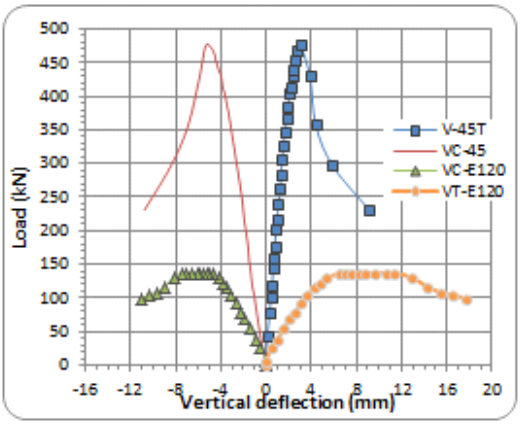

Figure 41. Load versus deflection for columns C3Φ20E120 and C3Φ20E45

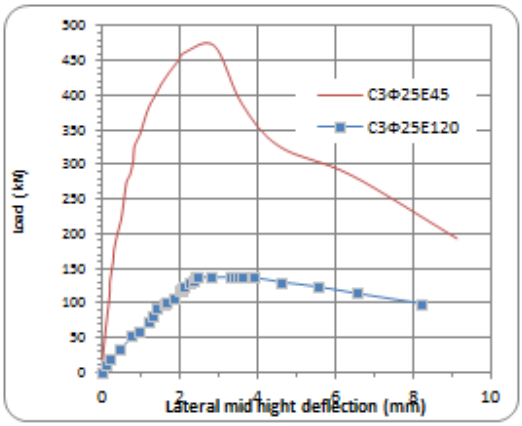

Figure 42. Load versus vertical deflection for columns C3Φ20E120 and C3Φ20E45

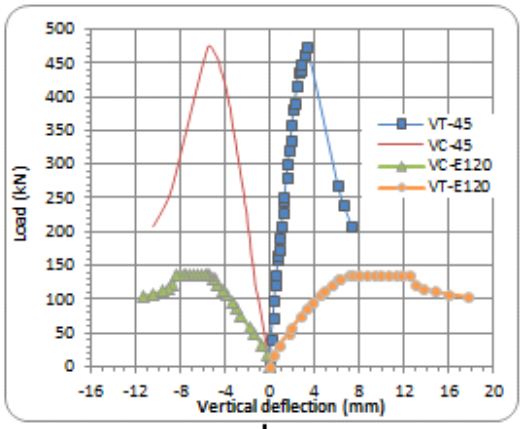

Figure 43. Load versus lateral mid-height deflection for columns C3Φ25E120 and C3Φ25E45

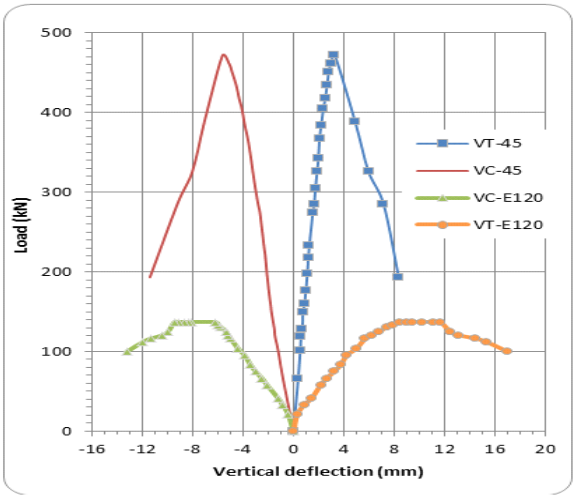

Figure 44. Load versus vertical deflection for columns C3Φ25E120 and C3Φ25E45.

Figure 45. Column C1Φ0E0 (group A), after testing

Figure 46. Column C1Φ20E0 (group A), after testing

(a) Compression face (b) Tension face

Figure 47. Column C1Φ15E45 (group A), after testing

(a) Compression face (b) Tension face

Figure 48. Column C3Φ20E45 (group B), after testing

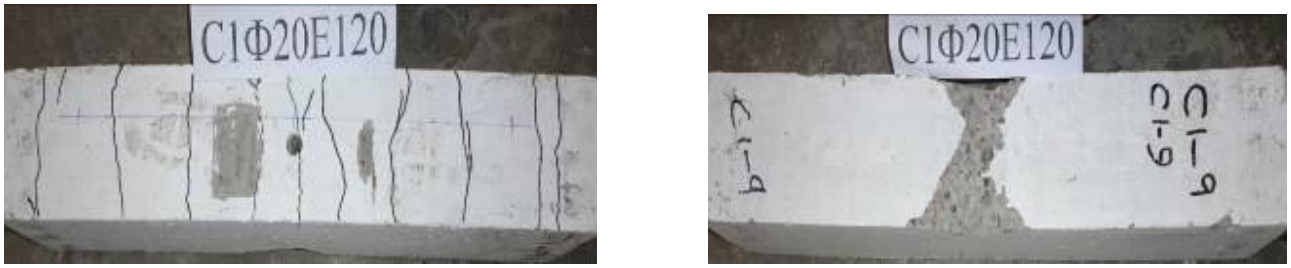

(a) Compression face (b) Tension face

Figure 49.Column C1Φ20E120 (group A), after testing

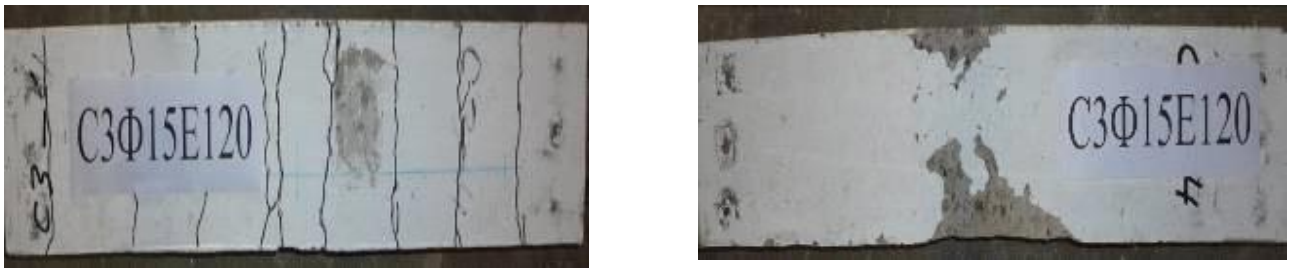

(a) Compression face (b) Tension face

Figure 50. Column C3Φ15E120 (group B), after testing.

Buckling Loads and Effective Length Factor for Non-Prismatic Columns

Taghreed Hassan Ibrahim
Assistant Lecture
Department of Civil Engineering
College of Engineering-University of Baghdad
E-mail: tegreed@yahoo.com

ABSTRACT

Based on a finite element analysis using Matlab coding, eigenvalue problem has been formulated and solved for the buckling analysis of non-prismatic columns. Different numbers of elements per column length have been used to assess the rate of convergence for the model. Then the proposed model has been used to determine the critical buckling load factor (γ_{cr}) for the idealized supported columns based on the comparison of their buckling loads with the corresponding hinge supported columns . Finally in this study the critical buckling factor (γ_{cr}) under end force (P) increases by about 3.71% with the tapered ratio increment of 10% for different end supported columns and the relationship between normalized critical load and slenderness ratio was generalized.

Keywords: Buckling load, non-prismatic, finite element, eigenvalue.

أحمال الانبعاج ومعامل الطول الفعال للأعمدة غير المنشورية

تغريد حسن إبراهيم
مدرس مساعد
قسم الهندسة المدنية
كلية الهندسة – جامعة بغداد

الخلاصة

بالاعتماد على نظرية تحليل العناصر المحددة وباستخدام برنامج الماتلاب تمت صياغة مشكلة القيمة الذاتية وحلها وفقا لتحليل الانبعاج للأعمدة غير المنشورية. تم استخدام أعداد مختلفة من العناصر على امتداد طول العمود لتقييم معدل التقارب للنموذج الأمثل. لقد تم استخدام النموذج المقترح لتحديد معامل الانبعاج الحرج(γ_{cr}) لأعمدة مثالية الإسناد وذلك للمقارنة بين أحمال الانبعاج لحالات إسناد مختلفة للأعمدة مع حالة الإسناد البسيط. وأخيرا كانت الزيادة لمعامل الانبعاج الحرج (γ_{cr}) بحدود 3,71% لكل 10% زيادة في نسبة التدبب لمختلف حالات الإسناد وكذلك تم تعميم العلاقة بين الحمل الحرج ونسبة النحافه للاعمدة.

الكلمات الرئيسية: حمل الانبعاج، غير منشوري، العناصر غير المحددة، القيمة الذاتية.

1. INTRODUCTION

Determination of critical buckling load for elastic column is a key problem in engineering design. Non-prismatic or tapered compression members are often used to achieve economy in many practical applications**, Shengmin, 1996**. The first study on elastic stability is attributed to **Euler, 1744**, who used the theory of calculus of variations to obtain the equilibrium equation and buckling load of a compressed elastic column. Since many studies in this field have been made such as **Gere, et al., 1962**, derived exact buckling solutions for many types of tapered columns with simple boundary conditions. **Ermopoulos, 1986** studied the buckling of the tapered columns under axially concentrated loads at any position along the length direction for the parabolically varying bending stiffness**, Gere, et al., 1962**. **Groper, et al., 1987,** developed a method for predicting the critical buckling load for the particular case of concentrically loaded

columns with variations in cross-sectional area. **Rzaiee, et al., 1995**, used a geometrical nonlinear analysis to solve non-prismatic or nonsymmetrical thin walled I-beam or columns, and by using a computer program they generalized the results in form of design tables. **Shengmin, 1996**, used a modified matrix technique to study the elastic and inelastic buckling capacity of non-prismatic members with a linear tapered I-shaped with a constant flange and a variable web. **Yossif, 2008**, derived the elastic critical load of a non-prismatic member using the equations of the modified stability functions for a wide range of taper ratio for rectangular or square cross sectional shapes. **Wei, et al., 2010**, analyzed the buckling of prismatic and non-prismatic rectangular columns under its weight and external axial force and discussed the influence of the taper ratio on the critical buckling load. **Al-Sadder, et al., 2004**, determined an exact secant stiffness matrix for a fixed-end forces vector for non-prismatic beam-column members under tension and compression axial force.

2. THEORY

In the displacement field approach, a structure is usually dividing into a number of finite elements and these elements are interconnecting at joints termed nodes as shown in **Fig. 1**. The displacements within each element are represented by simple functions. The displacement function is generally expressed in terms of a polynomial to be as or trigonometric function. For a one dimensional idealization structure, the displacement field can be assumed in Eq. (1)[4]:

$$\boldsymbol{v(x) = a_1 + a_2 x + a_3 x^2 + a_4 x^3} \qquad (\mathbf{1})$$

where:

$\boldsymbol{v(x)}$: Is the displacement function at any x along the element.

a_1, a_2, a_3 and a_4 :Is the coefficients of the generalized coordinates.

In a matrix form, $\boldsymbol{v(x)}$ can be represented as;

$$\boldsymbol{v = \begin{bmatrix} 1 & x & x^2 & x^3 \end{bmatrix} \begin{bmatrix} a_1 \\ a_2 \\ a_3 \\ a_4 \end{bmatrix}} \qquad (\mathbf{2})$$

The relation between the nodal degrees of freedom and the generalized coordinates can be expressed in Eq.(3):

$$\boldsymbol{v = [x]\{a\}} \qquad (\mathbf{3})$$

and

$$\boldsymbol{\theta = v' = \begin{bmatrix} 0 & 1 & 2x & 3x^2 \end{bmatrix} \begin{bmatrix} a_1 \\ a_2 \\ a_3 \\ a_4 \end{bmatrix}} \qquad (\mathbf{4})$$

Hence ; nodal displacements of an individual element will be expressed as:

$$[d]=\begin{bmatrix} v_1 \\ \theta_1 \\ v_2 \\ \theta_2 \end{bmatrix}=\begin{bmatrix} 1 & 0 & 0 & 0 \\ 0 & 1 & 0 & 0 \\ 1 & L & L^2 & L^3 \\ 0 & 1 & 2L & 3L^2 \end{bmatrix}\begin{bmatrix} a_1 \\ a_2 \\ a_3 \\ a_4 \end{bmatrix}$$

or

$$[d]=[A]\{a\} \quad (5)$$

then

$$\{a\}=[A]^{-1}\{d\} \quad (6)$$

Substitute Eq.(6) into Eq.(3) to get:

$$v = [x][A]^{-1}\{d\} \quad (7)$$

Where:

$$A^{-1}=\begin{bmatrix} 1 & 0 & 0 & 0 \\ 0 & 1 & 0 & 0 \\ \frac{-3}{L^2} & \frac{-2}{L} & \frac{3}{L^2} & \frac{-1}{L} \\ \frac{2}{L^3} & \frac{1}{L^2} & \frac{-2}{L^3} & \frac{1}{L^2} \end{bmatrix} \quad (8)$$

The total potential energy ($\prod p$) for a member that subjected to an axial force (P) is expressed in Eq. (9):

$\prod_p$= strain energy + potential energy of applied force [2]

$$\prod_p = \int_0^L \frac{EI}{2}\left(\frac{d^2v}{dx^2}\right)^2 dx + \int_0^L \frac{P}{2}\left(\frac{dv}{dx}\right)^2 dx \quad (9)$$

This equivalent assumed that the potential of the loads is considered to be due to the forces normal to the column length only. The summation of the two integrals of Eq. (9) is considered as $\prod p=0$.[4]

The term $\left(\left(\frac{dv}{dx}\right)^2/2\right)$ in the second integral expresses the strain due to rotation of the beam element a length of $\left(dx\left(\frac{ds-dx}{dx}\right)\right)$.

$$\frac{ds-dx}{dx}=\frac{(dx^2+dv^2)^{1/2}-dx}{dx}=[1+(v')^2]^{1/2}-1\approx\frac{(v')^2}{2}$$

Based on the above statements:

$$\prod_p = \int_0^L \frac{EI}{2} v_{,xx}^2 dx + \int_0^L \frac{P}{2} v_{,x}^2 dx \quad (10)$$

Where: $\boldsymbol{v_{,xx}} = \frac{\boldsymbol{d^2v}}{\boldsymbol{dx^2}}$, $\boldsymbol{v_{,x}} = \frac{\boldsymbol{dv}}{\boldsymbol{dx}}$

From Eq.(7) it will be get:

$$\boldsymbol{v_{,xx}} = \boldsymbol{\left[x''\right][A]^{-1}\{d\}} \quad (\mathbf{11})$$

And noting that , $\boldsymbol{v^2_{,xx}} = [\boldsymbol{v_{,xx}}]^{\boldsymbol{T}}[\boldsymbol{v_{,xx}}]$

$$\boldsymbol{v_{,xx}} = \boldsymbol{\lfloor B \rfloor . \{d\}} \quad (\mathbf{12})$$

Where:

$$\boldsymbol{\lfloor B \rfloor} = \boldsymbol{\left[x''\right] . [A]^{-1}}$$

$$\boldsymbol{\prod_p} = \frac{\boldsymbol{EI}}{\mathbf{2}} \int_{\mathbf{0}}^{\boldsymbol{L}} \boldsymbol{\{d\}^T_{1\times4} . \lfloor B \rfloor^T_{4\times1} . \lfloor B \rfloor_{1\times4} \{d\}_{4\times1} \, . dx} + \frac{\boldsymbol{P}}{\mathbf{2}} \int_{\mathbf{0}}^{\boldsymbol{L}} \boldsymbol{\{d\}^T . [A]^{-T} . \left[x'\right]^{-T} . \left[x'\right] . [A]^{-1} . \{d\} dx} \quad (\mathbf{13})$$

For a compressive force (P), we have $\boldsymbol{\prod_p} = \frac{\mathbf{1}}{\mathbf{2}}\boldsymbol{\{d\}^T[K]\{d\}} - \frac{\mathbf{1}}{\mathbf{2}}\boldsymbol{\{d\}^T P\left[K_g\right]\{d\}}$

Let $\boldsymbol{[K_e]} = \boldsymbol{[K]} - \boldsymbol{\left[K_g\right]}$=Equivalent stiffness matrix for a beam element of combined axial and a bending force actions.

Where:

$$\boldsymbol{[K]} = \boldsymbol{\int_0^L \lfloor B \rfloor^T . EI . \lfloor B \rfloor \, dx} \quad (\mathbf{14})$$

[K_g]=Geometric stiffness matrix

$$\boldsymbol{\left[K_g\right]} = \boldsymbol{P\left[\bar{k}\right]}$$

$$\boldsymbol{\left[K_g\right]} = \boldsymbol{P} \int_{\mathbf{0}}^{\boldsymbol{L}} \boldsymbol{[A]^{-T} . \left[x'\right]^{-T} . \left[x'\right] . [A]^{-1} . \{d\} \, dx} \quad (\mathbf{15})$$

$$\boldsymbol{\left[K_g\right]} = \frac{\boldsymbol{P}}{\boldsymbol{30L}} \begin{bmatrix} \mathbf{36} & \boldsymbol{3L} & \mathbf{-36} & \boldsymbol{3L} \\ \boldsymbol{3L} & \boldsymbol{4L^2} & \boldsymbol{-3L} & \boldsymbol{-L^2} \\ \mathbf{-36} & \boldsymbol{-3L} & \mathbf{36} & \boldsymbol{-3L} \\ \boldsymbol{3L} & \boldsymbol{-L^2} & \boldsymbol{-3L} & \boldsymbol{4L^2} \end{bmatrix} \quad (\mathbf{16})$$

The geometric stiffness matrix $\boldsymbol{\left[K_g\right]}$ can be obtained by the consistent geometric stiffness technique and the main advantage of this method that the eigenvalues were more accurate and were proven upper bounds to the exact solution.

For the non-prismatic or tapered member we derived equation for the moment of inertia (I_x) of the section at any distance (x) from the smallest end can be expressed in Eq. (17):

$$I_x = I_o + (\lambda - 1) I_o \frac{x}{L} \quad (17)$$

Where:
I_o *:* Is the moment of inertia for the smallest section at x=0.
λ: Is the tapered ratio that represents the increasing in the moment of inertia so it's defied as the ratio of the moment of inertia at the bottom of the column I-section (I_L) to the moment of inertia at the top of the column I-section (I_o) as shown in **Fig. 2**.

Substitutes Eq. (17) into Eq. (14) and analytical integrated by Matlab software, an implicit form has been derived for stiffness matrix [K].
Finally:

$$\left[[K] - \left[K_g\right]\right].\{D\} = \{F\} \quad (18)$$

For buckling problems: $\{F\} = \{0\}$, $\{D\} \neq \{0\}$ then

$$det\left|K - K_g\right| = 0$$

Eigenvalue problems were solved by using the finite element method written in Matlb program. The program used the element stiffness, mass matrix and modified the eigenvalue matrix equation with given constraints. The modified eigenvalue matrix equation contained fictitious zero eigenvalues in the same number of constraints. Finally solved this eigenvalue problem and determine the critical buckling load factor (γ_{cr}) for the lowest eignvalue. The critical buckling load is expressed as shown in Eq. (19):

$$P_{cr} = \gamma_{cr} \frac{\pi^2 EI}{L^2} \quad (19)$$

3. CASE STUDIES:

A tapered I-section column of a constant flange width and linear increasing in the web depth was adopted. It has a total length of (L) and under the effect of a concentrated axial load (P) on its top as shown in **Fig. 3.**

For the columns shown in **Fig. 3** there were different taper ratios (λ) of (1,1.1, 1.2, 1.3, 1.4, 1.5, 1.6, 1.7, 1.8, 1.9 and 2) with different boundary conditions of the hinged-hinged, clamped-free, clamped-hinged and clamped-clamped end supported columns have been considered. Critical buckling load factor (γ_{cr}) for the case studies has been summarized in **Table 1**.

The following notations were used to describe column boundary conditions for different end supports are summarized in **Table 2**.

4. VERIFICATION:

In order to investigate the validity of the results of the program we had to compare the buckling load factor for linear tapered I-sections column for the tapered ratio of one only because of the difference in the calculation of the studies for the tapered ratio where, **Wei,2010**, and **Yossif, 2008**, considered the tapered ratio as the ratio of width to length of a rectangular column section,

while in this study the tapered ratio is considered as the ratio of the moment of inertia at the bottom to the top of the I-section, since the verification is used tapered ratio of one only and the result was almost identical as shown in **Table 3**.

5. RESULTS AND DISCUSSIONS:

By using the finite element method in Matlab program to solve the eigenvlue problem in order to compute the critical buckling load factor for the non-prismatic or tapered I-shape steel column member, with linearly varied web height and with constant flange dimension.

Table 1 gave the critical buckling load factor ($\boldsymbol{\gamma_{cr}}$) of the web tapered column under axial force (P) acting at the top of the column for different boundary conditions. Different number of elements (from 4 to 11) along column length gave results that are quite close with a relative error not greater than (3%).

The results obtained from **Table 1** showed that average increasing in tapered ratio leads to increasing the buckling load factor about 4.17% for the hinged-hinged end supported column and about 3.6% for the clamped-free, clamped-hinged and clamped-clamped end supported columns, that mean for each 10% increase in the moment of inertia for the column section leads to average increasing of 3.71% for the hinged-hinged, clamped-free, clamped-hinged and clamped-clamped end supported columns.

To present the relationship between the normalized critical load defined by ($P_{cr}/f_y.A$) and the slenderness ratio (KL/r) as shown in **Table 4** and **Fig. 4**, the hinged-hinged column end supports was implemented with different tapered ratios of (1, 1.2, 1.4, 1.6, 1.8 and 2) and used the wide-flange section of (W30x211) as shown in **Table 5** to represents the section properties of the radius of gyration (r), moment of inertia (I), and area of the section (A). The modulus of elasticity (E) and the yield strength of steel (f_y) were considered as (200 GPa) and (250 MPa) respectively. The slenderness ratio was limited by the maximum short and intermediate column limit (Cc) factor which calculate from the Eq.(20) and the maximum long column limit (KL/r=200)[6].

$$\boldsymbol{C_c = \sqrt{\frac{2\pi^2 E}{f_y}}} \qquad (\mathbf{20})$$

Convergence for the critical buckling factor for the case of hinged-hinged column end supports could be obtained with three or more elements mesh as shown in **Fig. 5.**

6. CONCLUSIONS:

- The buckling of non-prismatic columns or tapered I-shaped steel column under tip force was analyzed by finite element method using Matlab coding.
- The boundary condition at both ends of column were processed in the program for the hinged-hinged, clamped-free, clamped-hinged and clamped-clamped end supported columns.

- The lowest eigenvlue gave the desired buckling load factor for different tapered ratios (λ) of (1,1.1, 1.2, 1.3, 1.4, 1.5, 1.6, 1.7, 1.8, 1.9 and 2) .
- The critical buckling factor (γ_{cr}) under end force (P) increases by about 3.71% with the tapered ratio increment of 10% for different end supported columns..
- Relationship between normalized critical load and limited slenderness ratio was generalized.
- For the hinged-hinged supports, from (3-7) elements along the column length obtained a fair convergence for the model for this study.

REFERENCES:

- Al-Sadder, S. Z., and Qasrawi, 2004, *Exact Secant Stiffness Matrix for Nonprismatic Beam-Columns with Elastic Semi rigid Joint Connections*, Emirates Journal for Engineering Research, Vol. 9, No.2, PP.127-135.
- Chandraupatla, T. R., and Belegunu, A. D., 1990, *Introduction to Finite Elements in Engineering*, U.S.A.
- Groper, M. and Kenig, M. J., 1987, *Inelastic Buckling of Non-prismatic Columns*, Journal of Engineering Mechanics, Vol.113, No.8, August, PP. 263-279.
- Iyengar , N. G. R., 1986, *Structural Stability Of Columns And Plates*, Affiliated East-West Press, New Delhi.
- Rzaiee-Pajand, M. and Moayedian, M., 1995, *Nonprismatic Beam and Column Design Table for Nonlinear Analysis*, Asian Journal of Structural Engineering, Vol.1, No.4, PP. 337-349.
- Shengmin, B. Wu., 1996, *Inelastic Buckling Loads for Nonprismatic Columns*, The Journal of Chaoyang, University of Technology Vol.6, No. 1, PP. 263-279.
- Timoshenko, S., and Gere, J. M., 1961, *Theory of Elastic Stability*, 2nd Edition, New York.
- Wei, D. J., Yan, S. X., Zhang, Li X.-F., 2010, *Critical Load for Buckling of Non-Prismatic Columns Under Self-Weight and Tip Force*, Mechanics Research Communications, Vol. 37, PP. 554–558.
- Yossif, W. V., 2008, *Elastic Critical Load of Tapered Members*, Journal of Engineering and Development, Vol. 12, No.1, PP. 148-160.
- Young, W. Kwan, Hyocoong Bang, 2000, *The Finite Element Method Using MATLAB*, 2nd Edition, NewYork.

NOMENCLATURE:

L = is the column length.
P = is the axial load.
P_{cr} = is the critical buckling load.
γ_{cr} = is the critical buckling factor.
λ = is the taper ratio.
r = is the radius of gyration.
A = is the area of column section.
I = is the moment of inertia.
I_x = is the moment of inertia for the section of the tapered member at any distance (x)
I_o = is the moment of inertia for the smallest section of the tapered member at x=0.
I_L = is the moment of inertia at the top of the column I-section.
E = is the steel modulus of elasticity
f_y = is the yield strength of steel.
Cc = is represents the theoretical demarcation line between inelastic and elastic behavior.

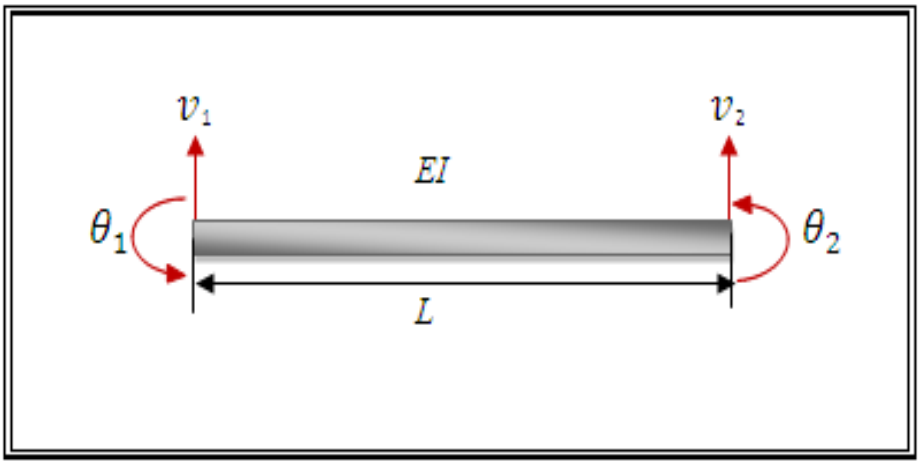

Figure 1. Beam Element.

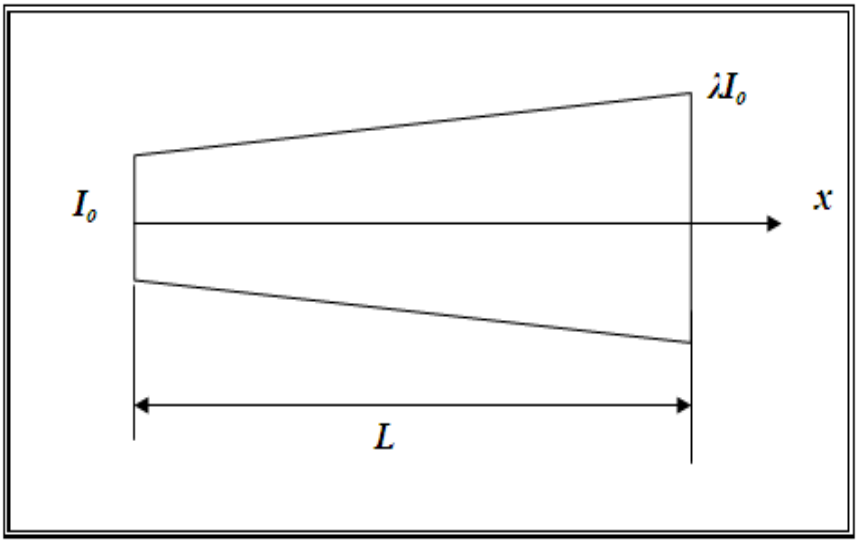

Figure 2. Tapered ratio of non-prismatic column member.

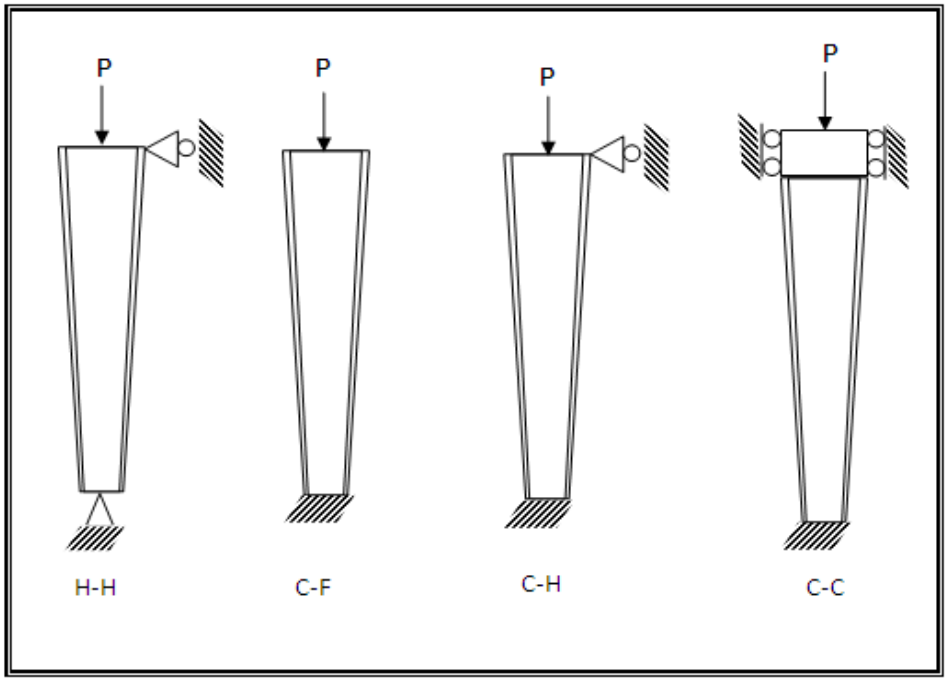

Figure 3. Schematic of tapered I-sections columns under tip force with different boundary conditions.

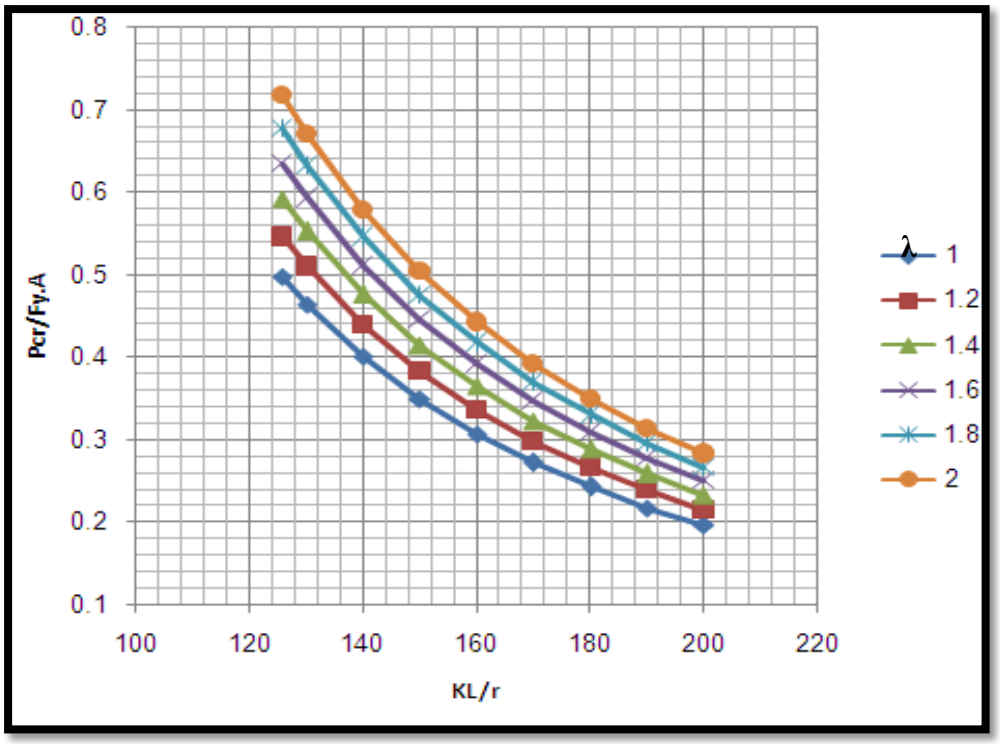

Figure 4. The normalized critical load verses the slenderness ratio.

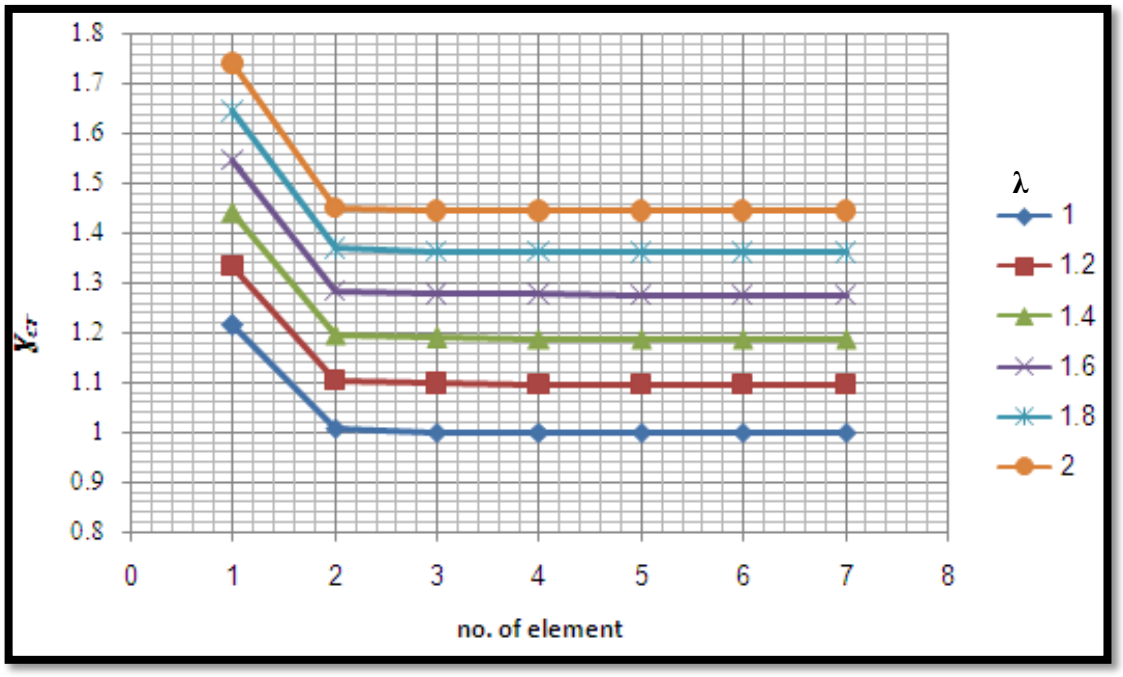

Figure 5. Relationship between the number of elements and the critical buckling factor for the hinged-hinged column end supports.

Table 1. The Critical Buckling Factor with Variable Tapered Ratio.

λ	(γ_{cr}) for H-H	No. of Element	(γ_{cr}) for C-F	No. of Element	(γ_{cr}) for C-H	No. of Element	(γ_{cr}) for C-C	No. of Element
1	1.000056	7	0.249999	7	2.046172	7	4.001155	9
1.1	1.049277	7	0.261711	8	2.140907	4	4.19873	8
1.2	1.097101	6	0.272958	7	2.237161	10	4.39124	7
1.3	1.143516	7	0.284103	7	2.324297	7	4.575643	9
1.4	1.188897	7	0.294864	7	2.416499	9	4.758021	7
1.5	1.233377	7	0.306293	10	2.501608	8	4.936345	7
1.6	1.276945	7	0.315715	7	2.582665	7	5.110617	7
1.7	1.361852	7	0.325847	7	2.669801	8	5.281849	7
1.8	1.403363	7	0.337499	10	2.755923	9	5.450041	7
1.9	1.403393	7	0.34753	11	2.841033	10	5.615194	7
2	1.444327	7	0.357459	11	2.925129	11	5.779029	7

Table 2. The Column Boundary Conditions of The Different End Supports.

Type of The Column End Supports	Boundary Conditions
(Hinged-Hinged) columns (H-H)	@x=0, v=0 @x=L, v=0
(Clamped-Free) columns (C-F)	@x=0, v=0 @x=0, $\boldsymbol{\theta}$=0
(Clamped-Hinged) columns (C-H)	@x=0, v=0 @x=0, $\boldsymbol{\theta}$=0 @x=L, v=0
(Clamped-Clamped) columns (C-C)	@x=0, v=0, @x=0, $\boldsymbol{\theta}$=0 @x=L, v=0, @x=L, $\boldsymbol{\theta}$=0

Table 3. Verification of the Critical Buckling Factor with Tapered Ratio(λ)=1.

Type of the Column End Supports	$(\boldsymbol{\gamma}_{cr})_{present\ study}$	$(\boldsymbol{\gamma}_{cr})_{Wie.\ 2010[8]}$	$(\boldsymbol{\gamma}_{cr})_{\ Yossif.2008[9]}$
(Hinged-Hinged) columns (H-H)	1.000056	1.0000401	1.000000
(Clamped-Free) columns (C-F)	0.249999	0.2499594	0.250000
(Clamped-Hinged) columns (C-H)	2.046172	2.045776	2.045752
(Clamped-Clamped) columns (C-C)	4.001155	3.999957	-

Table 4. The Non-dimensional Critical Load with Slenderness Ratio for the wide-flange section of (W30x211).

KL/r	$P_{cr}/f_y.A$ $\lambda=1$	$P_{cr}/f_y.A$ $\lambda=1.2$	$P_{cr}/f_y.A$ $\lambda=1.4$	$P_{cr}/f_y.A$ $\lambda=1.6$	$P_{cr}/f_y.A$ $\lambda=1.8$	$P_{cr}/f_y.A$ $\lambda=2$
125.66	0.4973	0.5456	0.5912	0.6349	0.6771	0.7181
130	0.4646	0.5007	0.5523	0.5932	0.6326	0.6709
140	0.4006	0.4395	0.4762	0.5115	0.5455	0.5785
150	0.3489	0.3827	0.4148	0.4455	0.4751	0.5039
160	0.3067	0.3365	0.3646	0.3916	0.4176	0.4429
170	0.2717	0.2981	0.323	0.3469	0.3699	0.3923
180	0.2423	0.2658	0.288	0.3093	0.3299	0.3499
190	0.2175	0.2386	0.2585	0.2776	0.296	0.314
200	0.196	0.215	0.233	0.2502	0.2668	0.283

Table 5. The Properties of Wide-Flange Section (W30x211).

Designation	Area (mm^2)	Web thickness(mm)	I $x10^6$ (mm^4)	r(mm)
W30x211	40100	19.7	4290	328

Study the Effects of Microwave Furnace Heat on The Mechanical Properties and Estimated Fatigue life of AA2024-T3

Dr. Ahmed Adnan AL-Qaisy
Lecturer
Mechanical Engineering Department
University of Technology
abomrem2004@gmail.com

Sameh Fareed Hasan
Engineer
Ministry of Science and Technology
Industrial Development & Research Director

Najmuldeen Yousif Mahmood
Assistant Lecturer
Mechanical Engineering Department
University of Technology
najmuldeen.uot@gmail.com

ABSTRACT

This research aims to study the effect of microwave furnace heat on the mechanical properties and fatigue life of aluminum alloy (AA 2024-T3). Four conditions were used inside microwave furnace (specimens subjected to heat as dry for 30 and 60min. and specimens subjected to heat as wet (water) for 30 and 60 min.), and compared all results with original alloy (AA 2024-T3). Tensile, fatigue, hardness and surface roughness tests were used in this investigation. It is found that hardness of dry conditions is higher than wet conditions and it increases with increasing of time duration inside microwave furnace for dry and wet conditions. Also, tensile strength has the same behavior of hardness, but it increases with decreasing of time. Dry condition for 60 min. shows the higher fatigue strength than other conditions. Surface roughness parameter (Ra) of dry conditions is higher than wet conditions and it decreases with increasing of duration of time.
Key words: Microwave Furnace, Mechanical Properties, Fatigue Life.

دراسة تأثير الحرارة الناجمة عن أفران المايكروويف على الخواص الميكانيكية وعمر الكلال لسبيكة الألومنيوم 2024-T3

د. أحمد عدنان عبد الجبار
مدرس
قسم الهندسة الميكانيكية
الجامعة التكنولوجية

سامح فريد حسن
مهندس
وزارة العلوم والتكنولوجيا
دائرة البحث والتطوير الصناعي

نجم الدين يوسف محمود
مدرس مساعد
قسم الهندسة الميكانيكية
الجامعة التكنولوجية

الخلاصة

يهدف هذا البحث لدراسة تأثير حرارة افران المايكرويف على الخواص الميكانيكية وعمر الكلال لسبيكة الالمنيوم (AA2024-T3). تم استخدام ابرع حالات داخل افران المايكرويف (عينات جافة تتعرض الى حرارة لمدة 30 دقيقة و 60 دقيقة و عينات رطبة (الماء) تتعرض الى حرارة لمدة 30 دقيقة و 60 دقيقة). في هذا البحث تم استخدام اختبار الشد ، الكلال ، الصلادة و خشونة السطح. وجدت ان الاصلادة للحالات الجافة اعلى من الحالات الرطبة وتتناقص الصلادة بزيادة الزمن داخل فرن المايكرويف بالنسبة للحالات الجافة والرطبة. مقاومة الشد لها نفس سلوك الصلادة ايضا ولكن تزداد مقاومة الشد بنقصان

الزمن. مقاومة الكلال للحالة الجافة ولمدة 60 دقيقية ظهرت اعلى من باقي الحالات. عامل خشونة السطح للحالة الجافة ولمدة 60 دقيقة اعلى من الحالة الرطبة وتتناقص بزيادة الزمن للحالتين الجافة والرطبة.

1. INTRODUCTION

It is well known that aluminum alloy has low density with normal strength and relatively a very good resistance for corrosive ware. Both strength and hardness of the material were extremely needed to be improved in any engineering applications. So, to apply this suitable heat treatment process is needed in order to improve the mechanical properties of such alloys. In many modern researches a microwave furnace heat energy has been used in a wide range of applications like medical therapy industrial modern application and food keeping processing etc. In this work, microwave furnace heat energy has been used, as one of the most modern applications and one of the greatest material processing techniques to improve mechanical properties of metals. At this work, a newer technique including microwave furnace post heat treatment of specimen surface were employed. A period microwave furnace was used efficiently to process AA 2024-T3. In microwave furnace processing, microwave furnace energy heats the alloy at the different heat levels، which will might leads to a uniformly bulk heating, conversely in the conventional heating systems, the alloy heated from surface to the inner core which produces thermal stress and/or longer time required for homogenization. A heat-treating process by microwave furnace can be used for a wide application of surface treatments such as carburizing, carbonating, chromizing, and bronzing. The fracture strength, toughness and hardness arrived from microwave furnace energy of treated specimen components were reported to be higher than others conventionally heat treated application ones , **Loganatha, et al., 2014**. Conventional heat treatment process exhibits higher porosity and coarse microstructure which affect the physical and mechanical properties of alloys, therefore, a new technique of microwave heating will be removing the bad effects of conventional heat treatment. Microwave heating process enhances the alloy uniformity way of providing unique microstructure and properties as a result of selective heating, **Rajkumar, et al., 2014** and **Rajan, et al., 2014**. In addition, microwave furnace is used for plant growth not only using as heat treatment of metal alloy, **Nasher, 2014**.

The research concentrated on the mechanical properties and estimated fatigue life affected by the microwave furnace energy heat treatment of the alloy used. In this work, AA 2024-T3 sheet was heat treated using microwave furnace energy at 4GHz and 1500W and the estimated fatigue life as long as its effect on mechanical properties**.**

2. MATERIAL AND APPARATUS

In this work, sheet metal of AA 2024-T3 is used with 3 mm thickness in order to make a standard tensile test specimen as shown as in **Fig. 1**. The tests were conducted at the Central Organization for Standardization and Quality Control (COSQC-Baghdad) according to the Iraqis Specification Quality (ISQ 1473/1989). The chemical composition tests were done at (COSQC-Baghdad) according to (ISQ 1473/1989) by the device (Spectrometer, ARC. MET 8000, 2009) as shown in **Fig.2**. These test result and standard are showed in **Table 1**.

2.1 Tensile and fatigue specimens preparation

The most important component of tensile testing test is specimen, because it could determine the actual physical and mechanical properties of the material which had been tested. The selected specimen for such tests must conform to exact physical dimensions and it must be free of heat distortion or induced cold working. Specimen must be personnel and accurately calibrated as long as the tensile machines and this is very important before applying the test, because these test

results were based on the accuracy and quality of the test specimen that been used. Tinius Olsen tensile machine is used in this investigation as showing in **Fig. 3**. A preparation steps including a precision milling machine, highly skilled machinist and considerably highly skills hand finishing can achieve the required configurations of the test specimen needed, **ASTM**, **2012.**

To achieve accurate results, a test specimen must be prepared accurately and properly. The following rules are suggested for general guidance:

a. Using Standard dimensions and sizes such as ASTM standards and like.
b. Surface finishing is very important in preparing tensile test specimens because it might be affecting on the results.

Other preparation concludes:

1. Grinding the specimen faces and sides with grinding papers (Silicon Carbide) starting from 120, 320, 500, 1000 and 2000 type .
2. Polishing the specimen by polishing instrument (Alumina Powder) of a grain size 0.5 μm.
3. Washing the specimen by water, oil soap and alcohol to remove grinding and polishing remained particles.
4. Finally, smoothly clean the specimen by soft silky fabric until you should almost see yourself on it. **Fig. 4** shows the specimen before and after polishing.

2.2 Fatigue Test Machine [Avery Standard Test]

In this research, a fully reversed reciprocating plane bending fatigue testing machine (Bend Test) type Avery Model 7305 with stress ratio R = -1 was used, see **Fig. 5**. To perform the tests, the following steps should be followed:

Step 1: Preparing the Machine:

As said, the machine should be calibrated to stress ratio R = -1 and for that two dial gages were used as shown in **Fig. 5**.

Step 2: Machine Calibration:

Static Calibration: In machines, it is importance to know exactly the speed of the machine, as an error in its speed corresponds might be to a doubled error in the applied load where the load is produced by centrifugal forces or by reciprocating masses. Therefore, the motor speed must be checked and calibrated with the standard. **Table 2** is illustrated the instruction manual of the machine.

Dynamic Calibration: During the operation of the testing machine, a new source of error sometimes appears; these errors come from the arrived vibration of rotating parts of the machine, which might lead to errors in the estimated results of the test. In the present work, a rubber isolator was used between the machine and the grand table to eliminate the inertia effects, **ASME**, **2009**.

2.3 Other Mechanical Properties Tests

Other tests included hardness test according to refrence, **ASTM E 110 – 82, 2002**, and surface roughness test according to Mitutoyo Standard Test. The first test was done by (Rockwell Hardness Testing Machine, the values are converted from Bernill Hardness value) as showing in **Fig. 6**, while the second test was done by Mitutoyo Surface Roughness Testing Machine as illustrated in **Fig. 7**, all tests were made by the COSQC-Baghdad according to the (ISQ 1475~1476/1989).

2.4 Experimental Work

Microwave furnace type Daewoo is used to achieve a heat treatment for all specimens as showing in **Fig. 8**. **Figs. 9** and **10** are showing tensile and fatigue specimens. There are 12^{th}

tensile specimens that using in this study and divided into four groups, three specimens each group. Firstly, dry condition for 60 min. in microwave, secondly, dry condition for 30 min. in microwave, thirdly, wet condition for 60 min. and the last, wet condition for 30 min in microwave. Temperature of microwave is 150°C. The general equation form of fatigue life is calculated by Basquin equation, **ASM Metals Handbook**, **2003,** and references, **Hantoosh, 2012, Mhesssan, 2012** and **Abdullatef, 2016,** are explained how to solve this equation according to S-N curves data, as follows:

$$\sigma_a = \sigma_f N^{-b} \quad \ldots (1)$$

Where:

σ_a: The applied stress at failure

N : The number of cycles at failure due to the applied stress σ_a

σ_f & b : Material constants that can be calculated by linearizing the S-N curve by rewriting equation (1) in logarithmic form.

3. RESULTS AND DISCUSSION

3.1 Hardness results

It has been showed that hardness of dry conditions is higher than wet conditions and it decreases with increasing of time duration inside microwave furnace. Increment of first group has 16% which higher than other groups (14%, 9% and 7.5% for group 1, 2 and 3 respectively), these results are illustrated in **Table 3**. These results lead to AA2024-T3 becomes harder when using of this type of heat treatment. These results are matched with references, **Loganathan, et al., 2014, Rajkumar, et al., 2014** and **Abdullatef, 2012,** which is studied the comparison between conventional heat treatment and microwave heat treatment.

3.2 Tensile strength results

From **Fig. 11** and **Table 4** results, it has been noticed that tensile strength of group 2 has higher result with improvement of 25% as compared with original alloy (2024-T3) than other groups. As above, material is become more brittle when using of microwave furnace, this is representing in total elongation. Group 4 has a higher total elongation (11.2 %) as compared with original alloy (12%), while group 1 has a lower value of total elongation (5.5%). Also, duration of time is effecting on elongation, when time increases, total elongation is decreased and verse versa. Microwave heat produces a hardening of surface of alloy only, while the center stills the same. When the surface is cooled, grains size of surface become smaller than grains size of center due to cooling is slower. Modulus of elasticity and Poisson's ratio has little change as compared with original alloy. These results have similar behavior with references, **Loganathan, et al., 2014** and **Abdullatef, 2012,** which is reported the effect of microwave furnace on the mechanical properties of AA6061 as compared with conventional heat treatment.

3.3 Fatigue strength results

The results showed that fatigue strength of dry conditions is higher than wet conditions as compared with original alloy. Also, time duration inside microwave furnace effects on fatigue strength, dry condition for 60 min. has fatigue strength higher than dry condition for 30 min, and

wet conditions have the same behavior, **Fig. 12** is illustrated that S-N curves of all groups as compared with original alloy.

For fatigue life, it has been found that group 1 has a major improvement as compared with other groups. When applying of equation (1) to produce a life of group 1, it can be written as follows in equation (2):

$$\sigma_a = 142\, N^{-0.0766} \quad \ldots (2)$$

Equation (3) represents a fatigue life of group 2 and as follows:

$$\sigma_a = 123\, N^{-0.0992} \quad \ldots (3)$$

Also, equation (4) represents a fatigue life form of original life and as follows:

$$\sigma_a = 165\, N^{-0.1085} \quad \ldots (4)$$

It has been not seen reports about fatigue strength of microwave furnace as a heat treatment of aluminum alloy, but, according to tensile strength, it is noticed that fatigue strength also has the same behavior.

3.4 Surface roughness results

Surface roughness parameter (Ra) of all groups are representing in **Table 4**. It has been found that group 1 has higher (Ra) than other groups and surface roughness parameter decreases with increasing of duration of time in microwave furnace.

4. CONCLUSION

1. Hardness of alloy that is subjected to microwave heat is a higher than conventional heat treatment.
2. Tensile and fatigue strength of alloy that is treated by microwave furnace have higher value as compared with conventional heat treatment.
3. Using of microwave furnace heat is not effect on modulus of elasticity and Poisson' ratio.
4. Using of microwaves furnace might be useful for shorten both time and cost of changing these properties into certain levels by only using suitable method and/or duration time and amount of heat.

5. REFERENCES

- Abdullatef, M. S., AlRazzaq, N., Hasan, M. M., 2016, *Prediction Fatigue Life of Aluminum Alloy 7075 T73 Using Neural Networks and Neuro-Fuzzy Models*, Eng. & Tech. Journal, Vol.34,Part (A), No.2.
- ASM Metals Handbook, 1992, *Properties and Selection: Nonferrous Alloys and Special-Purpose Materials*, vol.2.
- ASM Metals Handbook, 2003, *Mechanical Testing and Evaluation*, vol.8.
- ASME, 2009, *Standard Tensile Tests and Estimation of Mechanical Properties of AA7075*, Chicago, Illinois, USA.
- ASTM D 638 - 02a, 2003, *Standard Test Method for Tensile Properties of Plastics*, USA.
- ASTM E 110 – 82, 2002, *Standard Test Method for Indentation Hardness of Metallic Materials by Portable Hardness Testers*, USA.
- ASTM E 1251 – 94, 1999, *Standard Test Method for Optical Emission Spectrometric Analysis of Aluminum and Aluminum Alloys by the Argon Atmosphere, Point-to-Plane Unipolar Self-Initiating Capacitor Discharge*, USA.

- ASTM, 2012, *(ASTM) Standard Specification for Aluminum and Aluminum-Alloy Sheet and Plate*, USA.
- Hantoosh, Z. K., 2012, *Fatigue Life Prediction at Elevated Temperature under Low- High and High – Low Loading Based on Mechanical Properties Damage Model*, Eng. & Tech. Journal, Vol. 30, No.11.
- Loganathan, D., Gnanavelbabu, A., Rajkumar, K., and Ramadoss, R., 2014, *Effect of microwave heat treatment on mechanical properties of AA6061 sheet metal*, Elsevier Procedia Engineering, 97, PP. 1692 – 1697.
- Mhesssan, A. N., Hussein, H. A., and Alalkawi, H. J. M., 2012, *Effect of Temperature on Fatigue Transition life and Strength of Aluminum alloy*, Eng. & Tech. Journal, vol.30, N0.6.
- Nasher, S. H., 2014, *The Use of Microwave as Physical Method for Plant Growth Stimulation*, Eng. &Tech.Journal, Vol.32, Part (B), No.1.
- Rajan, P., Rajkumar, K., , and Charles, J. M. A., 2014, *Microwave heat treatment on Aluminum 6061 Alloy-Boron Carbide composite*, Elsevier Procedia Engineering, 86, PP.34-41.
- Rajkumar, K., Santosh, S., Ibrahim, S. J. S., and Gnanavelbabu, A., 2014, *Effect of electrical discharge machining parameters on microwave heat treatment Aluminum-Boron carbide-Graphite composites*, Elsevier Procedia Engineering, 97, PP. 1543-1550.
- Shulaev, N. S., Uleymanov, D. F., and Abutalipova, E. M., 2015, *A study on the effect of microwave radiation on the operational characteristics of insulating materials based on polyvinyl chloride*, International Scientific Forum, Butlerov Heritage, Kazan, The Republic of Tatarstan, Russia, Vol.42. No.5.

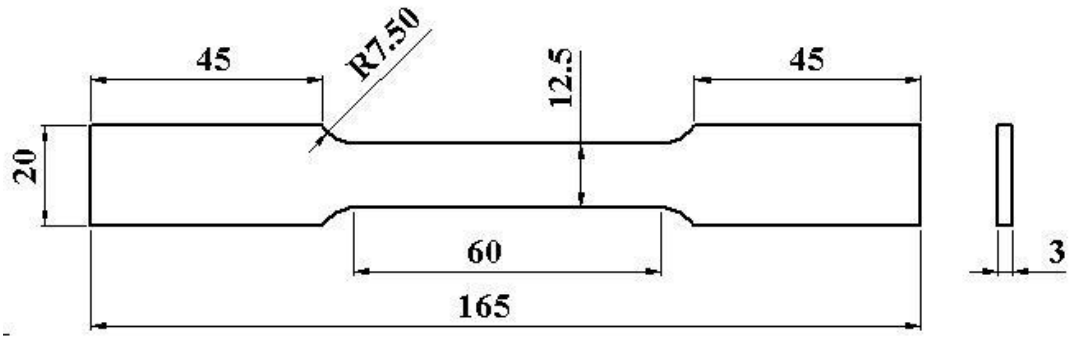

Figure 1. Tensile Test Specimen, **ASTM D 638 - 02a, 2003**. All dimensions are in mm.

Figure 2. AMETEK Material analysis division instrument**.**

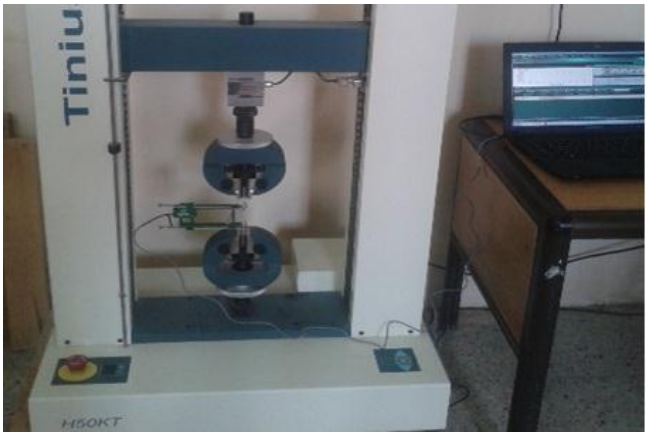

Figure 3. Tensile Test Machine Type Tinius Olsen.

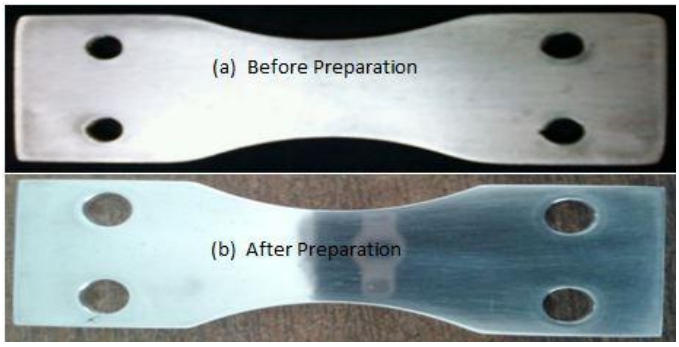

Figure 4. Standard Fatigue Test Specimen Before (a) and After (b) Preparation Steps**.**

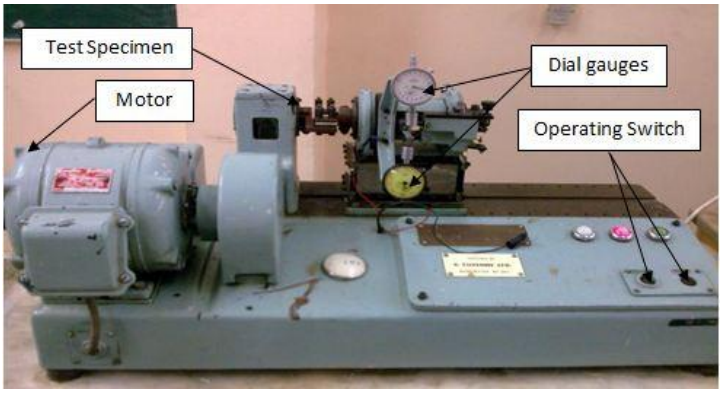

Figure 5. Bending Fatigue Testing Machine Type Avery Model 7305.

Figure 6. Rockwell Hardness Testing Machine**.**

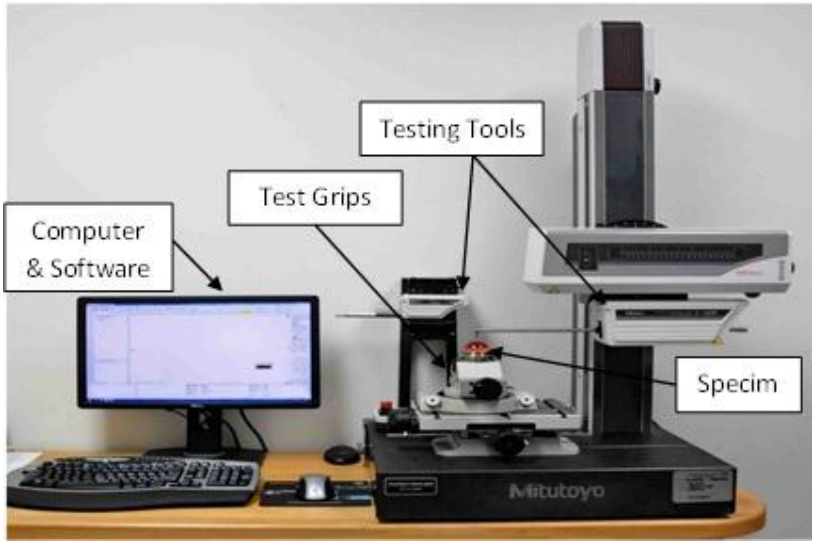

Figure 7. Surface Roughness Testing Machine Type Mitutoyo.

Figure 8. The Microwave Furnace used in this work Type Daewoo**.**

Figure 9. Tensile Test Specimens each three for specific group.

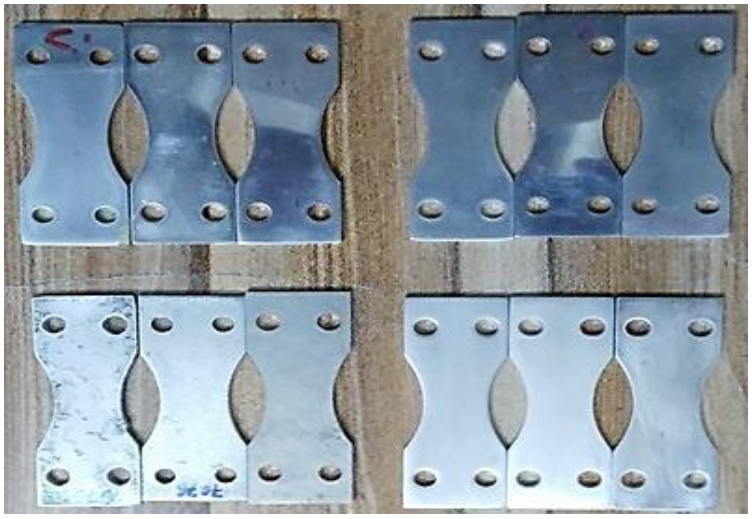

Figure 10. Fatigue Test Specimens according to Avery standard each three for specific group.

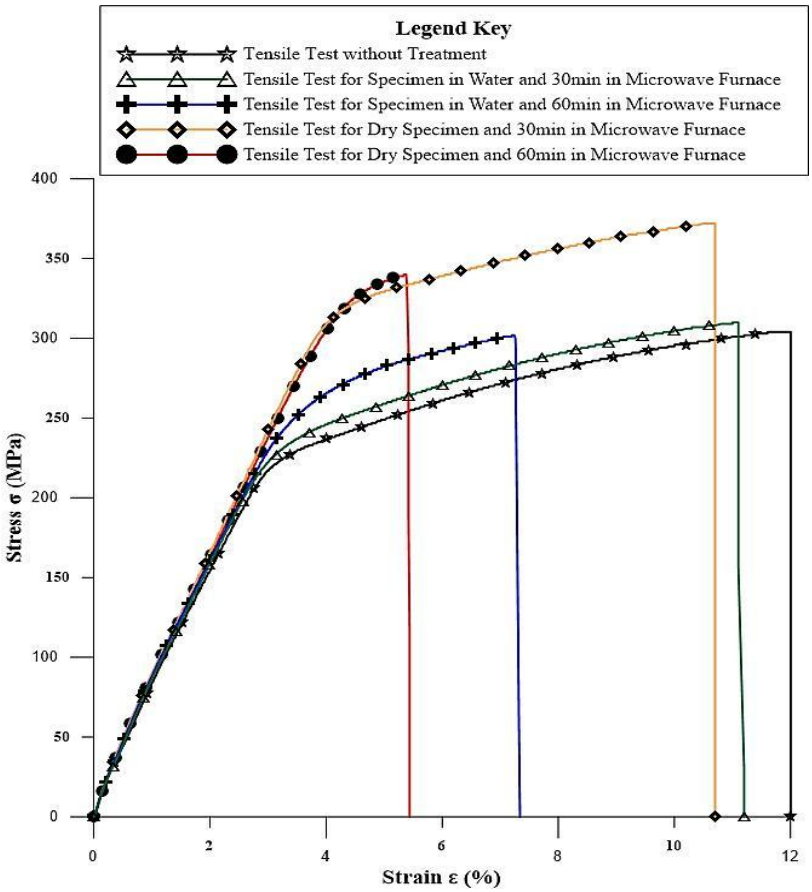

Figure 11. Stress – Strain diagram for the tensile test specimens.

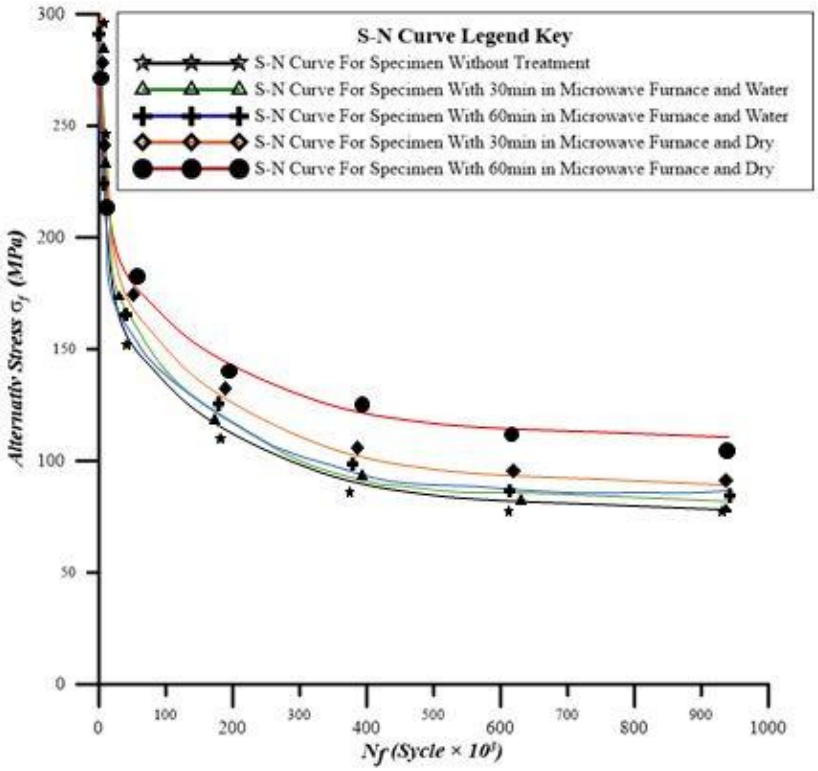

Figure 12. S – N Curves for the Fatigue test specimens.

Table 1. Chemical composition of AA2024-T3.

Component	% Si	% Fe	% Cu	% Mn	% Mg
Standard **(ASTM E 1251 – 94, 1999)**	≤ 0.5	≤ 0.5	3.8-4.9	0.3-0.9	1.2-1.8
Actual	0.25	0.09	4.53	0.81	1.51
Component	% Cr	% Zn	% Ti	% other	% Al
Standard **(ASTM E 1251 – 94, 1999)**	≤ 0.1	≤ 0.25	≤ 0.15	≤ 0.2	Reminder
Actual	0.014	0.13	0.014	0.065	Reminder

Table 2. Instruction manual of the fatigue test machine.

Power	1 HP
Maximum rating	1400 rpm
Current	2 Amperes
Voltage	380/440 Volts (3 Phases)
Frequency	50 Hz

Table 3. Mechanical Properties of all groups as compared with standard**.**

Group	Mechanical Properties	Test	Standard (ASM Metals Handbook, 1992)	Increment (%)
Group-1 Dry 60min in Microwave Furnace	Hardness, Rockwell B	93	80	16
	Ultimate Tensile Strength (MPa)	345	300	15
	Tensile Yield Strength (MPa)	325	225	44
	Modulus of Elasticity (GPa)	75.5	72	5
	Poisson's Ratio	0.333	0.35	5 (decrement)
	Fatigue Strength (MPa)	123	85	45
	Total Elongation (%)	5.5	12	54 (decrement)
Group-2 Dry 30min in Microwave Furnace	Hardness, Rockwell B	91	80	14
	Ultimate Tensile Strength (MPa)	375	300	25
	Tensile Yield Strength (MPa)	305	225	36
	Modulus of Elasticity (GPa)	74	72	4
	Poisson's Ratio	0.338	0.35	3 (decrement)
	Fatigue Strength (MPa)	105	85	24
	Total Elongation (%)	10.7	12	11 (decrement)
Group-3 Wet 60min in Microwave Furnace	Hardness, Rockwell B	87	80	9
	Ultimate Tensile Strength (MPa)	305	300	2
	Tensile Yield Strength (MPa)	265	225	18
	Modulus of Elasticity (GPa)	73	72	1
	Poisson's Ratio	0.343	0.35	2 (decrement)
	Fatigue Strength (MPa)	91	85	7
	Total Elongation (%)	7.5	12	37.5 (decrement)
Group-4 Wet 30min in Microwave Furnace	Hardness, Rockwell B	86	80	7.5
	Ultimate Tensile Strength (MPa)	315	300	5
	Tensile Yield Strength (MPa)	220	225	2 (decrement)
	Modulus of Elasticity (GPa)	72.5	72	0.7
	Poisson's Ratio	0.347	0.35	0.9 (decrement)
	Fatigue Strength (MPa)	88	85	3.5
	Total Elongation (%)	11.2	12	6.7 (decrement)

Table 4. Surface roughness results for all groups**.**

Alloys Type	AL 2024-T3			
Condition	Dry 60	Dry 30	Wet 60	Wet 30
Ra (μm) Read No.1	0.788	0.634	0.556	0.451
Ra (μm) Read No.2	0.784	0.637	0.550	0.452
Ra (μm) Read No.3	0.787	0.633	0.549	0.455
Ra (μm) Read No.4	0.785	0.630	0.547	0.454
Ra (μm) Average	0.786	0.634	0.552	0.453

E-ISSN 2520-3339

P-ISSN 1726-4073

Journal of Engineering

A Scientific Refereed Journal
Published by
College of Engineering
University of Baghdad

October
2017

Number 10
Volume 23

E-ISSN 2520-3339

P-ISSN 1726-4073

مجلة الهندسة

مجلة علمية محكمة تصدرها
كلية الهندسة ـ جامعة بغداد

العدد 10
المجلد 23

تشرين الاول
2017

رقم الايداع في دار الكتب والوثائق ببغداد
2231 لسنة 2017